










Therapeutic Strategies of COVID-19: from Natural Compounds to Vaccine Trials

Abdelhakim Bouyahya^{1,*} , Nasreddine El Omari ² , Nawal Elmeniyi ³ , Maryam Hakkour ⁴ ,
Abdelaali Balahbib ⁴ , Fatima-Ezzahrae Guaouguaou ⁵ , Taoufiq Benali ⁶ , Aicha El Baaboua ⁷ ,
Omar Belmehdi ⁷ 

¹ Laboratory of Human Pathologies Biology, Department of Biology, Faculty of Sciences, and Genomic Center of Human Pathologies, Faculty of Medicine and Pharmacy, Mohammed V University in Rabat, Morocco

² Laboratory of Histology, Embryology, and Cytogenetic, Faculty of Medicine and Pharmacy, Mohammed V University in Rabat, Morocco

³ Laboratory of Physiology, Pharmacology & Environmental Health, Faculty of Science, University Sidi Mohamed Ben Abdellah, Fez, Morocco

⁴ Laboratory of Zoology and General Biology, Faculty of Sciences, Mohammed V University in Rabat, Rabat, Morocco

⁵ Mohammed V University in Rabat, LPCMIO, Materials Science Center (MSC), Ecole Normale Supérieure, Rabat, Morocco

⁶ Laboratory of Natural Resources and Environment, Polydisciplinary Faculty of Taza, Sidi Mohamed Ben Abdellah University of Fez B.P.: 1223, Taza-Gare. Taza, Morocco

⁷ Biology and Health Laboratory, Biotechnology and Applied Microbiology Team, Department of Biology, Faculty of Science, Abdelmalek-Essaadi University, Tetouan, Morocco

* Correspondence: boyahya-90@hotmail.fr;

Scopus Author ID 57190813643

Received: 15.06.2020; Revised: 17.07.2020; Accepted: 18.07.2020; Published: 22.07.2020

Abstract: Severe Acute Respiratory Syndrome-Coronavirus 2 (SARS-CoV-2) is a novel coronavirus that caused a global epidemic named COVID-19. This disease continues to kill thousands of people around the world. Physiopathological studies showed that different organs such as lungs, brain, kidneys, immune system, and heart are affected directly and/or indirectly by this disease. With the absence of a vaccine, several treatments have been proposed, including old antiviral drugs, synthetic pharmacophores, and natural antiviral bioactive compounds. These molecules presented promising results with specific action on the virus. Moreover, other strategies are underway, such as the use of monoclonal antibodies, cell therapy, plasma therapy, and vaccine trials. In this work, we highlight the therapeutic strategies of COVID-19 natural compounds to vaccine trials.

Keywords: COVID-19; SARS-CoV-2; bioactive molecules; antiviral drug; targeted therapy.

© 2020 by the authors. This article is an open-access article distributed under the terms and conditions of the Creative Commons Attribution (CC BY) license (<https://creativecommons.org/licenses/by/4.0/>).

1. Introduction

Recently, a worldwide epidemic named COVID-19 (Coronavirus disease 2019) was produced by a novel virus named Severe Acute Respiratory Syndrome- Coronavirus 2 (SARS-CoV-2) [1, 2]. This virus belongs to the Coronaviridae family, SARS-CoV-2, and β -coronavirus genus with MERS-CoV and SARS-CoV [1, 2]. Molecularly, it is a positive-stranded RNA and contains four structural proteins on their surface (the membrane protein M, the envelope protein E, and the spike protein S). The spike protein is involved in virus tropism by its binding to host cell surfaces.

The rapid transmission of SARS-CoV-2 from human-to-human continues to cause real health dangers (cause the death of many people and causing enormous social, psychological, and economic impacts) [3, 4, 5].

With the absence of efficacy treatments, COVID-19 induces several clinical symptoms of patients infected by SARS-CoV-2 are different and include dry cough, high fever ($>38^{\circ}\text{C}$), fatigue, and some other symptoms such as vomiting myalgia, dyspnea, hemoptysis, sputum production, headache, and diarrhea [6–8]. Moreover, the detection of SARS-CoV-2 is based essentially on molecular diagnosis using on Real-Time Polymerase Chain Reaction (RT-PCR) technique [9].

Pharmacological strategies revealed the *in vitro* and *in vivo* efficacy drugs from different sources, while specific antiviral therapeutics and vaccines are the most effective methods to prevent and treat a viral infection. Up to date, there is any specific drug against the new coronavirus [10]. The lockdown is the only alternative solution to prevent and reduce the risk of transmission of this virus. Moreover, several studies are now being undertaken to set up treatments that target virus checkpoints such as penetration, de-encapsulation, transcription, replication, and assembly.

In this review, the latest advances *in vitro* and *in vivo* researches about anti-SARS-CoV-2 active drugs such as natural bioactive compounds and synthetic pharmacophores are scientifically explored and give promising results. Finally, all anti-COVID-19 therapeutic strategies at clinical trials using synthetic drugs, old antivirals, antibodies, cell therapy, plasma therapy, and current vaccine trials are also highlighted and critically discussed.

2. Preclinical therapeutic strategies

2.1. Natural bioactive compounds as possible drugs against SARS-CoV-2.

Since the outbreak of SARS, many researches dedicated themselves in order to find anti coronavirus agents, including the secondary metabolites as alkaloids, flavonoids, terpenoids, glycosides, tannins, etc., that exist in herbal medicines. In all studies, the hypotheses suggest that the receptor inhibitors, and the inhibition of proteins, which are essential for viral entry and replication of SARS-CoV, are the main attractive targets to discover a potential antiviral treatment for the human pathogen coronavirus. Table 1 summarizes all studies screened and confirmed the direct inhibition of SARS-CoV by some natural compounds *in silico*, *in vitro*, and *in vivo*.

Table 1. Anti-COVID effects of natural compounds isolated from medicinal plants

Chemical family	Compounds	Source	Experimental system (model cell line, <i>in silico</i> , <i>in vivo</i>)	Keys findings/mechanisms insights	References
Alkaloids	Capsaicin	<i>Allium sativum</i>	SARS-CoV-2 Protease Molecular Docking Analysis using MVD (molegro virtual dockers) software.	Stronger bond and high affinity to protease	[11]
	Bromocriptine, Celsentri, Delavirdine, Emend, Golvatinib, Maraviroc, Olysio, Saquinavir, Sovaprevir, Tanespimycin	-	SARS-CoV-2 Molecular Docking Analysis	Stronger bind the N-terminus and C-terminus of the homology model of SARS-CoV-2 Nsp14	[12]
	Agglutinin, nelfinavir	<i>Galanthus nivalis</i>	Feline coronavirus (FCoV)	Inhibited FCoV replication	

Chemical family	Compounds	Source	Experimental system (model cell line, <i>in silico</i> , <i>in vivo</i>)	Keys findings/mechanisms insights	References
			Feliscatus whole fetus-4 (fcwf-4) cells Cell viability: MTT assay microtitration infectivity-inhibition assay	Agglutinin more potent than nelfinavir with $IC_{50}=0.0088$ nM and 8.19 μ M, respectively at MOI 0.01 (2000 PFU/mL) Nelfinavir significantly blocked the induction of CPE foci at 9.41 μ M Agglutinin strong inhibitory activities at all concentrations Synergistic antiviral effect of two agents	[13]
	indirubin, tryptanthrin, indigodole A, indigodole B	<i>Strobilanthes cusia</i>	Human coronavirus NL63 (HCoV-NL63) infection MTT Cytotoxicity Test Cytopathic Effect Reduction and Virus Yield Inhibition Assays Infectivity Inhibition Assay Time-of-Addition/Removal Assay Assays on Virucidal	Potent antiviral activity Prevented the early ($IC_{50}=0.32$ μ M) and late stages ($IC_{50}=0.06$ μ M) of HCoV-NL63 replication Strong virucidal activity ($IC_{50}=0.06$ μ M) Anti-HCoV-NL63	[13]
	Indirubin, Indican, Sinigrin	<i>Isatis indigotica</i>	SARS-CoV 3CLpro	Sinigrin and hesperetin block the cleavage processing of the 3CL ^{pro} with $IC_{50}=217$ μ M and 8.3 μ M, respectively	[14]
	Lycorine	<i>Lycoris radiata</i>	SARS-CoV cytotoxicity assay	Potent antiviral activities against SARS-CoV EC_{50} value of 15.7 ± 1.2 nM CC_{50} value in the Vero E6 and HepG2 cell lines tested are 14980.0 ± 912.0 and 18810.0 ± 1322.0 nM, respectively selective index (SI) greater than 900	[14]
Flavonoids	Baicalein, Silibinin	-	SARS-CoV-2 Molecular Docking Analysis	Stronger bind the N-terminus and C-terminus of the homology model of SARS-CoV-2 Nsp14,	[12]
	(+)-catechin	-	Swine testicle cells Transmissible gastroenteritis virus (TGEV H16 strain) MTT assay Real-time PCR analysis	Inhibited TGEV replication in Swine testicle cells Reduced the viral yields Alleviated ROS conditions	[15]
	myricetin and scutellarein	-	SARS-coronavirus (CoV) induced severe acute respiratory syndrome (SARS) SARS helicase, nsP13, and the hepatitis C virus (HCV) helicase, NS3h Conducting fluorescence resonance energy transfer (FRET)-based double-strand (ds) DNA unwinding assay Colorimetry-based ATP hydrolysis assay.	Potently inhibit the SARS-CoV helicase protein Inhibited the ATPase activity of nsP13 by more than 90% at a concentration of 10 μ M With $IC_{50}=2.71\pm0.19$ μ M and 0.86 ± 0.48 μ M, respectively Any effect on the growth of MCF10A cells Any effect on the helicase activity of HCV virus	[16]
	tomentin A; Tomentin B; Tomentin C; Tomentin D; Tomentin	<i>Paulownia tomentosa</i>	SARS-CoV PL ^{pro} from <i>E. coli</i>	Inhibited PL ^{pro} in a dose-dependent manner	[17]

Chemical family	Compounds	Source	Experimental system (model cell line, <i>in silico</i> , <i>in vivo</i>)	Keys findings/mechanisms insights	References
	E; 3'-O-methyldiplacol; 4'-O-methyldiplacol; 3'-O-methyldiplacone; 4'-O-methyldiplacone; mimulone; diplacone; 6-geranyl-4',5,7-trihydroxy-3',5'-dimethoxyflavanone		SARS-CoV PL ^{pro} inhibition assay	IC ₅₀ ranging between 5.0 and 14.4 μM.	
	ACA, Galangin	<i>Curcuma sp.</i>	Molecular docking using the MOE 2010 program SARS-CoV-2 marker protein, RBD-S, PD-ACE2, and SARS-cov-2 protease	Highest affinity to bind the receptors Exhibited lowest energy binding with docking score of -13.51, -9.61, and -9.50 to the respected receptor of SARS-CoV-2 protease (6LU7), Spike glycoprotein-RBD (6LXT), and PD-ACE2 (6VW1) Better interaction to the SARS-CoV-2 protease compared to lopinavir Better interaction to Spike-RBD compared to nafamostat	[18]
	Tangeretin, Hesperetin, Nobiletin, Hesperidin, Naringenin,	<i>Caesalpinia sappan</i>	Molecular docking using the MOE 2010 program SARS-CoV-2 marker protein, RBD-S, PD-ACE2, and SARS-CoV-2 protease	Highest affinity to bind the receptors Exhibited lowest energy binding with docking score of -13.51, -9.61, and -9.50 to the respected receptor of SARS-CoV-2 protease (6LU7), Spike glycoprotein-RBD (6LXT), and PD-ACE2 (6VW1) Better interaction to the SARS-CoV-2 protease compared to lopinavir Better interaction to Spike-RBD compared to nafamostat	[18]
	naringenin, naringin, hesperetin, hesperidin, neohesperidin, nobiletin	<i>Citrus aurantium</i> <i>Citrus grandis</i> <i>Citrus reticulata</i>	LC-MS technique for analyzed six flavonoids Molecular docking Binding affinity of flavonoids to bind Angiotensin-Converting enzyme 2 (ACE 2)	Stronger binding affinity the ACE2. Naringin had highest binding activity to the ACE2 enzyme Docking energy of -6.85 kcal/mol The docking energy of naringin, hesperetin and naringenin binding to ACE2 were comparable with chloroquine.	[19]
	Hesperetin, Daidzein	<i>Isatis indigotica</i>	SARS-CoV 3CL ^{pro} cell-free assays cell-based cleavage assays	Sinigrin and hesperetin blocked the cleavage processing of the 3CL ^{pro} with IC ₅₀ =217 μM and 8.3 μM respectively	[14]
	kaempferol, morin, herbacetin, rhoifolin, pectolinarin, Daidzein	-	SARS-CoV 3CL ^{pro} Studied interaction of the three flavonoids using a tryptophan-based fluorescence method induced-fit docking analysis	Efficiently blocked the enzymatic activity of SARS-CoV 3CL ^{pro} . IC ₅₀ of SARS-CoV 3CL ^{pro} inhibitory activity=33.17, 27.45, and 37.78 μM, respectively	[20]

Chemical family	Compounds	Source	Experimental system (model cell line, <i>in silico</i> , <i>in vivo</i>)	Keys findings/mechanisms insights	References
			FRET protease assays with the SARS-CoV 3CL ^{pro} FRET protease assays with the SARS-CoV 3CL ^{pro} in the presence of Triton X-100		
	Quercetin, daidzein, puerarin, epigallocatechin, epigallocatechin gallate, gallic acid, gallic acid gallate, ampelopsin	<i>Pichia pastoris</i>	SARS-CoV 3C-like protease (SARS-CoV 3CL ^{pro}) Molecular docking Inhibition assay	Good inhibition toward 3CL ^{pro} with IC ₅₀ values of 73, 73, and 47 μ M, respectively gallic acid gallate showed a competitive inhibition pattern with K _i value of 25 \pm 1.7 μ M gallic acid gallate displayed a binding energy of -14 kcal mol ⁻¹ to the active site of 3CL ^{pro}	[21]
	amentoflavone, bilobetin, ginkgetin, sciadopitysin	<i>Torreanucifera</i>	SARS-CoV 3CL ^{pro} Molecular docking study Enzymatic assays SARS 3C-like protease (3CL ^{pro}) inhibition assay	Most potent 3CL ^{pro} inhibitory effect (IC ₅₀ =8.3 μ M)	[22]
Terpenoids	Limonene	<i>Elettaria</i>	SARS-CoV-2 Protease Molecular Docking Analysis using MVD (molegro virtual docker) software.	Stronger bond and high affinity to protease	[11]
	Thymol	<i>Mentha pulegium</i>	SARS-CoV-2 Protease Molecular Docking Analysis using MVD (molegro virtual docker) software.	Stronger bond and high affinity to protease	[11]
	ferruginol, dehydroabieta-7-one, sugiol, [8 β -hydroxyabieta-9(11),13-dien-12-one], 6,7-dehydroroleanone, pinusolidic acid, α -cadinol	<i>Chamaecyparis obtuse</i> var <i>formosana</i>	SARS-CoV-induced cytopathogenic effect on Vero E6 cells Cell-Based Assay Utilizing CPE on Vero E6 Cells via SARS-CoV Infection cell-based assay Cytotoxic Effects: MTT assay Inhibition of Viral Replication in SARS-CoV-Infected Vero E6 Cells SARS-CoV 3CL Protease Inhibition Assay Computer Modeling of SARS-CoV 3CL Protease Inhibition.	Significant levels (++ to +++) of anti-SARS-CoV activity at concentrations between 3.3 and 10 μ M. Significant inhibition on 3CL protease	[23]
	, 3 β ,12-diacetoxyabieta-6,8,11,13-tetraene, cedrane-3 β ,12-diol, betulonic acid	<i>Juniperus formosana</i>	SARS-CoV-induced cytopathogenic effect on Vero E6 cells Cell-Based Assay Utilizing CPE on Vero E6 Cells via SARS-CoV Infection cell-based assay Cytotoxic Effects: MTT assay Inhibition of Viral Replication in SARS-	Significant levels (++ to +++) of anti-SARS-CoV activity at concentrations between 3.3 and 10 μ M. Significant inhibition on 3CL protease	[23]

Chemical family	Compounds	Source	Experimental system (model cell line, <i>in silico</i> , <i>in vivo</i>)	Keys findings/mechanisms insights	References
			CoV-Infected Vero E6 Cells SARS-CoV 3CL Protease Inhibition Assay Computer Modeling of SARS-CoV 3CL Protease Inhibition.		
	cryptojaponol, 7 β - hydroxydeoxycryptojaponol	<i>Cryptomeria japonica</i>	SARS-CoV-induced cytopathogenic effect on Vero E6 cells Cell-Based Assay Utilizing CPE on Vero E6 Cells <i>via</i> SARS-CoV Infection cell-based assay Cytotoxic Effects: MTT assay Inhibition of Viral Replication in SARS-CoV-Infected Vero E6 Cells SARS-CoV 3CL Protease Inhibition Assay Computer Modeling of SARS-CoV 3CL Protease Inhibition.	SARS-CoV activity at concentrations between 3.3 and 10 μ M. Significant inhibition on 3CL protease	[23]
	Betulin	<i>Strobilanthes cusia</i>	Human coronavirus NL63 (HCoV-NL63) infection MTT Cytotoxicity Test Cytopathic Effect Reduction and Virus Yield Inhibition Assays Infectivity Inhibition Assay Time-of-Addition/Removal Assay Assays on Virucidal Activity	Potent antiviral activity Prevented the early (IC ₅₀ =0.32 μ M) and late stages (IC ₅₀ =0.06 μ M) of HCoV-NL63 replication Strong virucidal activity (IC ₅₀ =0.06 μ M) Anti-HCoV-NL63 activity with IC ₅₀ values of 1.52 μ M and 0.30 μ M in LCC-MK2 and Calu-3 cells, respectively	[13]
	Betulin, 18-hydroxyferruginol, hinokiol, ferruginol, 18-oxoferruginol, O-acetyl-18-hydroxyferruginol, methyl dehydroabietate, isopimaric acid, kayadiol	<i>Torreya nucifera</i>	SARS-CoV 3CL ^{pro} Molecular docking study Enzymatic assays SARS 3C-like protease (3CL ^{pro}) inhibition assay	Most potent 3CL ^{pro} inhibitory effect (IC ₅₀ =8.3 μ M)	[22]
Tanins	Phloroglucinol, triphloretol A, eckol, dioxinodehydroeckol, 2-phloroeckol, 7-phloroeckol, fucodiphloroethol G, dieckol, phlorofucofuroeckol A	<i>Ecklonia cava</i>	SARS-CoV 3CL ^{pro} SARS-CoV 3CL ^{pro} trans-cleavage assay SARS-CoV 3CL ^{pro} cis-cleavage assay Real-time analysis of ligand interaction with SARS-CoV 3CL ^{pro} by surface plasmon resonance (SPR) Molecular docking simulation study	Inhibitory activities in a dose-dependently and competitive manner Most potent SARS-CoV 3CL ^{pro} trans/cis-cleavage Inhibitory effects (IC ₅₀ s=2.7 and 68.1 μ M, respectively). Significantly blocking the cleavage of SARS-CoV 3CL ^{pro} in a cell-based assay Exhibited a high association rate in the SPR sensorgram Formed extremely strong hydrogen bonds to the catalytic dyad (Cys145 and	[24]

Chemical family	Compounds	Source	Experimental system (model cell line, <i>in silico</i> , <i>in vivo</i>)	Keys findings/mechanisms insights	References
				His41) of the SARS-CoV 3CL ^{pro}	
	Phloroglucinol, Eckol, 7-Phloroeckol, Phlorofucofuroeckol, Dieckol	<i>Ecklonia cava</i>	Porcine epidemic diarrhea virus (PEDV) MTT assay Antiviral assay Hemagglutination inhibition (HI) assay Real-time PCR analysis Western blot analysis Confocal fluorescence imaging	In the simultaneous-treatment assay, IC ₅₀ =10.8±1.4 µM In post-treatment assay, IC ₅₀ =12.2±2.8 µM Blocked the binding of viral spike protein to sialic acids at less than 36.6 µM	[25]
	geraniin, tellimagradin, punicalin, castalin, strictinin, granatin A, pedunculagin, casuarinin, tercatain, bicornin	-	SARS-CoV-2 Molecular docking modeling Molecular Operating Environment (MOE v2009) software	Interacted with the receptor binding site and catalytic dyad (Cys145 and His41) of SARS-CoV-2 Successfully inhibit the protease enzyme of SARS-CoV-2	[26]
Quinone	Hypericin, Idarubicin	-	SARS-CoV-2 Molecular Docking Analysis	Stronger bind the N-terminus and C-terminus of the homology model of the SARS-CoV-2 Nsp14,	[12]
	Emodin, Promazine, Rhein, 1,4-bis-(1-anthraquinonylamino)-anthraquinone	<i>Rheum officinale</i> and <i>Polygonum multiflorum</i> ,	SARS-CoV S Biotinylated ELISA Immunofluorescence assay (IFA) 3-(4,5-Dimethylthiazol-2-yl)-2,5-diphenyltetrazolium bromide (MTT) assay	Significantly blocked the S protein and ACE2 interaction Inhibited the infectivity of S protein-pseudotyped retrovirus to Vero E6 cells. Percent inhibition of emodin at 50 µM was 94.12±5.90%	[27]
	Emodin	-	Coronavirus HCoV-OC43 Rhabdomyosarcoma cells Measurement of virus using real-time PCR Plaque reduction assay	Inhibited the 3a ion channel of coronavirus SARS-CoV and HCoV-OC43 as well as virus release from HCoV-OC43 K _{1/2} =20 µM	[28]
	Aloeemodin	<i>Isatis indigotica</i>	SARS-CoV 3CL ^{pro} cell-free assays cell-based cleavage assays	Sinigrin and hesperetin blocked the cleavage processing of the 3CL ^{pro} with IC ₅₀ =217 µM and 8.3 µM, respectively	[14]
	Coumarin	<i>Glycyrrhiza glabra</i>	SARS-CoV-2 Protease Molecular Docking Analysis using MVD (molegro virtual docker) software.	Stronger bond and high affinity to protease	[11]
Coumarin	psoralen, bergapten, xanthotoxin, isopimpinellin	<i>Angelica keiskei</i>	SARS-CoV a chymotrypsin-like protease (3CL ^{pro}) and a papain-like protease (PL ^{pro}) SARS-CoV 3CL ^{pro} cell-free trans-cleavage inhibition assay SARS-CoV 3CL ^{pro} cell-based cis-cleavage inhibition assay SARS-CoV PL ^{pro} inhibition assay Deubiquitination activity assay	Exhibited the most potent 3CL ^{pro} and PL ^{pro} inhibitory activity with IC ₅₀ values of 11.4 and 1.2 µM. Inhibited cell-free trans-cleavage of SARS-CoV 3CL ^{pro} with IC ₅₀ =11.4±1.4 µM Inhibited cell-based cis-cleavage activities of SARS-CoV 3CL ^{pro} with IC ₅₀ =7.1±0.8 µM Exhibited the most potent activity with a selectivity	[29]

Chemical family	Compounds	Source	Experimental system (model cell line, <i>in silico</i> , <i>in vivo</i>)	Keys findings/mechanisms insights	References
			DeISGylation activity assay Chymotrypsin activity <i>In silico</i> molecular simulation study AutoDock version 3.0.5 using AutoDock version 3.0.5	index (SI $\frac{1}{4}$ CC ₅₀ /EC ₅₀) value of 9.2. IC ₅₀ of Deubiquitination activity=2.6±0.7 µM IC ₅₀ of DeISGylation activity=5.2±0.4 µM	
Steroidal alkaloids	Verticinone 3-beta-D-glucoside, Imperialine-3-β-D-glucoside, pseudojervine, zhebeininoside, Veratroylzygadenine, Zhebeinone-3-β-D-glucoside, Mulberroside E, Hupehenisine, verdineverticinone-3-β-D-glucoside, (E)-Resveratrol 3,5-O-β-diglucoside, peimisine, 15-O-(2-Methylbutanoyl)-3-O-veratroylprotoverine, 3-Acetylzygadenine, Polydatin IV, Piceatannol 3,4'-di-β-D-glucopyranoside, puqietinone	“Agsirga” species	SARS-CoV-2 HPLC-Q-Exactive high-resolution mass spectrometry molecular docking technology AutoDock molecular docking software	blocked the binding of ACE2 and SARS-CoV-2 S-protein at the molecular level	[30]
Steroids	Sitosterol	<i>Strobilanthes cusia</i>	Human coronavirus NL63 (HCoV-NL63) infection MTT Cytotoxicity Test Cytopathic Effect Reduction and Virus Yield Inhibition Assays Infectivity Inhibition Assay Time-of-Addition/Removal Assay Assays on Virucidal Activity	Potent antiviral activity Prevented the early (IC ₅₀ =0.32 µM) and late stages (IC ₅₀ =0.06 µM) of HCoV-NL63 replication Strong virucidal activity (IC ₅₀ =0.06 µM) Anti-HCoV-NL63 activity with IC ₅₀ values of 1.52 µM and 0.30 µM in LCC-MK2 and Calu-3 cells, respectively	[13]
	Glycyrrhizic acid derivatives,	<i>Glycyrrhiza radix</i>	SARS-CoV strain FFM1 Immunocytochemical Staining of Viral Antigens and Visual CPE Assay Determination of Cytotoxicity using MTT assay	Seven derivatives inhibited SARS-CoV replication at lower concentrations compared to GL The introduction of N-acetylglucosamine into the glycoside chain of GL (1) increased the anti SARS-CoV activity about 9 times compared to GL Compound 11 more active against SARS-CoV with an EC ₅₀ =5±3 µM High cytotoxicity effect with CC ₅₀ =15±3 µM Selectivity index (SI)=3 The immunocytochemical staining showed >99% suppression of viral antigen expression	[31]

Chemical family	Compounds	Source	Experimental system (model cell line, <i>in silico</i> , <i>in vivo</i>)	Keys findings/mechanisms insights	References
	Beta-sitosterol	<i>Isatis indigotica</i>	SARS-CoV 3CL ^{pro} cell-free assays cell-based cleavage assays	Sinigrin and hesperetin blocked the cleavage processing of the 3CL ^{pro} with IC ₅₀ =217 μM and 8.3 μM, respectively	[14]
Allyls	DiallylDisulfide	<i>Allium sativum</i>	SARS-CoV-2 Protease Molecular Docking Analysis using MVD (molegro virtual docker) software.	Stronger bond and high affinity to protease	[11]
Stilbenes	Curcumin	<i>Curcuma longa</i>	SARS-CoV-2 Protease Molecular Docking Analysis using MVD (molegro virtual docker) software.	Stronger bond and high affinity with protease	[11]
	Curcumin, DMC	<i>Citrus sp.</i>	Molecular docking using the MOE 2010 program SARS-CoV-2 marker protein, RBD-S, PD-ACE2, and SARS-CoV-2 protease	Highest affinity to bind the receptors Exhibited lowest energy binding with docking score of -13.51, -9.61, and -9.50 to the respected receptor of SARS-CoV-2 protease (6LU7), Spike glycoprotein-RBD (6LXT), and PD-ACE2 (6VW1) Better interaction to the SARS-CoV-2 protease compared to lopinavir Better interaction to Spike-RBD compared to nafamostat	[18]
Phenylpropanoids	Verbascoside	<i>Stachys schtschegleevi</i>	SARS-CoV-2 Protease Molecular Docking Analysis using MVD (molegro virtual dockers) software	Stronger bond and high affinity to protease	[11]
Glucosides	Glucuronic acid	<i>Astragalus gossypinus</i>	SARS-CoV-2 Protease Molecular Docking Analysis using MVD (molegro virtual dockers) software	Stronger bond and high affinity with protease	[11]
Lignoids	hinokinin, savinin	-	SARS-CoV-induced cytopathogenic effect on Vero E6 cells Cell-Based Assay Utilizing CPE on Vero E6 Cells via SARS-CoV Infection cell-based assay Cytotoxic Effects: MTT assay Inhibition of Viral Replication in SARS-CoV-Infected Vero E6 Cells SARS-CoV 3CL Protease Inhibition Assay Computer Modeling of SARS-CoV 3CL Protease Inhibition.	Significant levels (++ to +++) of anti-SARS-CoV activity at concentrations between 3.3 and 10 μM. Significant inhibition on 3CL protease	[23]

Chemical family	Compounds	Source	Experimental system (model cell line, <i>in silico</i> , <i>in vivo</i>)	Keys findings/mechanisms insights	References
Tanshinones	tanshinone IIA, tanshinone IIB, methyl tanshinonate, cryptotanshinone, tanshinone I, dihydrotanshinone I, rosmariquinone	<i>Salvia miltiorrhiza</i>	SARS-CoV 3CL ^{pro} and PL ^{pro} viral cysteine proteases. SARS-CoV 3CL ^{pro} inhibition assay SARS-CoV PL ^{pro} inhibition assay Kinetics of SARS-3CL ^{pro} activation, Analysis of SARS-CoV 3CL ^{pro} and PL ^{pro} inhibition progress curves	Tanshinone I (5) exhibited the most potent nanomolar level inhibitory activity toward deubiquitinating (IC ₅₀ =0.7 μM) Good inhibitors of both cysteine proteases Slight activity	[32]
	phloroglucinol, triphloretol A, eckol, dioxinodehydroeckol, 2-phloroeckol, 7-phloroeckol, fucodiphloroethol G, dieckol, phlorofucofuroeckol A	<i>Salvia miltiorrhiza</i>	SARS-CoV 3CL ^{pro} and PL ^{pro} SARS-CoV viral proteases inhibition using the FRET method SARS-CoV PL ^{pro} deubiquitination assay SARS-CoV PL ^{pro} deIS Gylation assay	Potent inhibitor of PL ^{pro} with an IC ₅₀ value of 3.7 μM inhibited SARS-CoV 3CL ^{pro} with an IC ₅₀ =103.6±17.4 μM Strongly inhibited the cleavage of both ubiquitin and ISG15 (IC ₅₀ =7.6 and 8.5 μM, respectively)	[33]
Alkylated chalcones	isobavachalcone, 4-hydroxyderricin, xanthoangelol, xanthoangelol F, xanthoangelol D, xanthoangelol E, xanthoangelol B, xanthoangelol G, xanthokeistal A	<i>Angelica keiskei</i>	SARS-CoV a chymotrypsin-like protease (3CL ^{pro}) and a papain-like protease (PL ^{pro}) SARS-CoV 3CL ^{pro} cell-free trans-cleavage inhibition assay SARS-CoV 3CL ^{pro} cell-based cis-cleavage inhibition assay SARS-CoV PL ^{pro} inhibition assay Deubiquitination activity assay DeISGylation activity assay Chymotrypsin activity <i>In silico</i> molecular simulation study AutoDock version 3.0.5 using AutoDock version 3.0.5	Exhibited the most potent 3CL ^{pro} and PL ^{pro} inhibitory activity with IC ₅₀ values of 11.4 and 1.2 μM. Inhibited cell-free trans-cleavage of SARS-CoV 3CL ^{pro} with IC ₅₀ =11.4±1.4 μM Inhibited cell-based cis-cleavage activities of SARS-CoV 3CL ^{pro} with IC ₅₀ =7.1±0.8 μM Exhibited the most potent activity with a selectivity index (SI ¼ CC ₅₀ /EC ₅₀) value of 9.2. IC ₅₀ of Deubiquitination activity=2.6±0.7 μM IC ₅₀ of DeISGylation activity=5.2±0.4 μM	[29]

2.1.1. Mechanism insights of natural alkaloids anti-SARS-CoV-2.

Some researchers have reported an important antiviral activity of alkaloids such as Capsaicin, Bromocriptine, Celsentri, Delavirdine, Emend, Golvatinib, Maraviroc, Olysio, Saquinavir, Sovaprevir, Tanespimycin, Agglutinin, nelfinavir, indirubin, tryptanthrin, indigodole A, indigodole B, Indirubin, Indican, Sinigrin, and Lycorine (Figure 1 and Table 1). Among them, Liu *et al.* [12] demonstrated, *in silico*, that Saquinavir and Bromocriptine could bind to the N-terminus and C-terminus of the homology model of SARS-CoV-2 Nsp14 which is important for replication and transcription of SARS and other coronaviruses, meaning that these compounds may be useful in the treatment of early stages of virus cycle.

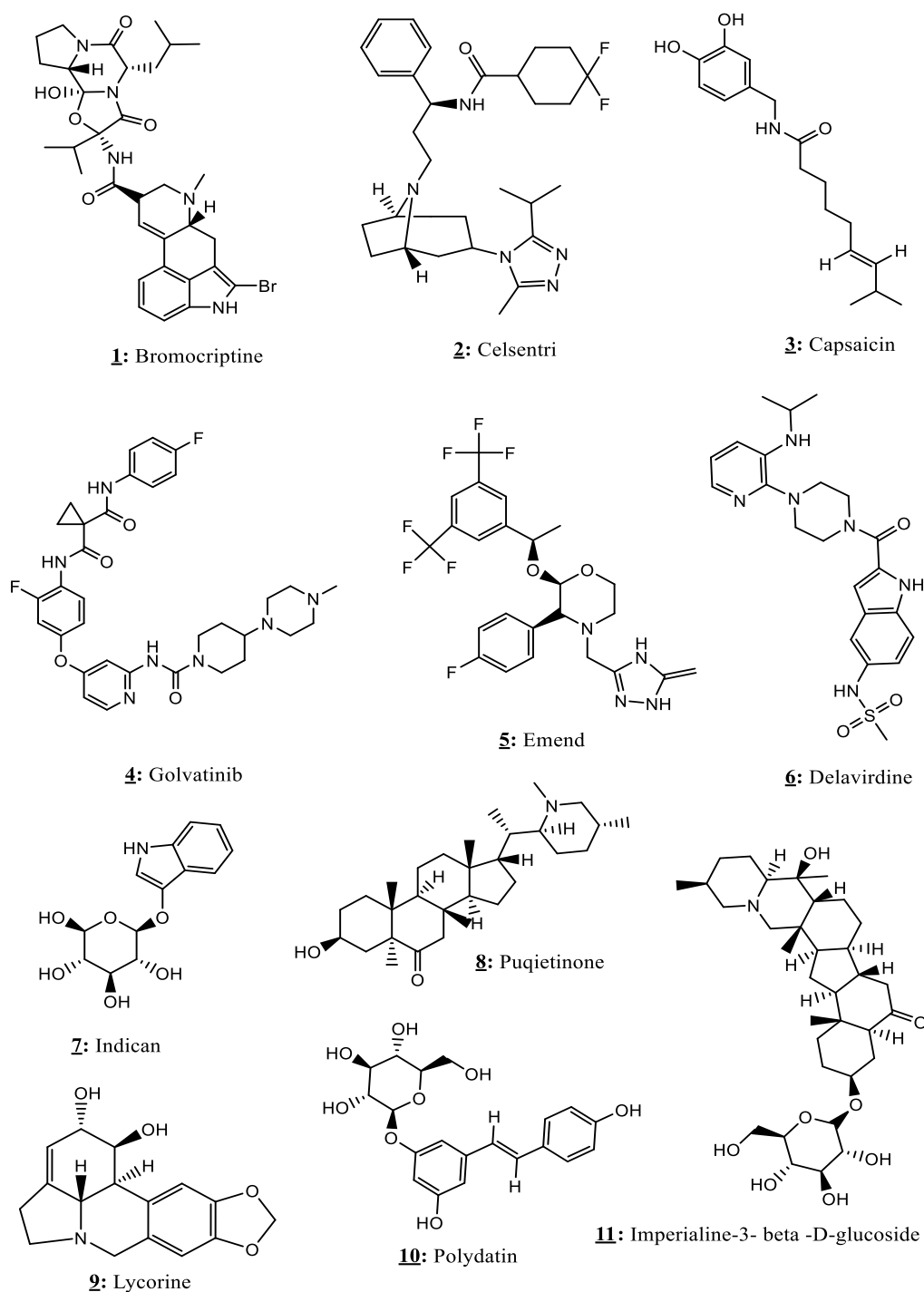


Figure 1. Chemical structures of natural alkaloids isolated from medicinal plants with anti-SARS-CoV-2 activities (these structures were drawn by ChemDraw).

In another study carried out *in vitro*, Tsai *et al.* [13] evaluated, in the first step, the antiviral activity of tryptanthrin against HCoV-NL63 using the CPE reduction assay. The results showed that at 40µM, tryptanthrin exhibits an important antiviral effect with a significant reduction in HCoV-NL63-induced CPE in LLC-MK2 cells 36 and 48 h post-infection. In the same study, the infectivity assay with immunofluorescent staining demonstrated that this alkaloid compound exhibits a strong inhibitory activity in the early and late stages of HCoV-NL63 replication.

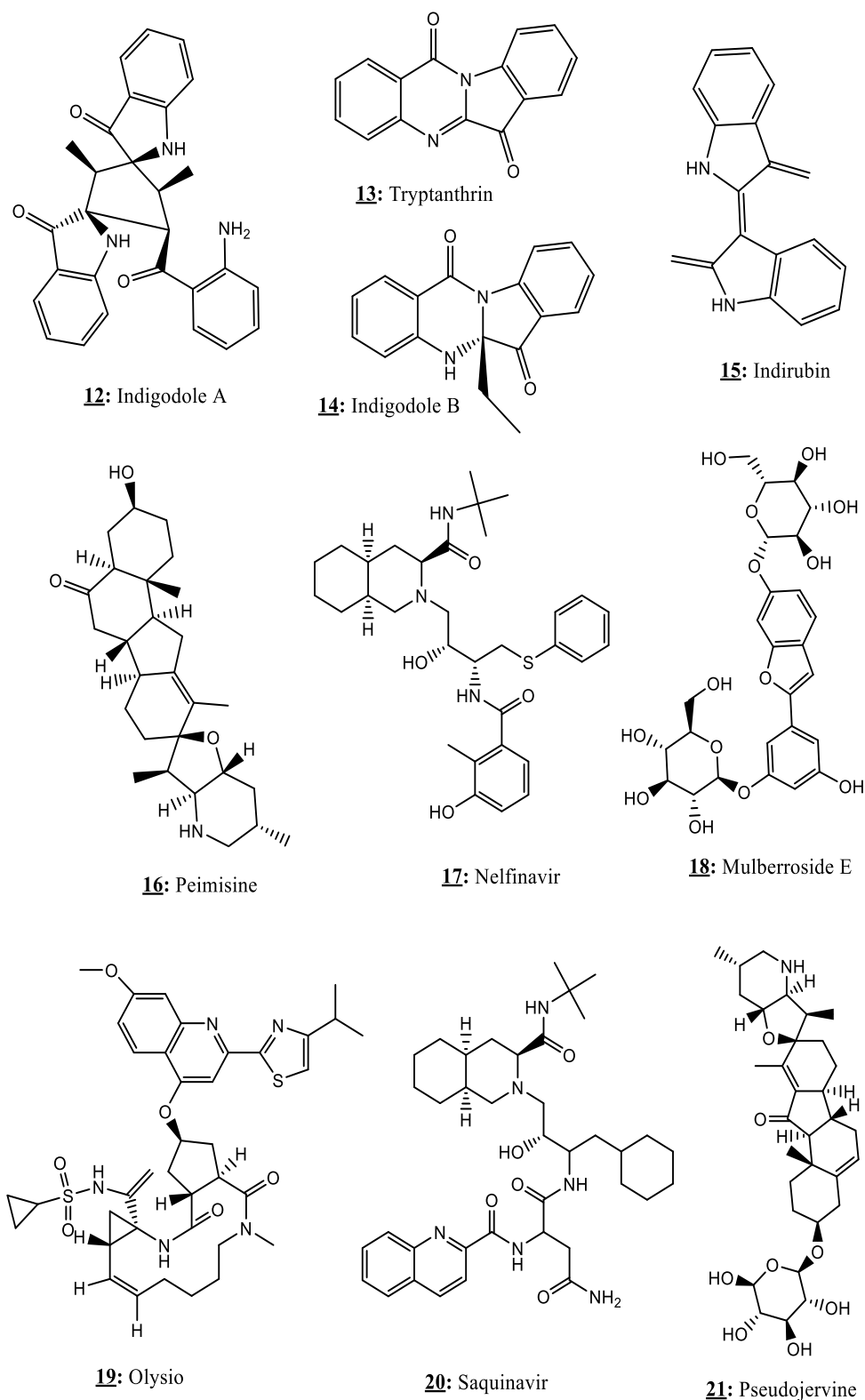


Figure 1. Continued.

However, tryptanthrin was less potent in impeding the early ($IC_{50}=0.32 \mu M$) than the late-stage ($IC_{50}=0.06 \mu M$); and considerably decreased the production of extracellular virions in these two stages. More interesting, this study indicated that tryptanthrin significantly attacked the viral enzymes such as RNA-dependent RNA polymerase and PLP2 during the late stages of HCoV-NL63 replication, indicating that the viral RNA genome synthesis and progeny virus production were moderated. Thus, tryptanthrin demonstrated important virucidal activity against HCoV-NL63 ($IC_{50}=0.06\mu M$). Tryptanthrin could be used against human coronaviruses

as an inhibitor targeting the viral replication cycle. Another alkaloid compound, namely sinigrin, exhibits a good antiviral effect. Indeed, Lin *et al.* [14] studied its anti-SARS coronavirus 3C-like protease effect. According to this study, the use of the cell-based assay revealed that sinigrin ($IC_{50}=217\ \mu M$) significantly blocks the cleavage processing of the viral protease 3CL^{pro}. In addition, sinigrin ($CC_{50}>10\ mM$) was not toxic to Vero cells; this compound may be considered as a potential alternative to develop an inhibitor of SARS-CoV 3CL^{pro} [14]. In addition, using cytotoxicity assay, the authors demonstrated an interesting anti-SARS-CoV effect of lycorine with an EC_{50} value of $15.7\pm 1.2\ nM$. The results suggested that this alkaloid compound is a candidate for new anti-SARS-CoV drug development.

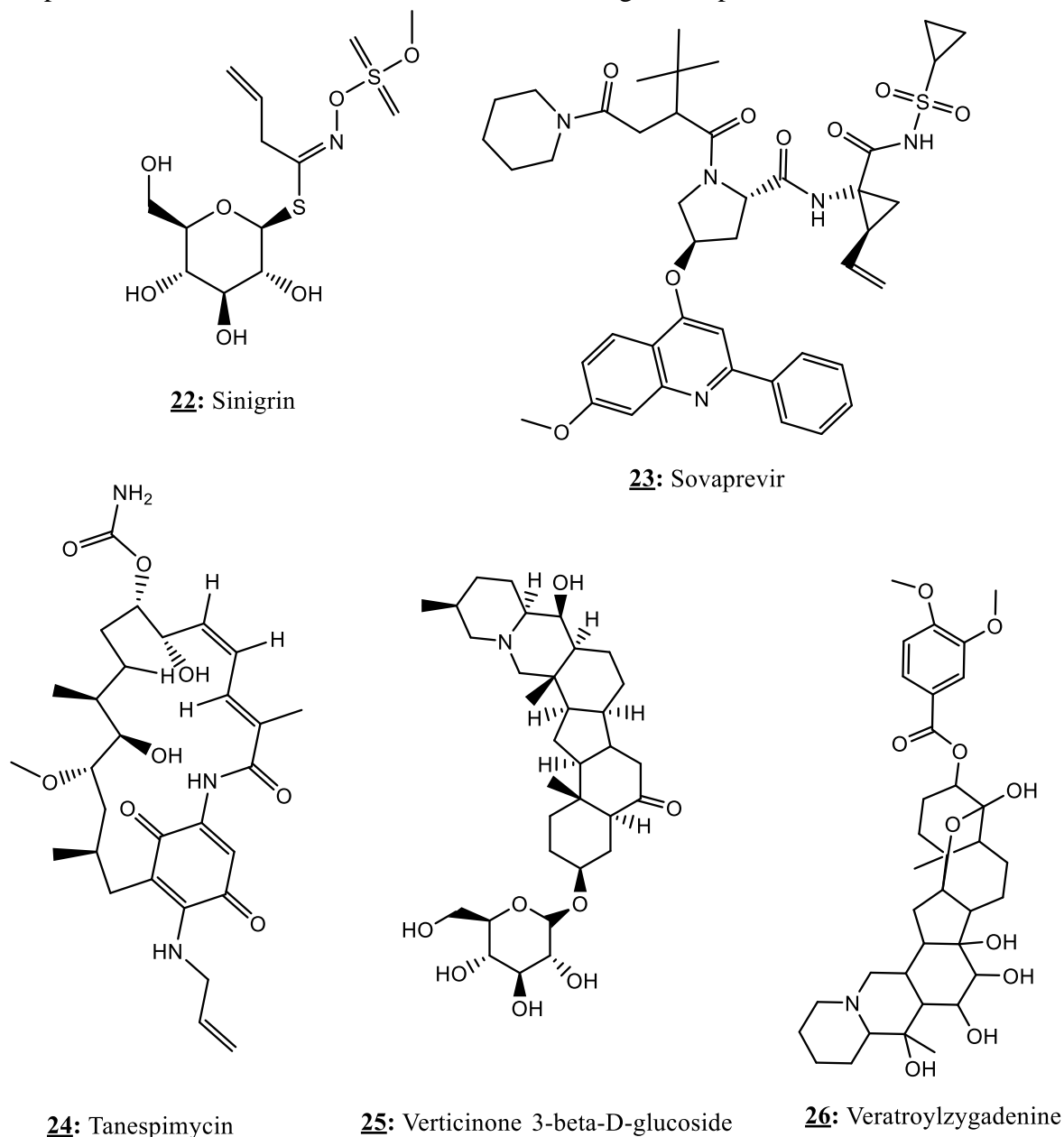


Figure 1. Continued.

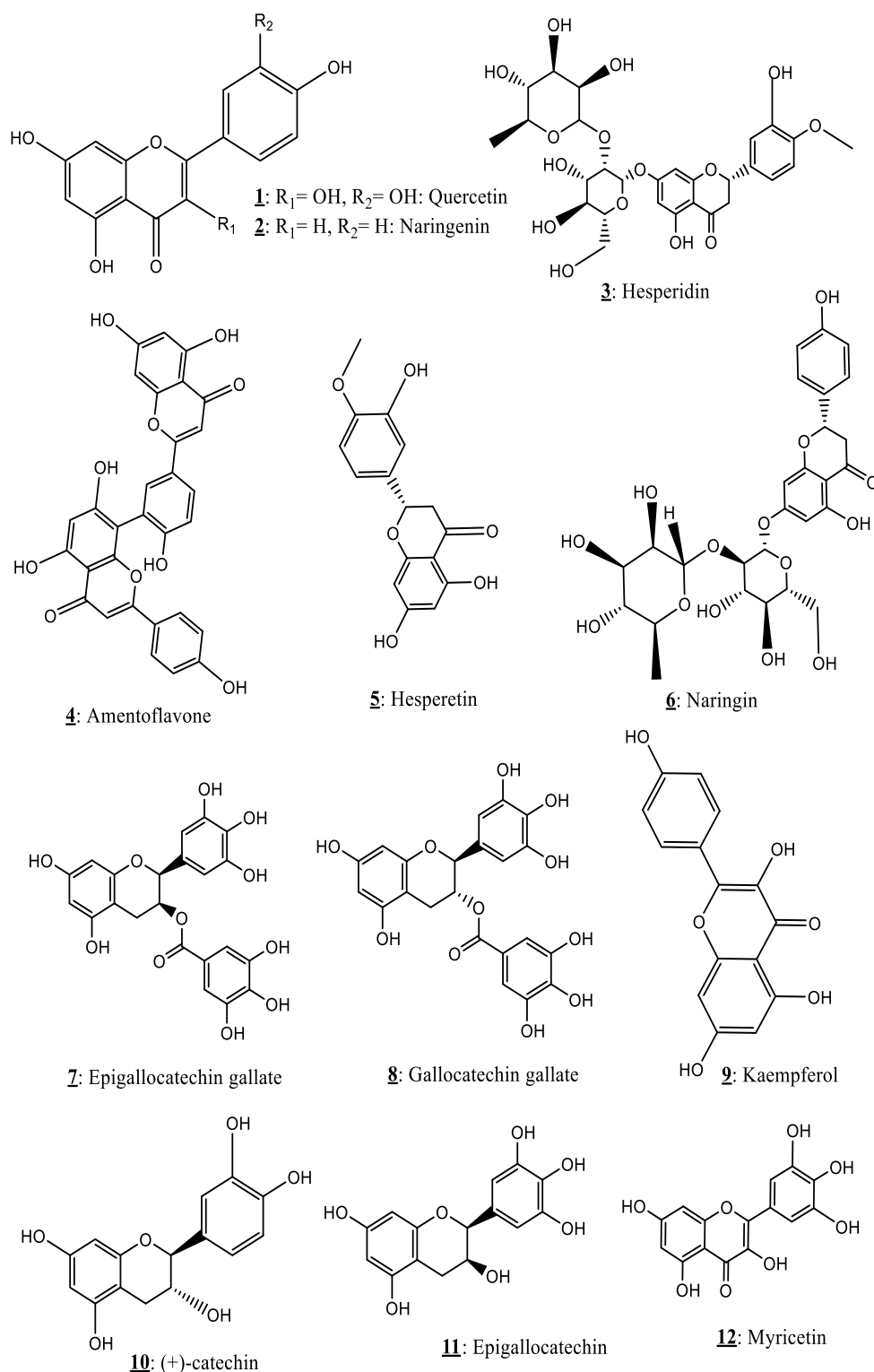


Figure 2. Chemical structures of natural flavonoids isolated from medicinal plants with anti-SARS-CoV-2 activities (these structures were drawn by ChemDraw).

2.1.2. Mechanism insights of flavonoids anti-SARS-CoV-2.

Other secondary metabolites namely flavonoids confirmed the anti-SARS effects such as baicalein, silibinin, myricetin, and scutellarein, (+)-catechin tomentin A; Tomentin B; Tomentin C; Tomentin D; Tomentin E; 3'-O-methyldiplacol; 4'-O-methyldiplacol; 3'-O-methyldiplacone; 4'-O-methyldiplacone; mimulone; diplacone; 6-geranyl-4',5,7-trihydroxy-3',5'-dimethoxyflavanone, Tangeretin, Hesperetin, Nobiletin, Hesperidin, Naringenin, ACA, Galangin, naringenin, naringin, hesperetin, hesperidin, neohesperidin, nobiletin, kaempferol,

morin, herbacetin, rhoifolin, pectolinarin, daidzein, quercetin, daidzein, puerarin, epigallocatechin, epigallocatechin gallate, galocatechin gallate, ampelopsin, amentoflavone, bilobetin, ginkgetin, and sciadopitysin (Figure 2 and Table 1). Among these compounds, hesperidin was described as a potent inhibitor of SARS-CoV-2.

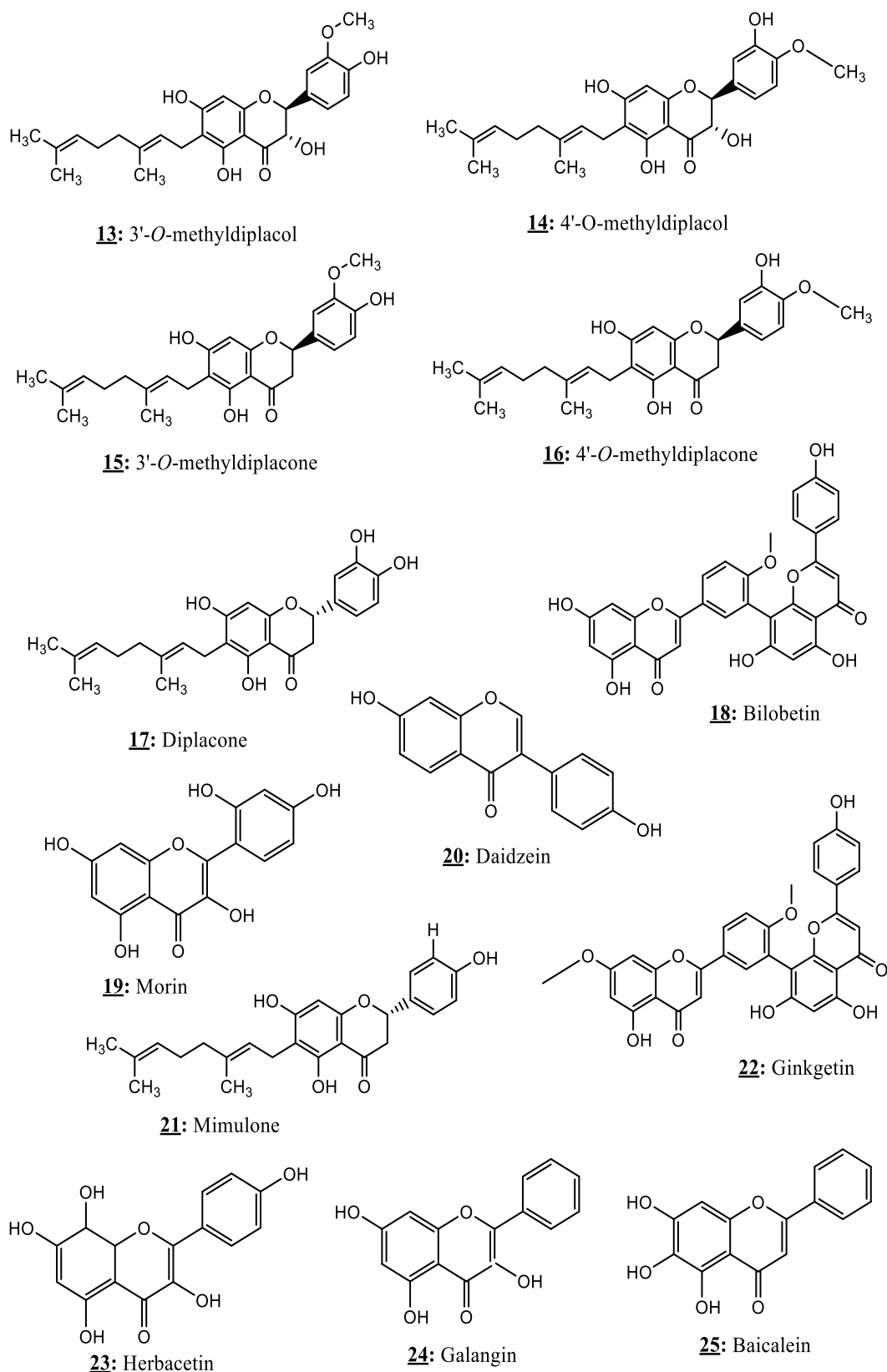


Figure 2. Continued.

Indeed, Utomo *et al.* [18] revealed, *in silico*, the anti-SARS-Cov-2 potential of hesperidin through its binding to RBDS, PD-ACE2, and SARS-CoV-2 protease. The results showed that hesperidin has the lowest docking score for all three protein receptors representing the highest affinity to bind the receptors tested. More importantly, this flavonoid compound has better interaction with the SARS-CoV-2 protease and to Spike-RBD compared to lopinavir and nafamostat [18]. These results suggest that hesperidin would be effective to block virus infection and replication.

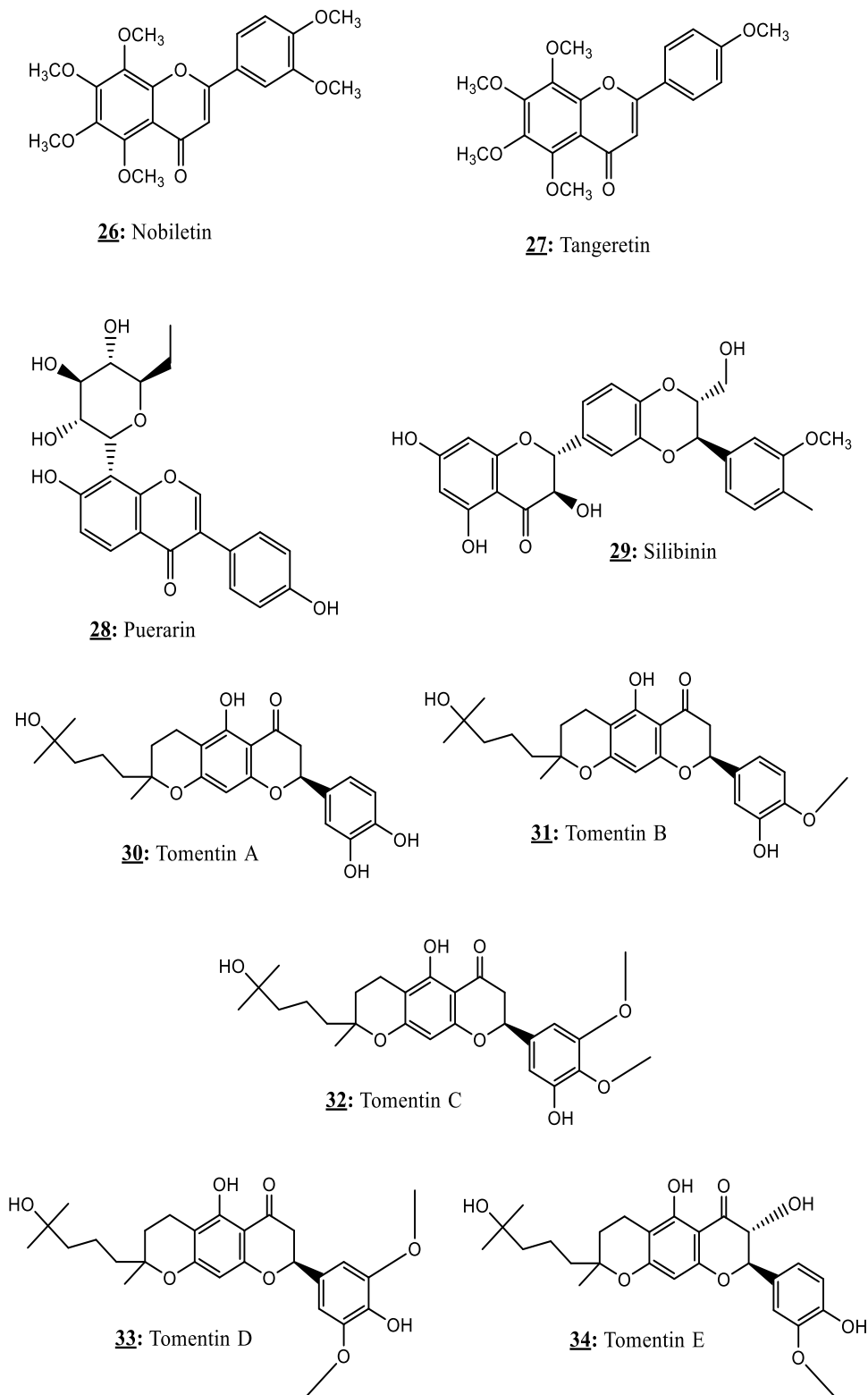


Figure 2. Continued.

In another study, herbacetin, rhoifolin, and pectolinarin (flavonoids) were reported as antiviral molecules against coronaviruses. The *in silico* results indicated that herbacetin, rhoifolin, and pectolinarin block the enzymatic activity of SARS-CoV 3CL^{pro} [35]. In addition, the confirmation of their interaction was performed using a tryptophan-based fluorescence assay; the *in silico* results demonstrated that S1, S2, and S30 sites are involved in binding with flavonoids, meaning that herbacetin, rhoifolin, and pectolinarin may be suggested to be inhibitors of the responsible enzyme for cleavage of the remaining 11 locations causing a release of a total of 16 nonstructural proteins (nsp) in both SARS- and MERS-CoV. Another study evaluated the antiviral effect of quercetin, epigallocatechin gallate, and gallic acid [21]. Indeed, these three flavonoid products exhibited a good inhibition of 3CL^{pro} with IC₅₀ values of 73, 73, and 47 μ M, for quercetin, epigallocatechin gallate, and gallic acid, respectively. Notably, gallic acid demonstrated a competitive inhibition pattern with $K_i=25\pm1.7$ μ M. *In silico*, gallic acid showed numerous hydrophobic and H-bonds interaction with amino acid residues in the active site pocket of 3CL^{pro}. In another work, the SARS-CoV 3CL^{pro} was the target of amentoflavone [22]. The results of fluorogenic methods showed that amentoflavone inhibits SARS-CoV 3CL^{pro} with an IC₅₀ value of 8.3 μ M. The characterization of the inhibitory mechanism of amentoflavone against SARS-CoV 3CL^{pro} activity was investigated. The results indicate that this compound exhibits non-competitive inhibition characteristics toward 3CL^{pro}. According to this study, an elucidation, performed *in silico*, of the interaction of SARS-CoV 3CL^{pro} with this compound supports the inferences drawn from the enzymatic assay, revealing its important inhibitory effect on SARS-CoV 3CL^{pro}. Thus, these results suggest amentoflavone, such as a natural therapeutic drug against SARS-CoV infection.

2.1.3. Mechanism insights of natural steroids anti-SARS-CoV-2.

The research is also interested in the antiviral activity of steroids such as glycyrrhizic acid derivatives, sitosterol, beta-sitosterol (Figure 3 and Table 1). Among these compounds, the glycyrrhizic acid derivatives demonstrated, *in vitro*, an important anti-SARS-CoV compared to glycyrrhizic acid [31]. The results of this study indicate that seven derivatives inhibited SARS-CoV replication at lower concentrations (EC₅₀ values varied between 5 ± 3 to 139 ± 20 μ M) compared to glycyrrhizic acid (EC₅₀= 365 ± 12 μ M).

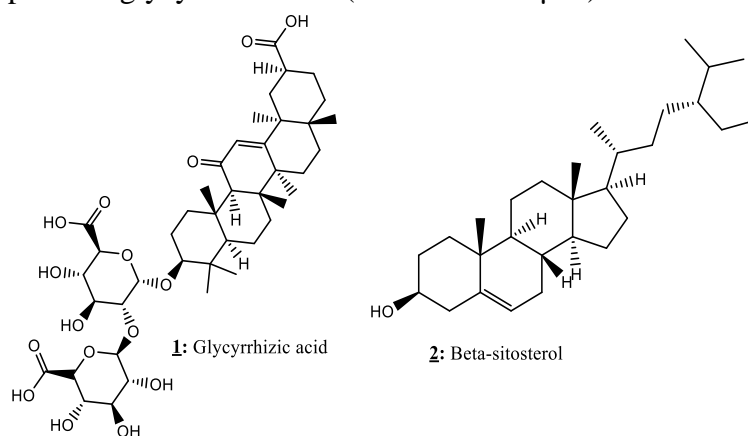


Figure 3. Chemical structures of natural steroids isolated from medicinal plants with anti-SARS-CoV-2 activities (these structures were drawn by ChemDraw).

Indeed, the anti-SARS-CoV activity of the compound resulting from the integration of *N*-acetylglucosamine into the glycoside chain of glycyrrhizic acid is nine times higher compared

to glycyrrhizic acid [31]. This derivative compound inhibited SARS-CoV replication at an EC_{50} of 40 μM . More importantly, the CC_{50} was superior to 3000 μM , and the resulting selectivity index (SI) is >75 ; thus, no CPE was detectable at a 500 μM of this compound, and the immunocytochemical staining indicated that the suppression of viral antigen expression was superior to 99%. Since the coronaviruses are known by their highly glycosylated, particularly in the S proteins which have been shown to be important for viral entry into cells by binding to the ACE2 receptor, the authors suppose that the addition of *N*-acetylglucosamine residues into the carbohydrate part of the basic structure of glycyrrhizic acid plays an important role in its interaction with S proteins, meaning that viral entry might be inhibited by these binding [31].

2.1.4. Mechanism insights of natural tannins anti-SARS-CoV-2.

Several tannins molecules have been tested against SARS-CoV. Such as phloroglucinol, triphloretol A, eckol, dioxinodehydroeckol, 2-phloroeckol, 7-phloroeckol, fucodiphloroethol G, dieckol, phlorofucofuroeckol A, phloroglucinol, eckol, 7-phloroeckol, phlorofucofuroeckol, geraniin, tellimagradin, punicalin, castalin, strictinin, granatin A, pedunculagin, casuarinin, tercatin, and bicornin (Figure 4 and Table 1). In this context, Khalifa *et al.* [26] analyzed, *in silico*, the biological activity of hydrosoluble tannins as natural anti-SARS-CoV-2 through the binding with the main protease of this virus [26].

Among the hydrosoluble tannins tested, pedunculagin, tercatin, and punicalin were found to have a stronger bond and high affinity with the receptor binding site and catalytic dyad (Cys145 and His41) of SARS-CoV-2 main protease, indicating their fruitful inhibition of the SARS-CoV-2 protease enzyme. These results anticipated that tannins might be more useful candidates for COVID-19 drug therapy. In another investigation of the antiviral effect of tannin compounds, Park *et al.* [24] targeted in their research SARS-CoV 3CL^{pro} which plays an important role in viral replication. Indeed, the results of the effect of nine phlorotannins 1-9 on the cell-free SARS-CoV 3CL^{pro} trans-cleavage assay demonstrated that among the products tested, the dieckol displayed a good inhibitory effect against SARS-CoV 3CL^{pro} cell-free cleavage with an IC_{50} value of 2.7 μM . The results of the kinetic mechanism investigation of the compound inhibitor and SARS-CoV 3CL^{pro} interaction indicated that dieckol had competitive inhibition profiles with K_i value of 2.4 μM . In addition, the authors determined the kinetic binding parameters, the association rate constant, and the dissociation rate constant using surface plasmon resonance [24]. Dieckol increased the SPR sensorgram in a significant and dose-dependent manner. The dissociation constant K_D (k_{off}/k_{on}) was calculated by globally fitting the kinetic data at various dieckol concentrations (12.5, 25, and 50 μM) to the Langmuir binding model ($K_D=10.3 \mu M$). The K_D for the dieckol interaction with $k_{on}=73.5 \mu M^{-1} S^{-1}$ and $k_{off}=0.000843 S^{-1}$, which quantitatively revealed a higher association rate than that of the positive control hesperetin ($K_D=24.5 \mu M$). To explain the inhibition mechanism of dieckol as an important potent inhibitor of SARS-CoV 3CL^{pro}, a docking experiment was performed. The results indicated that dieckol bound to the S1 site of SARS-CoV 3CL^{pro} through H-bonds, and formed strong hydrogen bonds to the catalytic dyad (Cys145 and His41) of SARS-CoV 3CL^{pro}. *In silico* experiments, support the results obtained with the enzymatic assay that revealed the important inhibitory action of dieckol on SARS-CoV 3CL^{pro} [24].

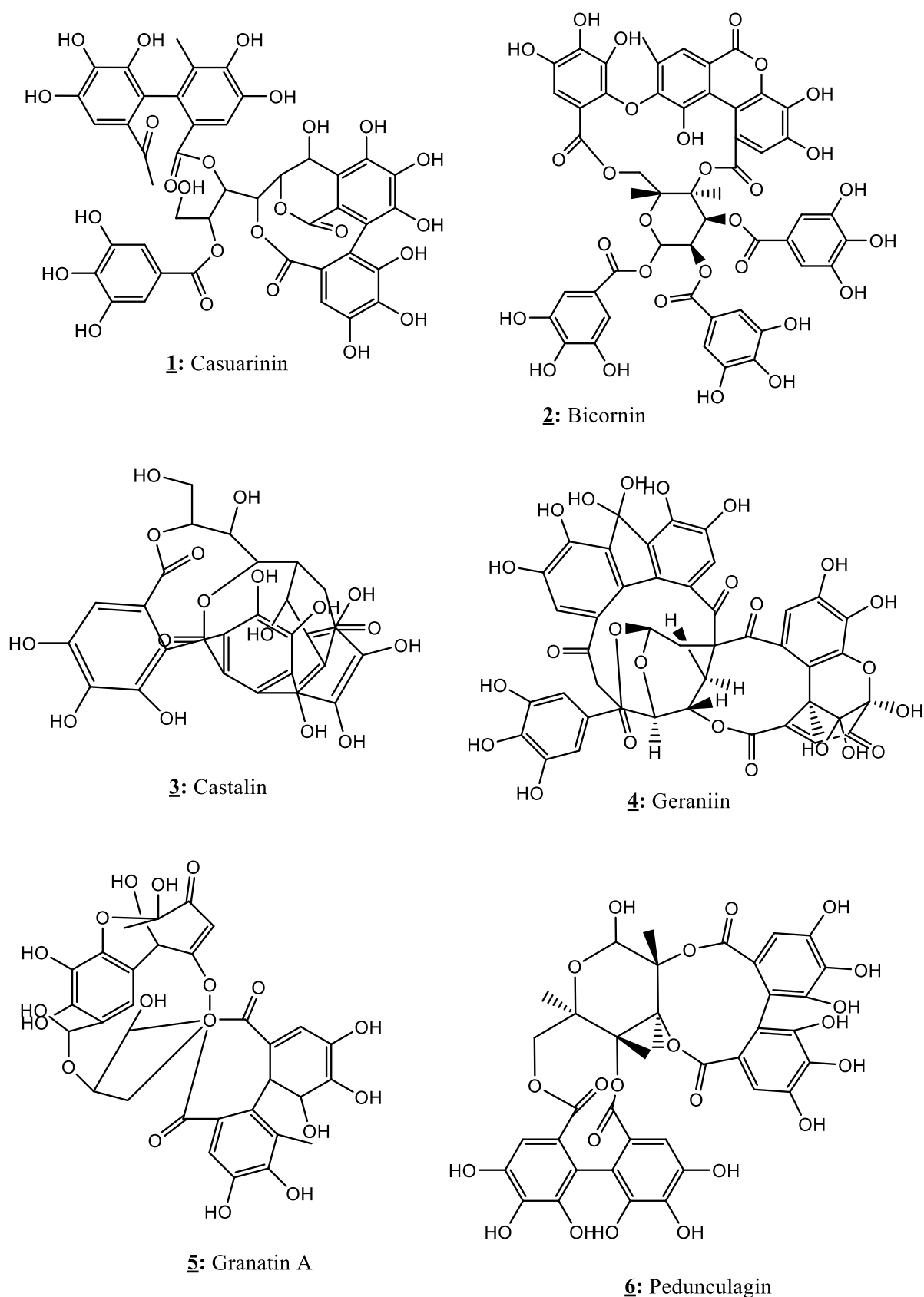


Figure 4. Chemical structures of natural tannins isolated from medicinal plants with anti-SARS-CoV-2 activities (these structures were drawn by ChemDraw).

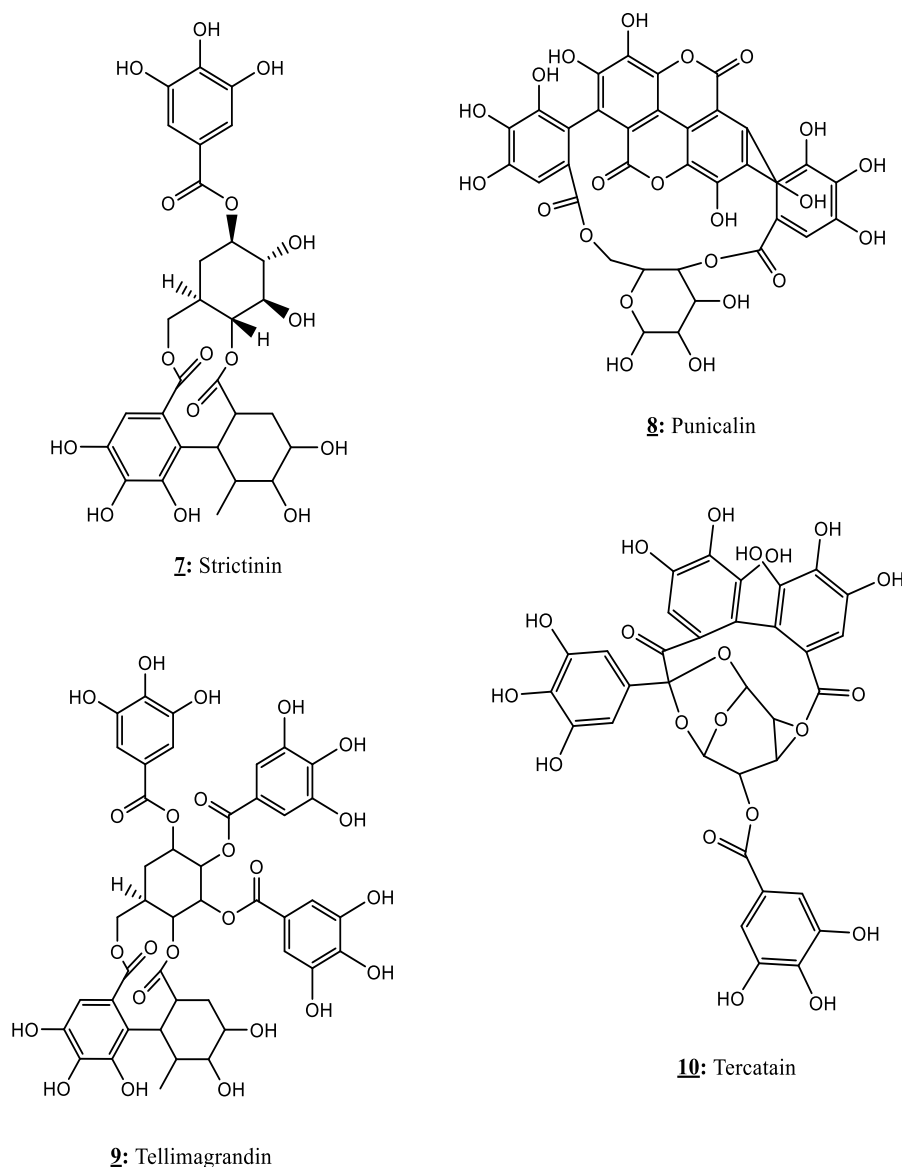


Figure 4. Continued.

2.1.5. Mechanism insights of natural quinone anti-SARS-CoV-2.

The quinone is one of the secondary metabolites studied for their antiviral activity. The hypericin, idarubicin, emodin, promazine, rhein, 1,4-bis-(1-anthraquinonylamino)-anthraquinone, emodin, and aloe-emodin are the most tested quinones (Figure 5 and Table 1). Among them, emodin has been confirmed as an anti-SARS-CoV compound [27]. According to this study, the results of the biotinylated ELISA assay showed that emodin blocked the binding of S protein to ACE2 in a dose-dependent manner with an IC_{50} value of 200 μ M. The inhibitory potential of emodin on the SARS-CoV S protein and Vero E6 cell interaction was also evaluated using IFA. Neither cytotoxic effect, nor cellular morphological change has been observed in emodin-treated cells. Treatment of Vero E6 cells with emodin/biotinylated S protein decreased the cell-associated fluorescence, indicating that this quinone compound is able to block the S protein and Vero E6 cell interaction. Additionally, the inhibitory potential of emodin was evaluated by the S protein-pseudotyped retrovirus infectivity [27]. The results showed that emodin inhibited the S protein-pseudotyped retrovirus infectivity in a dose-dependent manner, and at 50 μ M (without toxic effect) of emodin, the percent of inhibition was

94.12%. The finding of this study suggested that emodin was a novel anti-SARS-CoV compound and might be considered as a potential drug to treat the SARS infection [27].

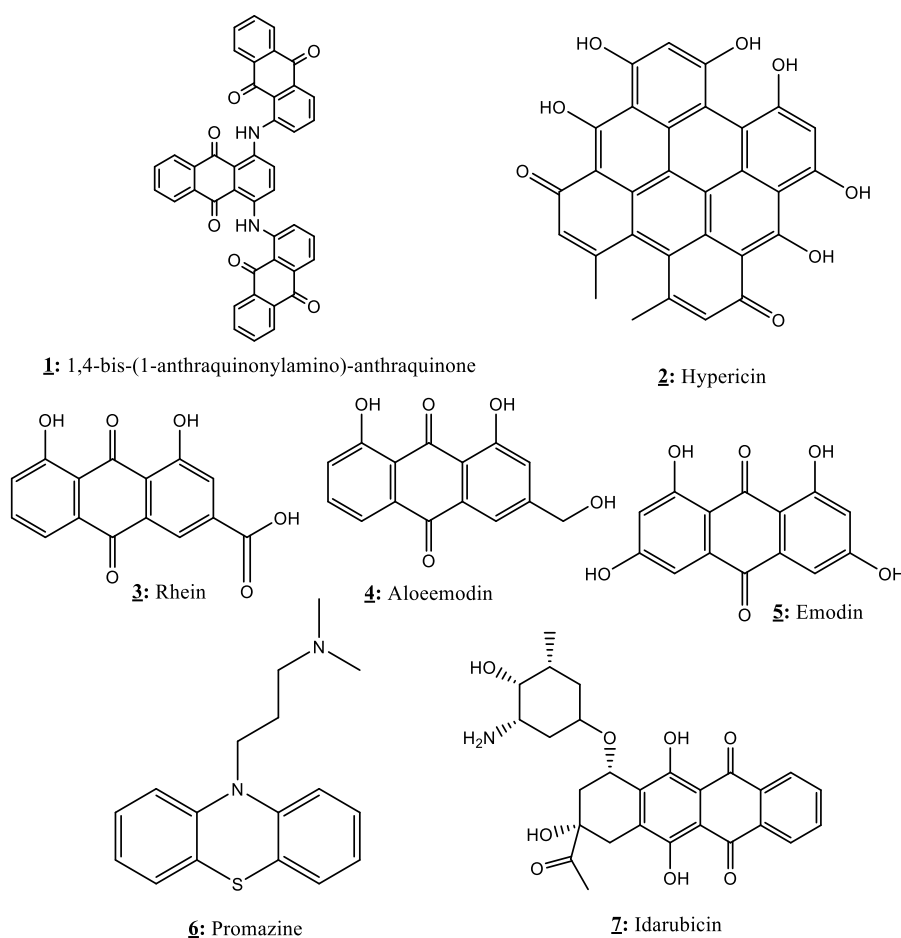


Figure 5. Chemical structures of natural quinones isolated from medicinal plants with anti-SARS-CoV-2 activities (these structures were drawn by ChemDraw).

In another work, Schwarz *et al.* [28] demonstrated that emodin inhibits HCoV-OC 43 release from infected RD cells with similar effectiveness of $K_{1/2} \approx 20 \mu\text{M}$ for inhibition of SNE-3a protein of SARS-CoV and HCoV-OC43. This inhibition of 3a ion channel could contribute to the reduction of virus release from the SARS-CoV-infected host. Therefore, reduced virus release from infected cells may provide the immune system sufficient time to improve the response against the infection [28].

2.1.6. Mechanism insights of natural stilbenes anti-SARS-CoV-2.

Curcumin compound, belonging to the stilbene's groups, has been reported as anti-SARS-CoV (Figure 6 and Table 1). Mohammed and Shaghghi, [11] evaluated the bioinformatics study of SARS-CoV-2 inhibition by a secondary metabolite of medicinal plants. The results showed that curcumin has a stronger bond and high affinity with protease [11].

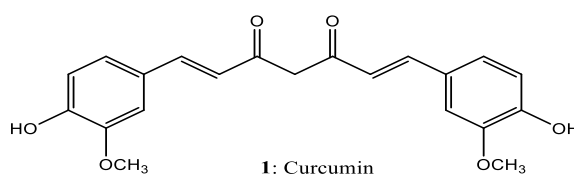


Figure 6. Natural chemical structures of stilbene isolated from medicinal plants with promising anti-SARS-CoV-2 activity (these structures were drawn by ChemDraw).

Finally, due to the high effectiveness function of plant compounds, the authors arrived at the conclusion that the coumarin compound may be considered as an effective anti-protease drug to treat COVID-19. Concerning the products belonging to other compound groups such as terpenoids, coumarin, steroidal alkaloids, allyls, phenylpropanoids, glucosides, lignoids, tanshinones, and alkylated chalcones, a detailed list of their anti-SARS activities is presented in Table 1.

2.2. Synthetic pharmacophores as possible drugs against SARS-CoV-2.

The search for new synthetic molecules as therapeutic drugs requires time for biological screening *in vitro* and *in vivo*. With the COVID-19 pandemic, the screening for therapeutic treatments, particularly targeted therapy using active molecules, could not be carried out routinely. Indeed, many research groups have started urgently to identify synthetic molecules with anti-SARS-CoV-2 properties (Table 2).

Table 2. Synthetic compounds with possible anti-SARS-CoV-2 effects.

Synthetic drugs	Experimental system (model cell line, <i>in silico</i> , <i>in vivo</i>)	Keys findings/mechanism insights	Authors
9a	Structure-guided design	IC ₅₀ =0.6μM Inhibition of MERS coronavirus 3CL protease.	[36]
10a	Structure-guided design	IC ₅₀ =0.4 μM Inhibition of MERS coronavirus 3CL protease.	[36]
9b	Structure-guided design	IC ₅₀ =0.7 μM Inhibition of MERS coronavirus 3CL protease.	[36]
10b	Structure-guided design	IC ₅₀ =0.6 μM Inhibition of MERS coronavirus 3CL protease.	[36]
9c	Structure-guided design	IC ₅₀ =0.8 μM Inhibition of MERS coronavirus 3CL protease.	[36]
10c	Structure-guided design	IC ₅₀ =0.7 μM Inhibition of MERS coronavirus 3CL protease.	[36]
9d	Structure-guided design	IC ₅₀ =0.7 μM Inhibition of MERS coronavirus 3CL protease.	[36]
10d	Structure-guided design.	IC ₅₀ =0.9 μM Inhibition of MERS coronavirus 3CL protease.	[36]
9e	Structure-guided design	IC ₅₀ =6.1 μM Inhibition of MERS coronavirus 3CL protease.	[36]
10e	Structure-guided design	IC ₅₀ =7.5 μM Inhibition of MERS coronavirus 3CL protease.	[36]
9f	Structure-guided design	IC ₅₀ =0.6 μM Inhibition of MERS coronavirus 3CL protease.	[36]
10f	Structure-guided design	IC ₅₀ =0.5 μM Inhibition of MERS coronavirus 3CL protease.	[36]
10a	Structure-guided design	EC ₅₀ =0.5 μM Inhibition of MERS coronavirus 3CL protease.	[36]
10c	Structure-guided design	EC ₅₀ =0.8 μM Inhibition of MERS coronavirus 3CL protease.	[36]
SP-4 (residues 192–203)	Expression and purification of recombinant SARS-CoV S protein Biotinylated enzyme-linked immunosorbent assay (ELISA)	Significantly blocked the interaction between S protein and ACE2. IC ₅₀ =4.30±2.18 nmol.	[37]
SP-8 (residues 483–494)	Expression and purification of recombinant SARS-CoV S protein Biotinylated enzyme-linked immunosorbent assay (ELISA)	Significantly blocked the interaction between S protein and ACE2. IC ₅₀ =6.99±0.71 nmol.	[37]
SP-10 (residues 668–679)	Expression and purification of	Significantly blocked the interaction between S protein and ACE2.	[37]

Synthetic drugs	Experimental system (model cell line, <i>in silico</i> , <i>in vivo</i>)	Keys findings/mechanism insights	Authors
	recombinant SARS-CoV S protein Biotinylated enzyme-linked immunosorbent assay (ELISA)	Blocked both binding of the S protein and infectivity of S protein-pseudotyped retrovirus to Vero E6 cells. IC ₅₀ =1.88±0.52 nmol.	
Compound 1	Computation tool Autodock 3.0.5	Inhibitory activity against recombinant 3C-like protease. IC ₅₀ =58.35±1.41µM.	[38]
Compound 2	Computation tool Autodock 3.0.5	Inhibitory activity against recombinant 3C-like protease. IC ₅₀ =62.79±3.19 µM.	[38]
Compound 3	Computation tool Autodock 3.0.5	Inhibitory activity against recombinant 3C-like protease. IC ₅₀ =101.38±3.27µM.	[38]
Compound 4	Computation tool Autodock 3.0.5.	Inhibitory activity against recombinant 3C-like protease. IC ₅₀ =77.09±1.94µM.	[38]
Compound 5	Computation tool Autodock 3.0.5	Inhibitory activity against recombinant 3C-like protease. IC ₅₀ =90.72±5.54µM.	[38]
Compound 6	Computation tool Autodock 3.0.5	IC ₅₀ =38.57±2.41µM. Competitive inhibition of 3C-like protease (K _i =9.11±1.61µM).	[38]
Compound 7	Computation tool Autodock 3.0.5	IC ₅₀ =41.39±1.17µM. Competitive inhibition of 3C-like protease (K _i =9.93±0.44µM).	[38]
cmp3	SARS-CoV-2 M ^{pro} Molecular docking study	Exhibited favorable electrostatic energy (ΔGelec=-21.38 kcal/mol)	[39]
cmp12	SARS-CoV-2 M ^{pro} Molecular docking study	Total binding free energy (ΔGtol) = -45.22 kcal/mol) ligand RMSD values after 20ns=0.91 Å Exhibited favorable electrostatic energy (ΔGelec=-26.16 kcal/mol)	[39]
cmp14	SARS-CoV-2 M ^{pro} Molecular docking study	Total binding free energy (ΔGtol) = -44.91kcal/mol Ligand RMSD values after 20ns=1.18Å Exhibited favorable electrostatic energy (ΔGelec=-33.56 kcal/mol)	[39]
cmp17	SARS-CoV-2 M ^{pro} Molecular docking study	Total binding free energies (ΔGtol) = -41.72kcal/mol Ligand RMSD values after 20ns=0.84 Å Exhibited favorable electrostatic energy (ΔGelec=-36.65 kcal/mol)	[39]
cmp18	SARS-CoV-2 M ^{pro} Molecular docking study	Total binding free energies (ΔGtol) = -44.55kcal/mol Ligand RMSD values after 20ns=1.03 Å Exhibited favorable electrostatic energy (ΔGelec=-5.39 kcal/mol)	[39]
cmp2	SARS-CoV-2 Nsp12 RdRp Molecular docking study	Exhibited favorable electrostatic energy (ΔGtol=-41.74 kcal/mol) Formed three H-bonds with motif C (Ser759), motifD (Lys798) and motif E (Ser814)	[39]
cmp17a	SARS-CoV-2 Nsp12 RdRp Molecular docking study	Exhibited favorable electrostatic energy (ΔGtol=-34.37kcal/mol) Formed five H-bonds with Arg624 (motif A),Thr680 and Ser682 (motif B), Ser756 (motif C) and Lys798 (motif D)	[39]
cmp21	SARS-CoV-2 Nsp12 RdRp Molecular docking study	Exhibited favorable electrostatic energy (ΔGtol=-24.9 kcal/mol) Formed four H-bonds with motif A (Asp623), motif F (Arg553 and Arg555), and motif C (Ser759)	[39]
cmp1	SARS-CoV-2 Nsp13 helicase Molecular docking study	Estimated favourableΔGtol(-37.29kcal/mol),	[39]
cmp3a	SARS-CoV-2 Nsp13 helicase Molecular docking study	Estimated favorable ΔGtol (-40.08 kcal/mol)	[39]
cmp11	SARS-CoV-2 Nsp13 helicase Molecular docking study	Estimated favorable ΔGtol (-49.73 kcal/mol)	[39]

Synthetic drugs	Experimental system (model cell line, <i>in silico</i> , <i>in vivo</i>)	Keys findings/mechanism insights	Authors
cmp15	SARS-CoV-2 Nsp13 helicase Molecular docking study	Estimated favorable ΔG_{tol} (-30.56kcal/mol)	[39]
A novel series of fused 1,2,3-triazoles derivatives	HEL cells <i>In silico</i> studies.	Inhibition of 3CL protease. Promising antiviral properties for compounds 14d, 14n, 14q, 18f, and 18i against human coronavirus 229E.	[40]
1	Molecular docking study	Inhibitory activity against SARS-CoV 3CL ^{pro} .	[41]
2	Molecular docking study	IC ₅₀ =10 μ M. Inhibitory activity against SARS-CoV 3CL ^{pro} .	[41]
3	Molecular docking study	IC ₅₀ =0.60 μ M. Inhibitory activity against SARS-CoV 3CL ^{pro} .	[41]
4	Molecular docking study	IC ₅₀ =9.1 μ M. K _i =0.66 μ M. Inhibitory activity against SARS-CoV 3CL ^{pro} .	[41]
5	Molecular docking study	K _{inact} /K _i =1900 M ⁻¹ s ⁻¹ . Inhibitory activity against SARS-CoV 3CL ^{pro} .	[41]
6	Molecular docking study	IC ₅₀ =0.065 μ M. Inhibitory activity against SARS-CoV 3CL ^{pro} .	[41]
7	Molecular docking study	K _i =2.2 μ M. Inhibitory activity against SARS-CoV 3CL ^{pro} .	[41]
8	Molecular docking study	IC ₅₀ =1.7 μ M. K _i =0.0041 μ M. Inhibitory activity against SARS-CoV 3CL ^{pro} .	[41]
9	Molecular docking study	K _i =0.0031 μ M. Inhibitory activity against SARS-CoV 3CL ^{pro} .	[41]
10	Molecular docking study	K _i =3.2 μ M. Inhibitory activity against SARS-CoV 3CL ^{pro} .	[41]
11	Molecular docking study	IC ₅₀ =323 μ M. Inhibitory activity against SARS-CoV 3CL ^{pro} .	[41]
12	Molecular docking study	K _i =0.065 μ M. Inhibitory activity against SARS-CoV 3CL ^{pro} .	[41]
13	Molecular docking study	IC ₅₀ =0.37 μ M. Inhibitory activity against SARS-CoV 3CL ^{pro} .	[41]
14	Molecular docking study	K _i =0.0075 μ M. Inhibitory activity against SARS-CoV 3CL ^{pro} .	[41]
15	Molecular docking study	IC ₅₀ =6.1 μ M. Inhibitory activity against SARS-CoV 3CL ^{pro} .	[41]
16	Molecular docking study	IC ₅₀ =6.8 μ M. Inhibitory activity against SARS-CoV 3CL ^{pro} .	[41]
17	Molecular docking study	IC ₅₀ =17.2 μ M. Inhibitory activity against SARS-CoV 3CL ^{pro} .	[41]
25a	Molecular docking study	K _i =5.90 μ M. Inhibitory activity against SARS-CoV 3CL ^{pro} .	[41]
25b	Molecular docking study	K _i =23.0 μ M. Inhibitory activity against SARS-CoV 3CL ^{pro} .	[41]
25c	Molecular docking study	K _i =0.46 μ M. IC ₅₀ =21.0 μ M. Inhibitory activity against SARS-CoV 3CL ^{pro} .	[41]
25d	Molecular docking study	K _i =1.60 μ M. Inhibitory activity against SARS-CoV 3CL ^{pro} .	[41]
25e	Molecular docking study	K _i =1.71 μ M. Inhibitory activity against SARS-CoV 3CL ^{pro} .	[41]
25f	Molecular docking study	K _i =29.0 μ M. Inhibitory activity against SARS-CoV 3CL ^{pro} .	[41]
25g	Molecular docking study	K _i =9.40 μ M. Inhibitory activity against SARS-CoV 3CL ^{pro} .	[41]
25h	Molecular docking study	K _i =1.20 μ M. Inhibitory activity against SARS-CoV 3CL ^{pro} .	[41]
26a	Molecular docking study	K _i =3.20 μ M. Inhibitory activity against SARS-CoV 3CL ^{pro} .	[41]
26b	Molecular docking study	K _i =0.42 μ M. IC ₅₀ =43.0 μ M. Inhibitory activity against SARS-CoV 3CL ^{pro} .	[41]

Synthetic drugs	Experimental system (model cell line, <i>in silico</i> , <i>in vivo</i>)	Keys findings/mechanism insights	Authors
26c	Molecular docking study	$K_i=0.61\mu\text{M}$. Inhibitory activity against SARS-CoV 3CL ^{pro} .	[41]
26d	Molecular docking study	$K_i=7.4\mu\text{M}$. Inhibitory activity against SARS-CoV 3CL ^{pro} .	[41]
26e	Molecular docking study	$K_i=0.69\mu\text{M}$. Inhibitory activity against SARS-CoV 3CL ^{pro} .	[41]
26f	Molecular docking study	$K_i=0.70\mu\text{M}$. Inhibitory activity against SARS-CoV 3CL ^{pro} .	[41]
26g	Molecular docking study	$K_i=1.30\mu\text{M}$. Inhibitory activity against SARS-CoV 3CL ^{pro} .	[41]
26h	Molecular docking study	$K_i=0.56\mu\text{M}$. $\text{IC}_{50}=24.0\mu\text{M}$. Inhibitory activity against SARS-CoV 3CL ^{pro} .	[41]
26i	Molecular docking study	$K_i=1.56\mu\text{M}$. Inhibitory activity against SARS-CoV 3CL ^{pro} .	[41]
26j	Molecular docking study	$K_i=8.4\mu\text{M}$. Inhibitory activity against SARS-CoV 3CL ^{pro} .	[41]
26k	Molecular docking study	$K_i=0.84\mu\text{M}$. Inhibitory activity against SARS-CoV 3CL ^{pro} .	[41]
26l	Molecular docking study	$K_i=3.20\mu\text{M}$. Inhibitory activity against SARS-CoV 3CL ^{pro} .	[41]
26m	Molecular docking study	$K_i=0.39\mu\text{M}$. $\text{IC}_{50}=10.0\mu\text{M}$. Good inhibitory activity against 3CL ^{pro} .	[41]
26n	Molecular docking study	$K_i=0.33\mu\text{M}$. $\text{IC}_{50}=14.0\mu\text{M}$. Good inhibitory activity against 3CL ^{pro} .	[41]
27a	Molecular docking study	$K_i=0.66\mu\text{M}$. Inhibitory activity against SARS-CoV 3CL ^{pro} .	[41]
27b	Molecular docking study	$K_i=37.0\mu\text{M}$. Inhibitory activity against SARS-CoV 3CL ^{pro} .	[41]
27c	Molecular docking study	$K_i=52.0\mu\text{M}$. Inhibitory activity against SARS-CoV 3CL ^{pro} .	[41]
27d	Molecular docking study	$K_i=2.50\mu\text{M}$. Inhibitory activity against SARS-CoV 3CL ^{pro} .	[41]
1	Molecular docking study	$\text{IC}_{50}=0.5\mu\text{M}$. Inhibitory activity against SARS-CoV 3CL ^{pro} .	[42]
2	Molecular docking study	$\text{IC}_{50}=5\mu\text{M}$. Inhibitory activity against SARS-CoV 3CL ^{pro} .	[42]
3	Molecular docking study	$\text{IC}_{50}=11.1\mu\text{M}$. Inhibitory activity against SARS-CoV 3CL ^{pro} .	[42]
4	Molecular docking study	$\text{IC}_{50}=30\text{nM}$. Inhibitory activity against SARS-CoV 3CL ^{pro} .	[42]
5	Molecular docking study	$\text{IC}_{50}=13\mu\text{M}$. Inhibitory activity against SARS-CoV 3CL ^{pro} .	[42]
6	Molecular docking study	$\text{IC}_{50}=1.5\mu\text{M}$. Inhibitory activity against SARS-CoV 3CL ^{pro} .	[42]
7	Molecular docking study	$\text{IC}_{50}=6.2\mu\text{M}$. Inhibitory activity against SARS-CoV 3CL ^{pro} .	[42]
9a	Molecular docking study	Inactive.	[42]
9b	Molecular docking study	Inactive.	[42]
9c	Molecular docking study	Inactive.	[42]
10a	Molecular docking study	Inactive.	[42]
10b	Molecular docking study	Inactive.	[42]
10c	Molecular docking study	$\text{IC}_{50}=11\mu\text{M}$. Inhibitory activity against SARS-CoV 3CL ^{pro} .	[42]
12	Molecular docking study	$\text{IC}_{50}>20\mu\text{M}$.	[42]
13a	Molecular docking study	$\text{IC}_{50}=7.72\mu\text{M}$. Inhibitory activity against SARS-CoV 3CL ^{pro} .	[42]
13b	Molecular docking study	$\text{IC}_{50}=25.3\mu\text{M}$. Inhibitory activity against SARS-CoV 3CL ^{pro} .	[42]
13c	Molecular docking study	$\text{IC}_{50}=6.9\mu\text{M}$. Inhibitory activity against SARS-CoV 3CL ^{pro} .	[42]

Synthetic drugs	Experimental system (model cell line, <i>in silico</i> , <i>in vivo</i>)	Keys findings/mechanism insights	Authors
13d	Molecular docking study	IC ₅₀ =4.1 μM. Inhibitory activity against SARS-CoV 3CL ^{pro} .	[42]
13e	Molecular docking study	IC ₅₀ =22.5 μM. Inhibitory activity against SARS-CoV 3CL ^{pro} .	[42]
13f	Molecular docking study	IC ₅₀ =9.1 μM. Inhibitory activity against SARS-CoV 3CL ^{pro} .	[42]
13g	Molecular docking study	IC ₅₀ =3.8 μM. Inhibitory activity against SARS-CoV 3CL ^{pro} .	[42]
13h	Molecular docking study	IC ₅₀ =100 μM. Inhibitory activity against SARS-CoV 3CL ^{pro} .	[42]
13i	Molecular docking study	Inactive.	[42]
13j	Molecular docking study	IC ₅₀ =100 μM. Inhibitory activity against SARS-CoV 3CL ^{pro} .	[42]
13k	Molecular docking study	IC ₅₀ =26 μM. Inhibitory activity against SARS-CoV 3CL ^{pro} .	[42]
13l	Molecular docking study	Inactive.	[42]
16a	Molecular docking study	IC ₅₀ =2.9 μM. Inhibitory activity against SARS-CoV 3CL ^{pro} .	[42]
16b	Molecular docking study	IC ₅₀ =3.6 μM. Inhibitory activity against SARS-CoV 3CL ^{pro} .	[42]
16c	Molecular docking study	IC ₅₀ =13.3 μM. Inhibitory activity against SARS-CoV 3CL ^{pro} .	[42]
16d	Molecular docking study	IC ₅₀ =3.4 μM. Inhibitory activity against SARS-CoV 3CL ^{pro} .	[42]
16e	Molecular docking study	IC ₅₀ =4.1 μM. Inhibitory activity against SARS-CoV 3CL ^{pro} .	[42]
16f	Molecular docking study	IC ₅₀ =8.1 μM. Inhibitory activity against SARS-CoV 3CL ^{pro} .	[42]
16g	Molecular docking study	IC ₅₀ =22.1 μM. Inhibitory activity against SARS-CoV 3CL ^{pro} .	[42]
16h	Molecular docking study	IC ₅₀ =100 μM. Inhibitory activity against SARS-CoV 3CL ^{pro} .	[42]
16i	Molecular docking study	IC ₅₀ =10.3 μM. Inhibitory activity against SARS-CoV 3CL ^{pro} .	[42]
16j	Molecular docking study	IC ₅₀ =2.1 μM. Inhibitory activity against SARS-CoV 3CL ^{pro} .	[42]
16k	Molecular docking study	IC ₅₀ =1.5 μM. Inhibitory activity against SARS-CoV 3CL ^{pro} .	[42]
17a	Molecular docking study	IC ₅₀ =0.051 μM. Inhibitory activity against SARS-CoV 3CL ^{pro} .	[42]
17b	Molecular docking study	IC ₅₀ =0.97 μM. Inhibitory activity against SARS-CoV 3CL ^{pro} .	[42]
17c	Molecular docking study	IC ₅₀ =0.70 μM. Inhibitory activity against SARS-CoV 3CL ^{pro} .	[42]
17d	Molecular docking study	IC ₅₀ =2.0 μM. Inhibitory activity against SARS-CoV 3CL ^{pro} .	[42]
17e	Molecular docking study	IC ₅₀ =12.5 μM. Inhibitory activity against SARS-CoV 3CL ^{pro} .	[42]
1	Normal human fibroblast cells (HS27) <i>In silico</i> studies	Activity against HCV (EC ₅₀ =0.8 μM). Activity against SCV (IC ₅₀ >50 μM for ATPase activity, IC ₅₀ =11 μM for helicase activity).	[43]
3	Normal human fibroblast cells (HS27) <i>In silico</i> studies	Activity against HCV (EC ₅₀ =5 μM). Activity against SCV (IC ₅₀ >50 μM for ATPase activity, IC ₅₀ >50 μM for helicase activity).	[43]
4	Normal human fibroblast cells (HS27) <i>In silico</i> studies	Activity against HCV (EC ₅₀ =3 μM). Activity against SCV (IC ₅₀ >50 μM for ATPase activity, IC ₅₀ >50 μM for helicase activity).	[43]
1a	Vero 76 cells	Reduced cytopathic effect induced by human SARS CoV. EC ₅₀ =0.018 μM.	[44]
1c	Vero 76 cells	Reduced cytopathic effect induced by human SARS CoV. EC ₅₀ <0.005 μM.	[44]
1e	Vero 76 cells	Reduced cytopathic effect induced by human SARS CoV.	[44]

Synthetic drugs	Experimental system (model cell line, <i>in silico</i> , <i>in vivo</i>)	Keys findings/mechanism insights	Authors
		EC ₅₀ <0.005 μM.	
4a	Vero 76 cells	Reduced cytopathic effect induced by human SARS CoV. EC ₅₀ =0.34 μM.	[44]
4b	Vero 76 cells	Reduced cytopathic effect induced by human SARS CoV. EC ₅₀ =0.039 μM.	[44]

Researchers have greatly exploited the behavior of other coronaviruses (SARS-CoV and MERS) to be able to mimic the molecular action on pharmacodynamic targets, which are certainly similar. Indeed, as being the result of Darwinian adaptive mutations, SARS-CoV-2 uses the same molecular scenario in its parasitic behavior, which made it possible to test some molecules against the targets of other coronaviruses, which will certainly have pharmacodynamic actions and possibly therapeutic effects on SARS-CoV-2. In our research approach, a bibliometric study was carried out using the various databases in order to identify, index, and organize the studies that have been recently carried out on molecules that specifically attack SARS-CoV-2 or the molecular targets of other coronaviruses. Table 2 presents the research work on the properties of synthetic molecules that we have schematized by ChemDraw.

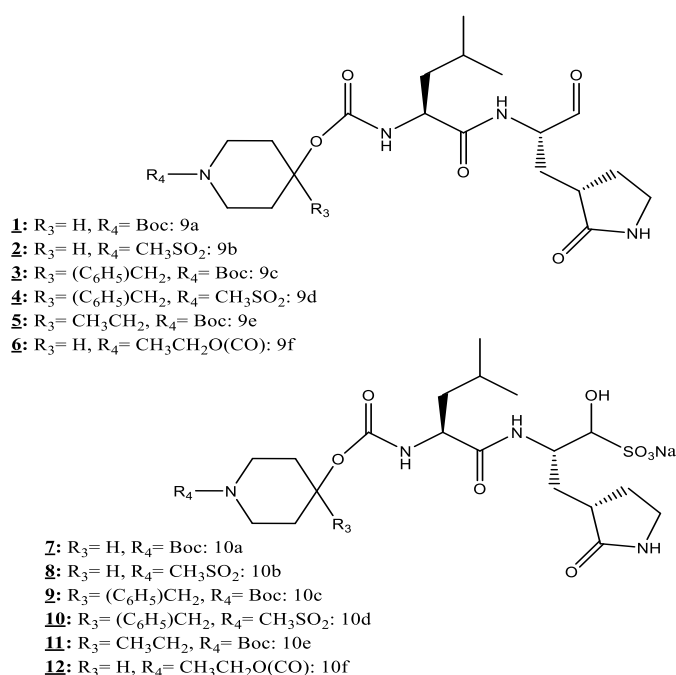


Figure 7. Structures of guided design inhibitor of SARS-CoV-2 (this structure was drawn by ChemDraw).

The CL3 protease protein is a molecule expressed by the virus to proteolyze non-functional viral proteins into functional function units. The inhibition of this protease is an important pharmacological target for blocking the assembly of the virus after its impossible and/or difficult replication. In this way, several studies have already confirmed the inhibitory action of certain synthetic molecules against CL3p (Table 2). Using an *in-silico* model, Galasiti Kankanamalage *et al.* [36] tested the action of fourteen synthetic molecules (Figure 7) on the 3CL protease of MERS coronavirus. The molecule 10a has been shown to be the most active in inhibiting this protein with an inhibition value of IC₅₀=0.6 μM. The two molecules 10f and

10a also revealed a strong inhibition ($IC_{50}=0.5 \mu M$), followed by 9f, 10b and 9a ($IC_{50}=0.6 \mu M$), then by 9b, 10c and 9d ($IC_{50}=0.5 \mu M$) [36].

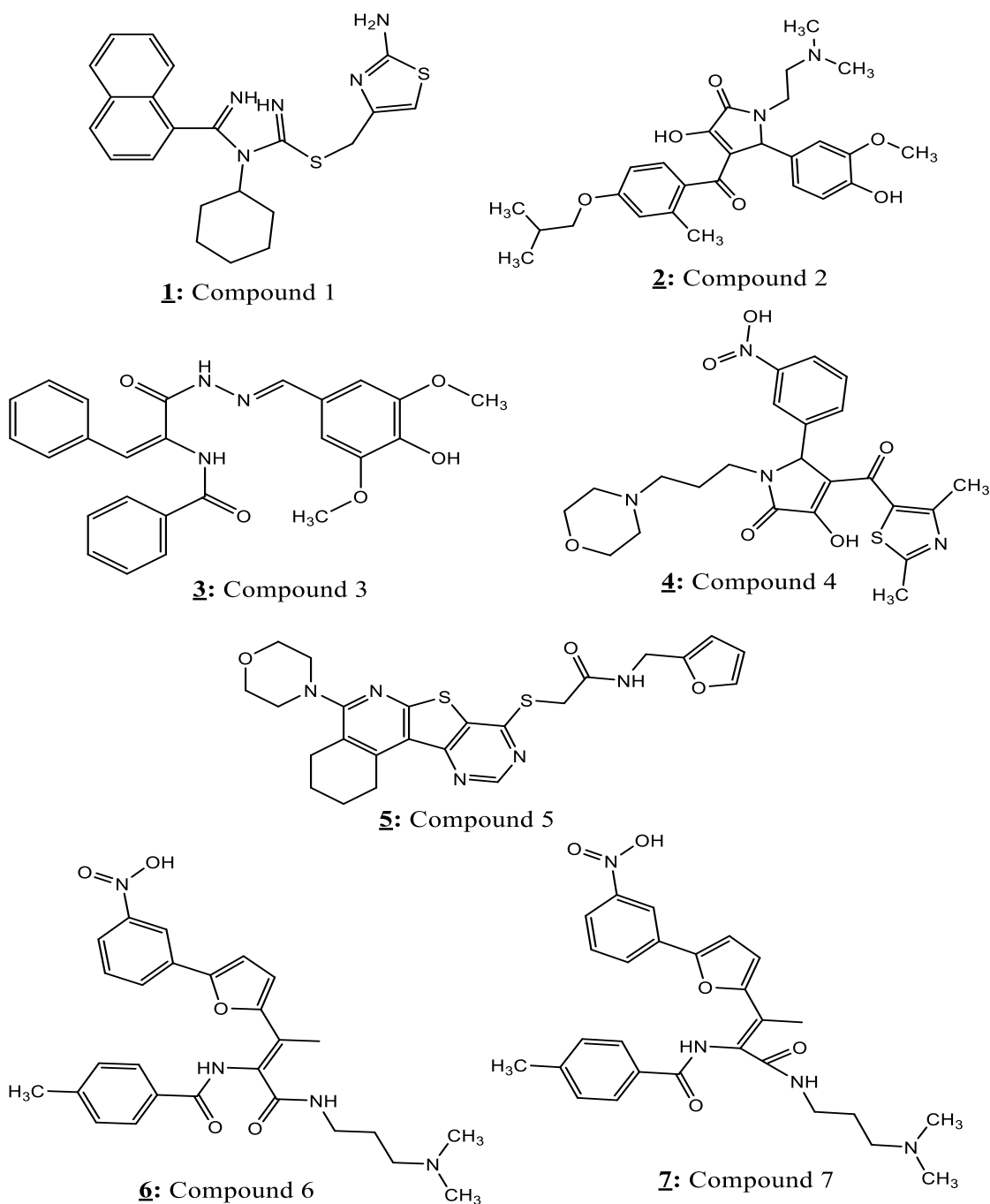


Figure 8. Chemical structure of the novel 3CL^{pro} inhibitors studied (these structures were drawn by ChemDraw).

In another work, the inhibitory action of seven synthetic molecules (Figure 8) was tested against CL3p [38]. Molecule 6 showed very strong inhibition with a low concentration ($IC_{50}=38.57\pm2.41 \mu M$) followed by molecule 7 ($IC_{50}=41.39\pm1.17 \mu M$).

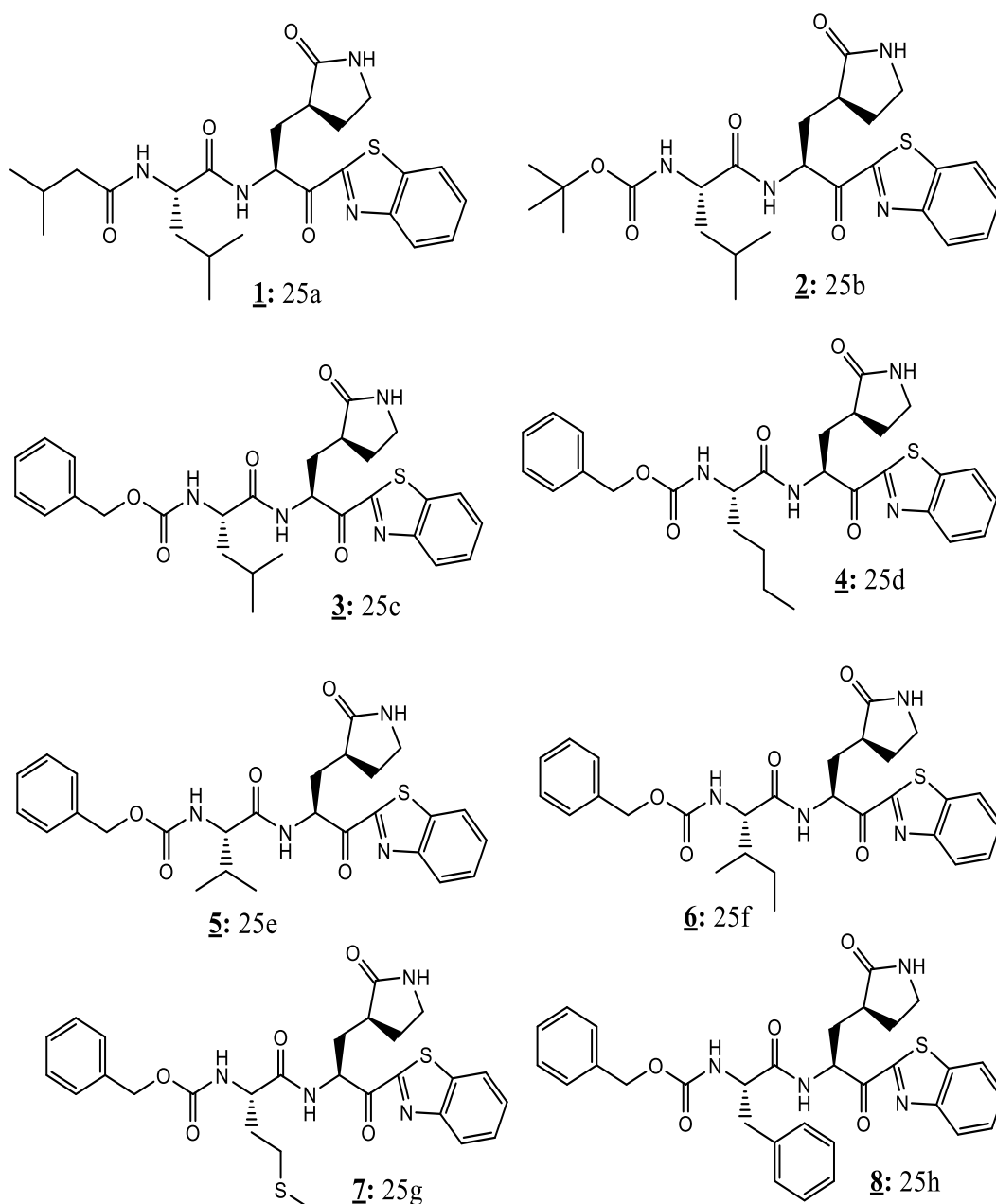


Figure 9. Structure of synthetic dipeptide-type SARS-CoV 3CL protease inhibitors (these structures were drawn by ChemDraw).

The authors have shown that the inhibitory action of these two molecules is a competitive action. However, molecules 1, 2, and 4 showed moderate inhibitory effects against CL3p with inhibitory concentrations of $IC_{50}=58.35\pm1.41$, $IC_{50}=62.79\pm3.19$, and $IC_{50}=77.09\pm1.94$ μ M, respectively. Other molecules showed the lowest inhibitory effects. A previous study highlighted the anti-SARS-CoV effects of 26 synthetic molecules (Figure 8) by studying, *in silico*, their interactions with the CL3 protease [41]. These molecules have shown a different inhibitory action to each other and give hope for their use as therapeutic drugs against COVID-19. Indeed, the results of this study allowed the identification of certain molecules with an important inhibitory action against CL3p.

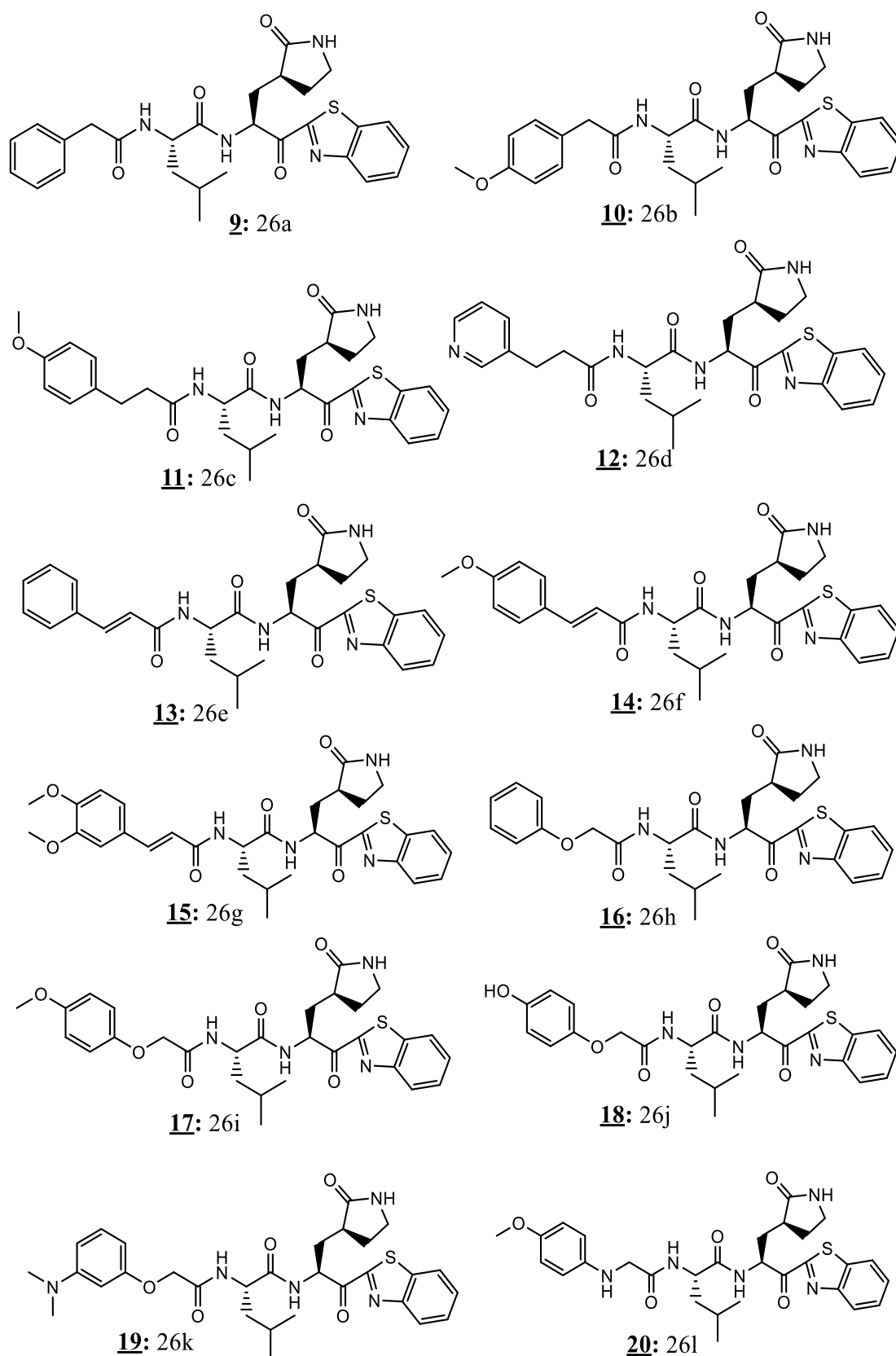


Figure 9. Continued.

The 25c molecule inhibited the CL3 protease at a low concentration ($IC_{50}=21.0 \mu M$) and a high degree of affinity ($K_i=0.46 \mu M$). The 26m molecule also showed significant inhibition ($IC_{50}=10.0 \mu M$) with a degree of a strong bond with CL3p ($K_i=0.39 \mu M$) [41].

In addition, the molecule 26n showed similar significant effects ($K_i=0.33 \mu M$ and $IC_{50}=14.0 \mu M$). The other molecules (Figure 9) also showed inhibitory effects against CL3p

but in a moderate way. These molecules deserve further investigations that could allow for highlighting anti-CL3p drugs for COVID-19 treatment [41].

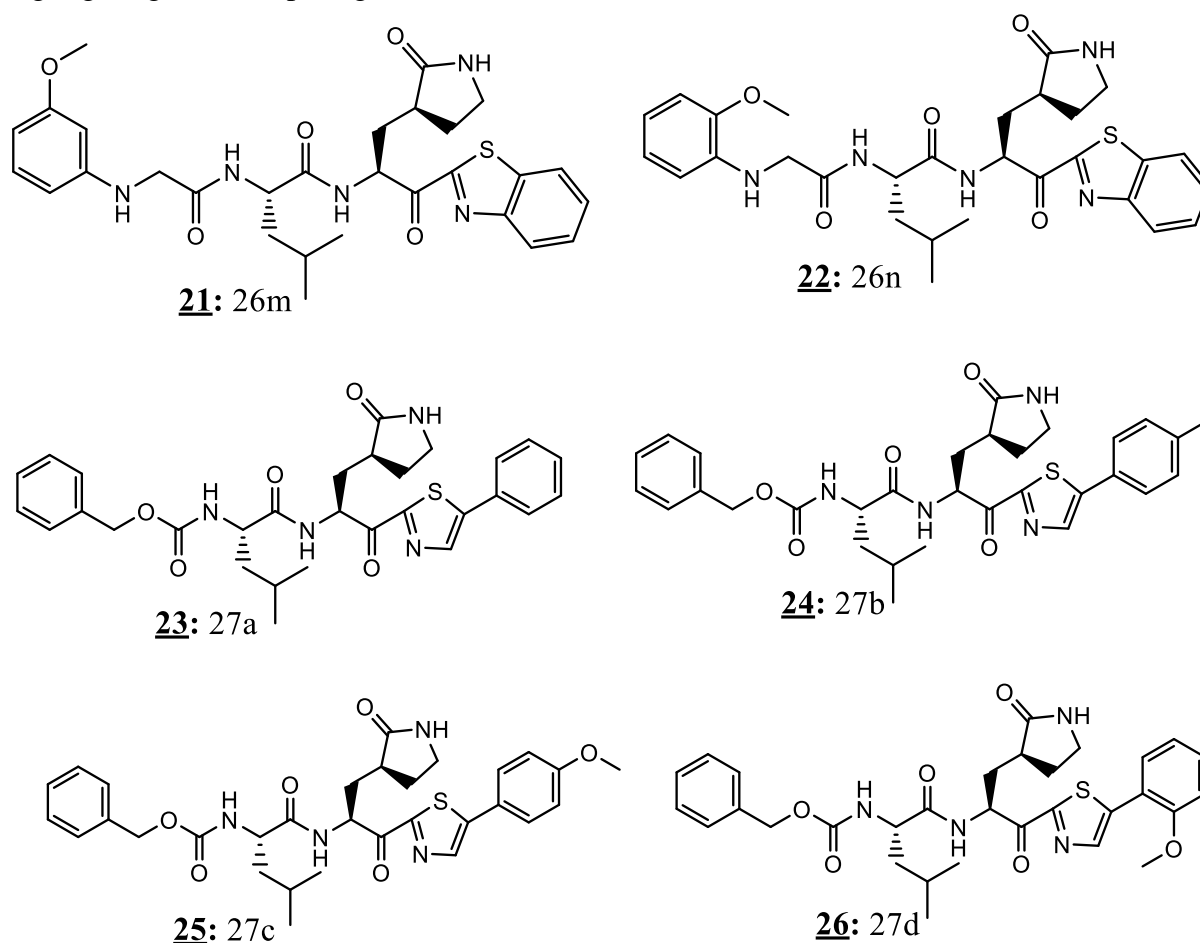


Figure 9. Continued.

Mirza and Froeyen, [39] have tested, *in silico*, the effect of 12 compounds (Figure 10) on SARS-CoV-2 protein targets Nsp12 RNA-dependent-RNA-polymerase, Nsp13 helicase, and M^{pro} protease (Table 2). All molecules presented important interactions with M protease. Indeed, the molecule cmp3, cmp12, cmp14, cmp17, and cmp18 (Figure 10) interacted positively to M^{pro} with electrostatic energy of $\Delta\text{Gelec} = -21.38$ kcal/mol, $\Delta\text{Gelec} = -26.16$ kcal/mol, $\Delta\text{Gelec} = -33.56$ kcal/mol, $\Delta\text{Gelec} = -36.65$ kcal/mol, and $\Delta\text{Gelec} = -5.39$ kcal/mol, respectively [39]. Non-structural proteins (nsps) such as RNA-dependent RNA polymerase (nsp 12) is essential for SARS-CoV-2 genome replication. Some synthetic molecules such as cmp2, cmp17a, and cmp21 (Figure 9) showed their capacity to block this target [39]. The molecule cmp2 showed important inhibition of Nsp12 RdRp by electrostatic energy ($\Delta\text{Gtol} = -41.74$ kcal/mol). Molecular interactions showed that this compound forms three H-bonds with motif C (Ser759), motifD (Lys798), and motif E (Ser814)[39]. However, cmp17a, also acted as electrostatic energy ($\Delta\text{Gtol} = -34.37$ kcal/mol), interacted with five H-bonds with Arg624 (motif A), Thr680 and Ser682 (motif B), Ser756 (motif C) and Lys798 (motif D). Moreover, such bounds (A (Asp623), motif F (Arg553 and Arg555), and motif C (Ser759)) were established between cmp21Nsp12 RdRp [39].

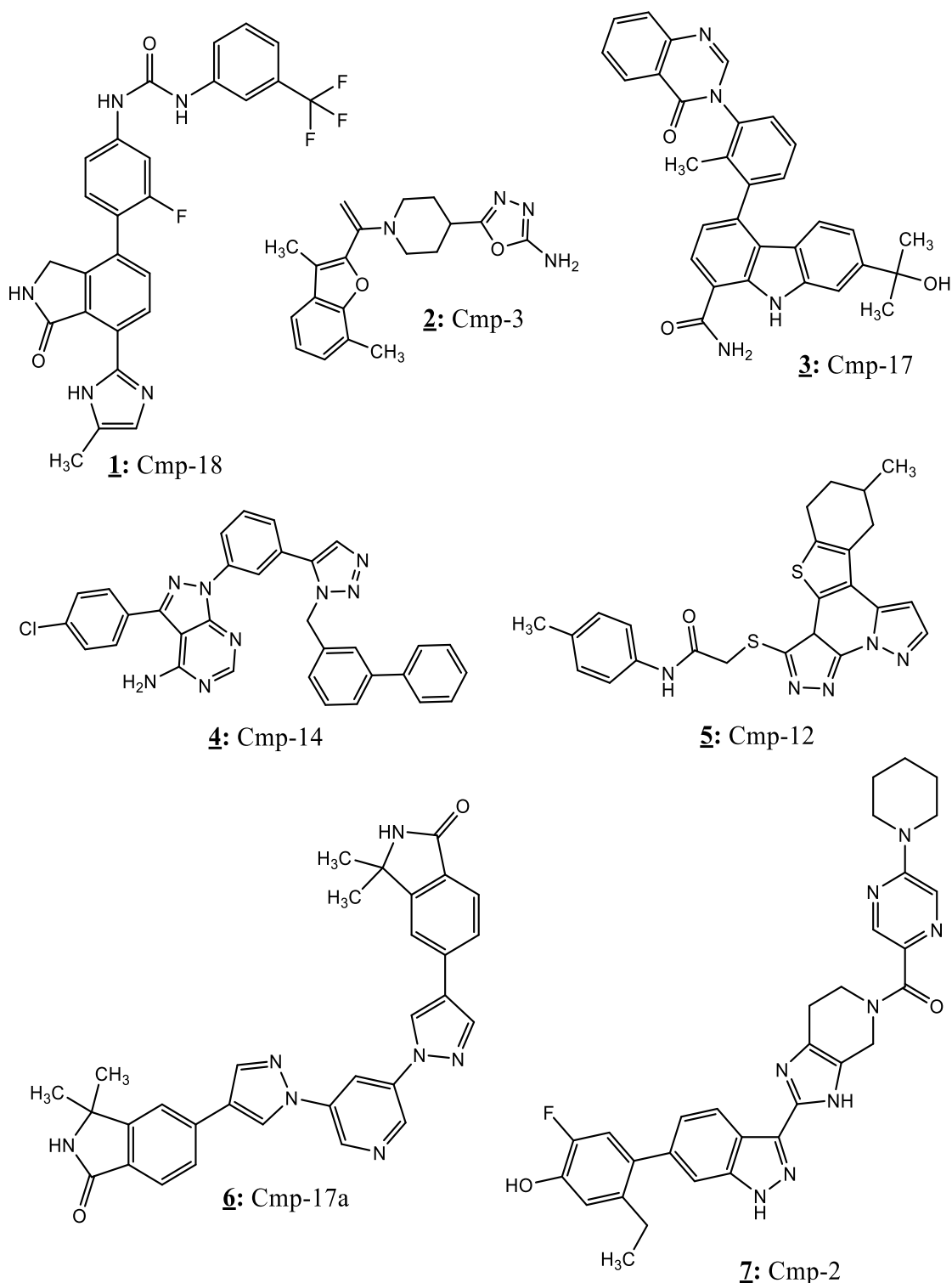


Figure 10. Chemical structures of synthetic inhibitors of against protease, Nsp12 and Nsp13 helicase of SRAS-CoV-2 (these structures were drawn by ChemDraw).

ACE2, a membrane receptor expressed in several human cells, is behind the penetration of SARS-CoV-2 into the host cell. Since the binding of SARS-CoV S protein to ACE2 is the first step in infection with this virus, this protein constitutes a major pharmacological target for inhibiting the penetration SARS-CoV-2. Consequently, several molecules have been tested, *in silico*, against this receptor. Ho *et al.* [37] analyzed the inhibitory powers of 14 synthesized peptides derived from S protein on the interaction of this protein and ACE2. By the ELISA test, they found that SP-10 (residues 668–679), SP-8 (residues 483–494), and SP-4 (residues 192–203) significantly inhibited the interaction in a dose-dependent manner with IC₅₀ values

of 1.88 ± 0.52 , 6.99 ± 0.71 , and 4.30 ± 2.18 nmol, respectively, with the definition of a novel region of receptor binding by a peptide-scanning method.

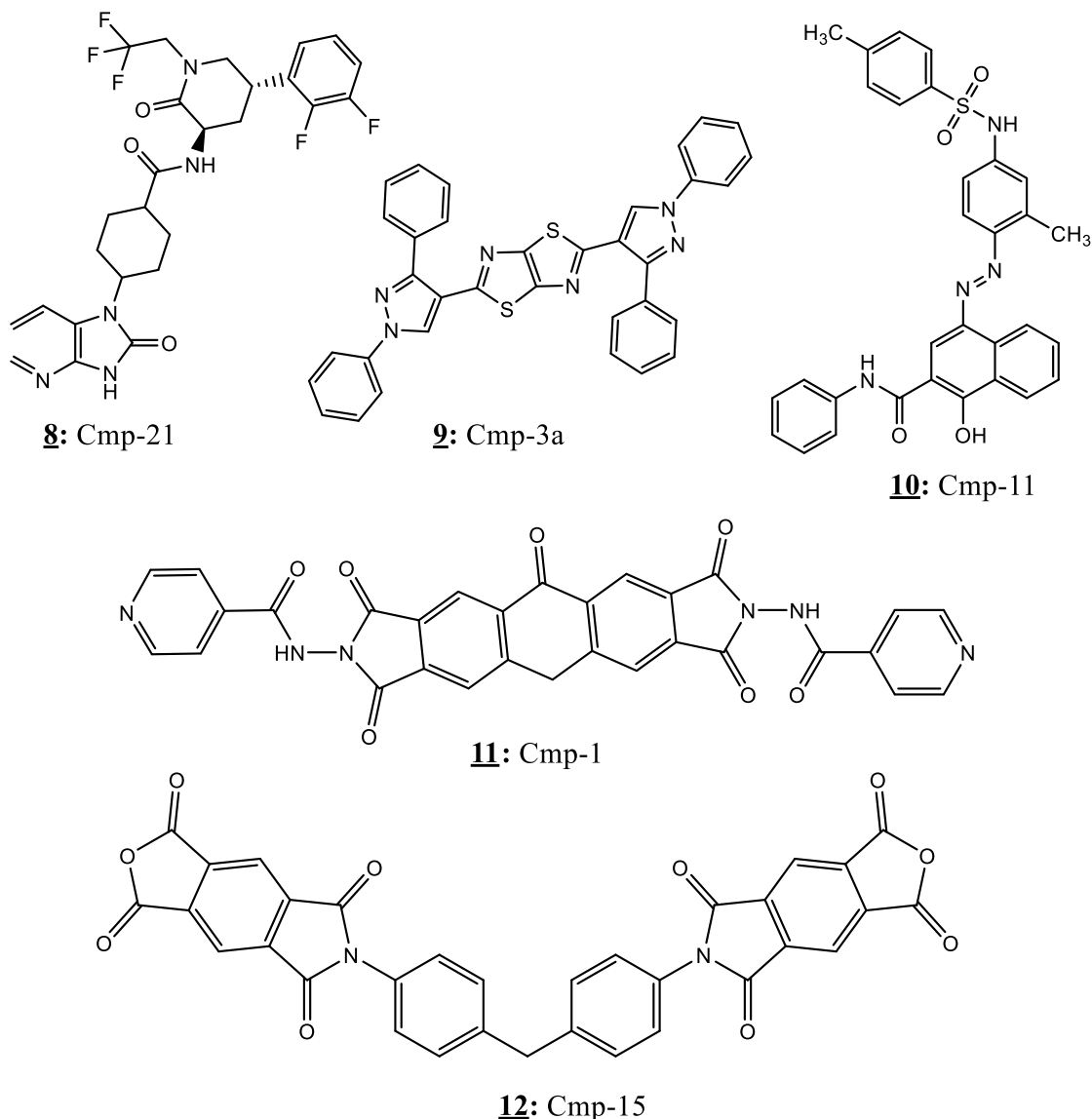


Figure 10. Continued.

In addition, they mentioned that SP-10 was a potent inhibitor of S protein binding to Vero E6 cells. Furthermore, Yang *et al.* [44] evaluated SARS-CoV-induced anti-CPE activity of the tylophorine compounds (1a, 1c, 1e, 4a, and 4b) (Figure 11) in Vero 76 cells and, consequently, these small molecules decreased the CPE induced by the virus, with EC_{50} values between 5 and 340 nM [44].

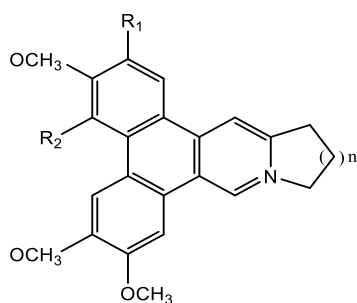
2.3. Old antiviral drugs against SARS-CoV-2.

In order to inhibit or delay a viral infection, the use of antivirals can be considered as an effective treatment. These molecules can limit the multiplication of viral particles by disrupting the viral replication cycle. Indeed, several studies have evaluated the mechanisms by which synthetic drugs act against different human coronaviruses (HCoV) [45-47]. In 2011, a Korean research team, using normal human fibroblast cells (HS27), showed that 5-hydroxychromone derivatives with two arylmethoxy substituents have antiviral activity

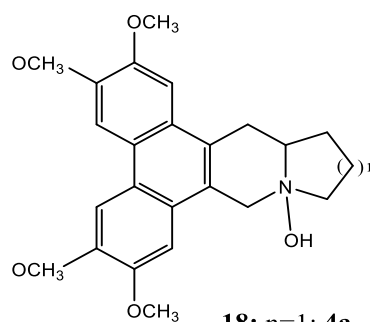
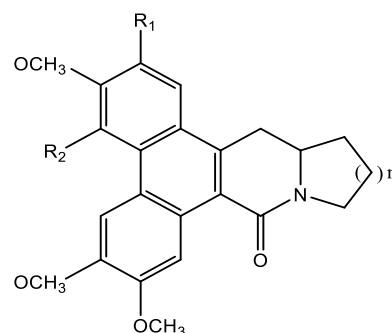
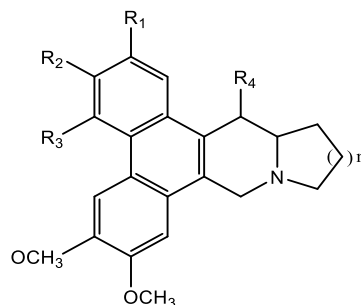
against SARS-associated coronavirus [48]. Among the molecules tested, 3-iodobenzoyloxy-substituted derivative 5e exhibited the most important activity ($IC_{50}=11 \mu M$ for helicase activity and $4 \mu M$ for ATPase activity) (Table 3).

- 1:** $R_1=R_2=OCH_3$, $R_3=R_4=H$, $n=1$: **1a** & **1a'**
2: $R_1=R_2=R_3=OCH_3$, $R_4=H$, $n=1$: **1b**
3: $R_1=R_2=OCH_3$, $R_3=R_4=H$, $n=2$: **1c**
4: $R_1=R_3=R_4=H$, $R_2=OCH_3$, $n=1$: **1d**
5: $R_1=R_3=H$, $R_2=OCH_3$, $R_4=OH$, $n=1$: **1e**
6: $R_1=R_3=H$, $R_2=OCH_3$, $R_4=OAc$, $n=1$: **1f**
7: $R_1=H$, $R_3=OCH_3$, $R_2=R_4=OH$, $n=1$: **1g**
8: $R_1=R_3=H$, $R_2=R_4=OH$, $n=1$: **1h**
9: $R_1=R_2=R_3=OCH_3$, $R_4=H$, $n=2$: **1i**
10: $R_1=R_3=R_4=H$, $R_2=OCH_3$, $n=2$: **1j**

- 11:** $R_1=OCH_3$, $R_2=H$, $n=1$: **2a**
12: $R_1=R_2=OCH_3$, $n=1$: **2b**
13: $R_1=OCH_3$, $R_2=H$, $n=2$: **2c**
14: $R_1=R_2=H$, $n=1$: **2d**



- 15:** $R_1=OCH_3$, $R_2=H$, $n=1$: **3a**
16: $R_1=R_2=OCH_3$, $n=1$: **3b**
17: $R_1=OCH_3$, $R_2=H$, $n=2$: **3c**



- 18:** $n=1$: **4a**
19: $n=2$: **4b**

Figure 11. Structures of phenanthroindolizines and phenanthroquinolizidines as inhibitors of coronavirus.

Table 3. Old antiviral drugs with possible anti-SARS-CoV-2 effects.

Antiviral	Experimental system (model cell line, <i>in silico</i> , <i>in vivo</i>)	Keys findings/mechanisms insights	Authors
Sofosbuvir	Construction of a model for Wuhan SARS-CoV-2 RdRp from sequence analysis, modeling and docking.	Effectiveness of molecules tested as potent drugs against the newly emerged HCoV disease.	[49]
IDX-184	Construction of a model for Wuhan SARS-CoV-2 RdRp from sequence analysis, modeling and docking.	Effectiveness of molecules tested as potent drugs against the newly emerged HCoV disease.	[49]
Ribavirin	Construction of a model for Wuhan SARS-CoV-2 RdRp from sequence analysis, modeling and docking.	Effectiveness of molecules tested as potent drugs against the newly emerged HCoV disease.	[49]
Remdisvir	Construction of a model for Wuhan SARS-CoV-2 RdRp	Effectiveness of molecules tested as potent drugs against the newly emerged HCoV disease.	[49]

Antiviral	Experimental system (model cell line, <i>in silico</i> , <i>in vivo</i>)	Keys findings/mechanisms insights	Authors
	from sequence analysis, modeling and docking.		
Pemirolast	Molecular docking (Autodock Tools)	Limiting the binding of the SARS-CoV-2 S-protein with the ACE2 receptor.	[50]
Isoniazid pyruvate	Molecular docking (Autodock Tools)	Limiting the binding of the SARS-CoV-2 S-protein with the ACE2 receptor.	[50]
Nitrofurantoin	Molecular docking (Autodock Tools)	Limiting the binding of the SARS-CoV-2 S-protein with the ACE2 receptor.	[50]
Eriodictyol	Molecular docking (Autodock Tools)	Limiting the binding of the SARS-CoV-2 S-protein with the ACE2 receptor.	[50]
Cepharanthine	Molecular docking (Autodock Tools)	Limiting SARS-CoV-2 virus-host interactions.	[50]
Ergoloid	Molecular docking (Autodock Tools)	Limiting SARS-CoV-2's virus-host interactions.	[50]
Hypericin	Molecular docking (Autodock Tools)	Limiting SARS-CoV-2's virus-host interactions.	[50]
Saquinavir	Molecular docking (Vina1.1.2)	Can bind to the NSP12-NSP7 interface as interfacial blocker.	[51]
Tipranavir	Molecular docking (Vina1.1.2).	Can bind to the NSP12-NSP7 interface as interfacial blocker.	[51]
Lonafarnib	Molecular docking (Vina1.1.2).	Can bind to the interface active pockets between the SARS-CoV-2 NSP12 and NSP7.	[51]
Tegobuvir	Molecular docking (Vina1.1.2).	Can bind to both of the interface active pockets of the SARS-CoV-2 NSP12-NSP7 and NSP12-NSP8.	[51]
Olysio	Molecular docking (Vina1.1.2).	Can bind to the interface active pockets of the SARS-CoV-2 NSP12-NSP8.	[51]
Filibuvir	Molecular docking (Vina1.1.2).	Can bind to the interface active pockets of the SARS-CoV-2 NSP12-NSP8	[51]
Cepharanthine	Molecular docking (Vina1.1.2)	Can bind to the interface active pockets of the SARS-CoV-2 NSP12-NSP8.	[51]
Trypsin	293T ACE2 and Vero E6 cells	Inhibition of cathepsin L (an endosomal protease sensitive to pH) prevents SARS coronavirus entry.	[52]
Peptide drugs	An autodock vina based docking simulation.	Inhibition of SARS-CoV-2 main protease.	[45]
Hexachlorophene	Mouse astrocytoma DBT and fibroblast 17Cl-1 cells.	Robust anti-coronavirus activities (a reduction of $8\log_{10}$) with an $IC_{50}=1.2 \mu M$.	[46]
Nitazoxanide	Mouse astrocytoma DBT and fibroblast 17Cl-1 cells.	Robust anti-coronavirus activities (a reduction $6\log_{10}$) with an $IC_{50}=1 \mu M$.	[46]
Homoharringtonine	Mouse astrocytoma DBT and fibroblast 17Cl-1 cells.	Robust anti-coronavirus activities (a reduction of $8\log_{10}$) with an $IC_{50}=12nM$.	[46]
6-Mercaptopurine	Molecular docking (DS Modeling 1.7 software).	Inhibition of MERS-CoV papain-like protease. Inhibition constant $K_{is}=14.3\pm 1.6\mu M$. IC_{50} of $25.8-26.9 \mu M$.	[47]
6-Thioguanine	Molecular docking (DS Modeling 1.7 software).	Inhibition of MERS-CoV papain-like protease. Inhibition constant $K_{is}=9.1\pm 1.2 \mu M$. IC_{50} of $12.4-24.4 \mu M$.	[47]
N-ethylmaleimide	Molecular docking (DS Modeling 1.7 software).	Inhibition of MERS-CoV papain-like protease. IC_{50} of $45.0 \mu M$.	[47]

Antiviral	Experimental system (model cell line, <i>in silico</i> , <i>in vivo</i>)	Keys findings/mechanisms insights	Authors
Mycophenolic acid	Molecular docking (DS Modeling 1.7 software).	Unable to inhibit SARS-CoV PL ^{pro} even at a concentration of 1 mM; nevertheless, it shows a dose-dependent inhibitory effect on the E168R mutant of SARS-CoV PL ^{pro} . Inhibition constant $K_{is}=263.7\pm13.8\mu\text{M}$. IC_{50} of 222.5–247.6 μM .	[47]
2,6-bis-(3-chloro-benzyloxy)-5-hydroxy- chromen-4-one (5b)	Normal human fibroblast cells (HS27).	$\text{IC}_{50}=10\mu\text{M}$ for ATPase activity. $\text{IC}_{50}=40\mu\text{M}$ for helicase activity. Inhibitory activity against SARS-associated coronavirus.	[43]
6-(3-chloro-benzyloxy)-2-(4-chloro- benzyloxy)-5-hydroxy- chromen-4-one (5c).	Normal human fibroblast cells (HS27).	$\text{IC}_{50}=28\mu\text{M}$ for ATPase activity. $\text{IC}_{50}=53\mu\text{M}$ for helicase activity. Inhibition activity against SARS-associated coronavirus.	[43]
6-(3-chloro-benzyloxy)-2-(3,5-dichloro- benzyloxy)-5-hydroxy- chromen-4-one (5d).	Normal human fibroblast cells (HS27).	$\text{IC}_{50}>50\mu\text{M}$ for ATPase activity. $\text{IC}_{50}>50\mu\text{M}$ for helicase activity. Inhibition activity against SARS-associated coronavirus.	[43]
6-(3-chloro-benzyloxy)-5-hydroxy- 2-(3-iodo- benzyloxy)-chromen-4-one (5e).	Normal human fibroblast cells (HS27).	The most potent inhibition activity against SARS-associated coronavirus. $\text{IC}_{50}=4\mu\text{M}$ for ATPase activity. $\text{IC}_{50}=11\mu\text{M}$ for helicase activity.	[43]
6-(3-chloro-benzyloxy)-5-hydroxy- 2-(4-iodo- benzyloxy)-chromen-4-one (5f).	Normal human fibroblast cells (HS27).	$\text{IC}_{50}=23\mu\text{M}$ for ATPase activity. $\text{IC}_{50}=31\mu\text{M}$ for helicase activity. Inhibition activity against SARS-associated coronavirus.	[43]
Remdesivir (RDV)	Vero CCL81 cells MERS CoV EMC 2012 and MERS-nLUC human lung epithelial cell line, Calu-3 2B4 MERS-CoV pathogenesis in <i>Ces1c</i> ^{-/-} and <i>hDPP4</i> mice.	RDV (WT $\text{EC}_{50}=0.12\mu\text{M}$; MERS-nLUC $\text{EC}_{50}=0.09\mu\text{M}$) in the human lung epithelial cell line, Calu-3 Significantly diminished MERS-CoV-induced weight loss in mice infected with $5\text{E}+04$ Significantly reduced ATS lung injury scores Reduced virus lung titers the most (>3 log reduction, vehicle median = $1.4\text{E}+05$ pfu/lobe, RDV median=50 pfu/lobe)	[53]
Lopinavir (LPV)	Vero CCL81 cells MERS CoV EMC 2012 and MERS-nLUC human lung epithelial cell line, Calu-3 2B4 MERS-CoV pathogenesis in <i>Ces1c</i> ^{-/-} and <i>hDPP4</i> mice.	EC_{50} values=11.6 μM with CC_{50} values $>50\mu\text{M}$ SI was >4.3 inhibition of MERS-CoV	[53]
Interferon beta (IFNb)	Vero CCL81 cells MERS CoV EMC 2012 and MERS-nLUC human lung epithelial cell line, Calu-3 2B4 MERS-CoV pathogenesis in <i>Ces1c</i> ^{-/-} and <i>hDPP4</i> mice.	$\text{EC}_{50}=175$ international units (IU)/mL CC_{50} values >2800 IU/mL and an SI >16 inhibition of MERS-CoV Significantly induced sustained expression of interferon gamma-induced protein 10 (IP-10, CXCL-10) in the serum of both strains of mice Induced dose dependent expression of interferon stimulated gene (ISG), Mx1, in peripheral blood mononuclear cells (PBMCs) in <i>Ces1c</i> ^{-/-} mice	[53]
Ritonavir (RTV)	Vero CCL81 cells MERS CoV EMC 2012 and MERS-nLUC human lung epithelial cell line, Calu-3 2B4	EC_{50} values=24.9 μM with CC_{50} values $>50\mu\text{M}$ SI for RTV was >2 , inhibition of MERS-CoV	[53]

Antiviral	Experimental system (model cell line, <i>in silico</i> , <i>in vivo</i>)	Keys findings/mechanisms insights	Authors
	MERS-CoV pathogenesis in <i>Ces1c</i> ^{-/-} and <i>hDPP4</i> mice.		
Remdesivir	SARS-CoV-2 Vero E6 cells (ATCC-1586) CCK8 assay RT-PCR (qRT-PCR) Virus nucleoprotein (NP) expression through Immunofluorescence microscopy	EC ₅₀ =0.77 μM; CC ₅₀ > 100 μM; SI > 129.87	[54]
Ribavirin	SARS-CoV-2 Vero E6 cells (ATCC-1586) CCK8 assay RT-PCR (qRT-PCR) Virus nucleoprotein (NP) expression through Immunofluorescence microscopy	EC ₅₀ =109.50 μM, CC ₅₀ > 400 μM, selectivity index (SI) >3.65	[54]
Penciclovir	SARS-CoV-2 Vero E6 cells (ATCC-1586) CCK8 assay RT-PCR (qRT-PCR) Virus nucleoprotein (NP) expression through Immunofluorescence microscopy	EC ₅₀ =95.96 μM, CC ₅₀ > 400 μM, SI > 4.17	[54]
Favipiravir	SARS-CoV-2 Vero E6 cells (ATCC-1586) CCK8 assay RT-PCR (qRT-PCR) Virus nucleoprotein (NP) expression through Immunofluorescence microscopy	EC ₅₀ =61.88 μM, CC ₅₀ > 400 μM, SI > 6.46	[54]
Nafamostat	SARS-CoV-2 Vero E6 cells (ATCC-1586) CCK8 assay RT-PCR (qRT-PCR) Virus nucleoprotein (NP) expression through Immunofluorescence microscopy	EC ₅₀ =22.50 μM, CC ₅₀ > 100 μM, SI > 4.44	[54]
Nitazoxanide	SARS-CoV-2 Vero E6 cells (ATCC-1586) CCK8 assay RT-PCR (qRT-PCR) Virus nucleoprotein (NP) expression through Immunofluorescence microscopy	EC ₅₀ =2.12 μM, CC ₅₀ > 35.53 μM, SI > 16.76	[54]
Chloroquine	SARS-CoV-2 Vero E6 cells (ATCC-1586) CCK8 assay RT-PCR (qRT-PCR) Virus nucleoprotein (NP) expression through Immunofluorescence microscopy	EC ₅₀ =1.13 μM, CC ₅₀ > 100 μM, SI > 88.50	[54]
Hydroxychloroquine	SARS-CoV-2 infected Vero cells PBPK models	Inhibiting SARS-CoV-2 with EC ₅₀ =0.72 Mm	[55]
Chloroquine	SARS-CoV-2 infected Vero cells PBPK models	Inhibiting SARS-CoV-2 with EC ₅₀ =5.47 μM	[55]
Alisporivir	MERS-CoV infected Vero cells	EC ₅₀ =3.6±1.1 μM, CC ₅₀ =26.4±1.0 μM, SI=7.3	[56]

Antiviral	Experimental system (model cell line, <i>in silico</i> , <i>in vivo</i>)	Keys findings/mechanisms insights	Authors
Alisporivir	SARS-CoV infected Vero E6 cells	EC ₅₀ =8.3±1.0 µM, CC ₅₀ >50 µM, SI >6.0	[56]

Moreover, Cao *et al.* [46] assessed the ability of three drugs (homoharringtonine, nitazoxanide, and hexachlorophene) to inhibit viral infection in mouse astrocytoma DBT and fibroblast 17Cl-1 cells. Consequently, they showed dose-dependent anti-coronavirus activities with a reduction of 6 to 8 log₁₀ in viral load and IC₅₀ values varying between 1 µM for nitazoxanide and hexachlorophene, and 12 nM for homoharringtonine. Also, the authors carried out the second part of the experiment, where they selected 11 drugs to treat cells *via* the inhibition of luciferase activity (1 hour before or 3 hours after viral infection) (Table 3). They found that these drugs had strong inhibition at different times; this indicates that they inhibit viral infection at the stage of viral replication (post-entry stage). In the same year, Cheng *et al.* [47] tested the effect of two thiopurine analogs (6-Mercaptopurine and 6-Thioguanine) and mycophenolic acid on MERS-CoV by inhibiting the papain-like protease (PL^{pro}) of the virus, which is an important antiviral target. As a result, they showed that these three inhibitors were effective against MERS-CoV PL^{pro} with IC₅₀s of 24.4, 26.9, and 247.6 µM for 6-thioguanine (6TG), 6-mercaptopurine (6MP), and mycophenolic acid, respectively [47]. Additionally, the interaction of these compounds with the target was competitive for 6MP and 6TG and non-competitive for mycophenolic acid. Also, the authors reported that the binding of these inhibitors together synergistically improves their inhibitory capacity against MERS-CoV PL^{pro} (Table 3).

Two years later, de Wilde *et al.* [56] investigated the inhibitory potential of alisporivir (ALV), a cyclophilin inhibitor, on MERS- and SARS-coronavirus replication in cell culture. Three days after infection, they found that this molecule prevented virus-induced CPE (cytopathic effect) in a dose-dependent manner in MERS-CoV EMC/2012-infected Vero cells (EC₅₀=3.6 µM) and MERS-CoV EMC/2012-infected Huh7 cells (EC₅₀=3.4 µM). Also, they observed in VeroE6 cells, inhibition of SARS-CoV strain Frankfurt 1 (EC₅₀=8.3 µM), and SARS-CoV strain MA-15 (mouse-adapted) (EC₅₀=1.3 µM). Furthermore, at the concentration of 10 µM of ALV, they noted a 4-to 5-log reduction of the virus yield (MERS-CoV) in Vero, Huh7, and LLC-MK2 cells with EC₅₀ of 3.9, 2.8, and 4.0 µM, respectively [56]. The same efficacy in reducing viral production was observed in two other coronaviruses; human coronavirus 229E (HCoV-229E) and murine hepatitis virus (MHV-A59) on Huh7 and 17Cl1 cells, respectively, using different doses. Likewise, the authors tested combination therapy of ALV with ribavirin (MERS-CoV replication inhibitor) in LLC-MK2 cells, which potentiated antiviral activity. However, this association had no additive effect on SARS-CoV infection in a mouse model (Table 3).

Very recently, numerous studies, *in silico*, have tested synthetic compounds against the new HCoV that appeared in Wuhan (COVID-19) [45, 49–51]. Indeed, Elfiky and collaborators tested four anti-HCV molecules (IDX-184, Remdisvir, Ribavirin, Sofosbuvir) against viral RNA dependent RNA polymerase (RdRp) by molecular docking also using the structure of SARS HCoV as a model which has more than 97% of sequence identical to SARS-CoV-2 RdRp [49]. They found that these drugs were able to bind tightly to SARS-CoV-2 and SARS HCoV RdRps and therefore exhibit potent inhibition of this new HCoV.

Since the development of new drug therapies takes years, Smith and Smith, [50] reused already characterized small molecules, that could have an action against the novel coronavirus, by using docking calculations to identify those which are able to bind either to the viral spike protein (S-protein) or to the S protein-human ACE2 interface. Therefore, they identified seven compounds (Isoniazid pyruvate, Pemirolast, Eriodictyol, Cepharanthine, Ergoloid, Hypericin, Nitrofurantoin) capable of limiting the binding of the viral S-protein with the ACE2 receptor, thereby restricting the host-virus interactions and the SARS-CoV-2 infection pathway.

Moreover, to combat SARS-CoV-2, the NSP12-NSP7-NSP8 complex of the virus may be a potential therapeutic target. In this context, Ruan *et al.* [51] created two homologous models (NSP12-NSP8 interface model and NSP12-NSP7 interface model). Subsequently, they selected seven compounds (Tipranavir, Saquinavir, Tegobuvir, Lonafarnib, Olysio, Cepharanthine, Filibuvir) for the calculation of binding free energy, based on docking scores and virtual screening. They found that all of these compounds show a good combination with NSP12-NSP7-NSP8 in the homologous model. Furthermore, Zhang and colleagues identified and designed peptide drugs against SARS-CoV-2 main protease, which is also a major target, through virtual drug screening using DFCNN (densely fully connected neural network) [45]. Consequently, they noted that these drugs have the ability to bind well to this target protein.

Other recent studies have also evaluated the anti-coronavirus activity of synthetic drugs either tested for the first time or already used as antivirals on cell cultures (*in vitro*) [52-53] [54] [55]. Effectively, Simmons *et al.* [52] tested the effect of certain compounds on inhibiting cathepsin L, a pH-sensitive endosomal protease, and blocking the entry of SARS-CoV, using 293T ACE2 and Vero E6 cells. Indeed, compounds like MDL28170, trypsin, and leupeptin effectively prevented viral infection by inhibiting the activity of the endosomal protease during viral entry.

Sheahan and collaborators investigated the anti-MERS-CoV activity (*in vitro* and *in vivo*) of four well-known drugs as broad-spectrum antivirals like remdesivir (RDV), ritonavir (RTV), lopinavir (LPV), and interferon-beta (IFN β), by comparing the therapeutic and prophylactic efficacy of RDV with the RTV/LPV-IFN β combination [53]. Regarding *in vitro* antiviral tests, the authors found that RDV had significant activity on MERS-nLUC (EC₅₀=0.09 μ M) and MERS-CoV EMC 2012 strain (EC₅₀=0.12 μ M) in Calu-3, a human lung epithelial cell line. In parallel, RTV and LPV showed inhibitory effects against MERS-CoV of 24.9 and 11.6 μ M, respectively, while their combinatorial effect was 8.5 μ M. Similarly, IFN β was very effective with an EC₅₀ of 175 IU/mL, and CC50 values >2800 IU/mL, and the combination with RTV/LPV (EC₅₀=160 IU/mL) did not improve its activity. This indicates that the antiviral activity of IFN β and RDV is higher than that of RTV and LPV *in vitro*. On the other hand, using the *Ces1c*^{-/-} *hDPP4* mouse model, they observed that the administration of prophylactic RDV (25 mg/kg) one day before infection; significantly attenuated the weight loss induced by MERS-CoV in infected animals and prevented the mortality of mice treated with a lethal dose. Simultaneously, RDV prophylaxis significantly reduced lung hemorrhage, characteristics of acute lung injury, and lung viral load > 3 logs over the 4- and 6-days following infection. In the same animal model, therapeutic RDV substantially diminished lung hemorrhage, bodyweight loss, and virus replication during MERS-CoV infection. However, the therapeutic RTV/LPV-IFN β could not improve the previous parameters or survival after a lethal dose of the virus. Whereas the prophylactic RTV/LPV-IFN β caused a slight decrease in the lung viral load, and the IFN β alone did not affect the virus replication. Additionally, other researchers evaluated the *in vitro* antiviral efficiency of seven drugs on a clinical isolate of the novel Wuhan

coronavirus [54]. As a result, they recorded that the drugs tested were able to decrease viral infection at different concentrations, namely 109.50, 95.96, 61.88, 22.50, 2.12, 0.77, and 1.13 μM for ribavirin, penciclovir, favipiravir, nafamostat, nitazoxanide, remdesivir, and chloroquine, respectively. This showed that remdesivir and chloroquine were the most potent inhibitors against SARS-CoV-2. In addition, chloroquine and its derivative (hydroxychloroquine), at increasing concentrations, were investigated *in vitro* for their inhibitory power against SARS-CoV-2 using infected Vero cells [55]. They reported that both molecules had a good activity with the ability to reduce viral replication in a dose-dependent manner. Likewise, hydroxychloroquine ($\text{EC}_{50}=0.72 \mu\text{M}$) was more powerful than chloroquine ($\text{EC}_{50}=5.47 \mu\text{M}$) to block virus infection.

3. Therapeutic strategies for clinical studies to combat Covid-19

The high mortality rate with the absence of effective treatments to combat COVID-19 has stimulated a number of research groups to start clinical trials quickly by exploiting all possible strategies. Many of the clinical trials are underway today. These are different therapeutic strategies such as the use of antiviral molecules with a wide spectrum of action, traditional natural molecules and / preparations especially based on traditional Chinese medicine, monoclonal antibodies directed in particular against the mediators of the immune system, mesenchymal cells as cell therapy, plasma therapy, and SARS-CoV-2 antigen vaccine trials.

3.1. Specific antiviral drugs.

With the emergence of COVID-19 pandemic, several clinical trials have been taken place to found clinically active drugs against SRAS-CoV-2 from old antiviral drugs. Indeed, several patents on clinical trials were deposited at different clinical phases (Table 4). As summarized in Table 5, these clinical patents include numerous drugs and/or combination of drugs such as arbidol hydrochloride tablets, ASC09/Ritonavir, lopinavir/ritonavir, aviptadil, azithromycin/chloroquine, baricitinib, bromhexine hydrochloride, carrimycin, colchicine, darunavir, dexamethasone, escin, fingolimod, and glucocorticoid. These drugs are in different clinical trials and could give promising applications in the future. For example, Azithromycin and Chloroquine used to fight against COVID-19 (to decrease COVID-19 complications) has been confirmed into phase 4 of clinical trials, which has been experienced on a large number of patients (NCT04322396). Moreover, other drugs such as arbidol hydrochloride tablets were also developed into phase 4 of clinical trials with promising results on SARS-CoV-2.

Table 4. Clinical trial patients of synthetic drugs targeted SARS-CoV2.

Patent number	Patent title	Target/key results	Organization	Priority date	Phase	Links
NCT04325633	Efficacy of Addition of Naproxen in the Treatment of Critically Ill Patients Hospitalized for COVID-19 Infection (ENACOVID).	Virus nucleoprotein.	Assistance Publique - Hôpitaux de Paris.	20200327	3	https://clinicaltrials.gov/ct2/show/NCT04325633?cond=COVID-19&draw=2&rank=5
NCT04304313	A Pilot Study of Sildenafil in COVID-19.	Not reported.	Tongji Hospital.	20200317	3	https://clinicaltrials.gov/ct2/show/NCT04304313?cond=COVID-19&draw=3&rank=13
NCT04304053	Treatment of COVID-19 Cases and Chemoprophylaxis of Contacts as Prevention (HCQ4COV19)	Decrease in viral load levels.	Fundacio Lluita Contra la SIDA.	20200324	3	https://clinicaltrials.gov/ct2/show/NCT04304053?cond=COVID-19&draw=3&rank=16

Patent number	Patent title	Target/key results	Organization	Priority date	Phase	Links
NCT04321993	Treatment of Moderate to Severe Coronavirus Disease (COVID-19) in Hospitalized Patients.	Not reported.	Dalhousie University.	20200311	2	https://clinicaltrials.gov/ct2/show/NCT04321993?cond=COVID-19&draw=3&rank=18
NCT04313023	The Use of PUL-042 Inhalation Solution to Prevent COVID-19 in Adults Exposed to SARS-CoV-2.	Prevention.	Pulmotect, Inc.	20200324	2	https://clinicaltrials.gov/ct2/show/NCT04313023?cond=COVID-19&draw=3&rank=19
NCT04307693	Comparison of Lopinavir/Ritonavir or Hydroxychloroquine in Patients With Mild Coronavirus Disease (COVID-19).	Decrease in viral load levels.	Asan Medical Center.	20200313	2	https://clinicaltrials.gov/ct2/show/NCT04307693?cond=COVID-19&draw=3&rank=20
NCT04323631	Hydroxychloroquine for the Treatment of Patients With Mild to Moderate COVID-19 to Prevent Progression to Severe Infection or Death.	Decrease in viral load levels.	Rambam Health Care Campus.	20200326	1	https://clinicaltrials.gov/ct2/show/NCT04323631?cond=COVID-19&draw=4&rank=21
NCT04292899	Study to Evaluate the Safety and Antiviral Activity of Remdesivir (GS-5734™) in Participants With Severe Coronavirus Disease (COVID-19).	Not reported.	Gilead Sciences.	20200402	3	https://clinicaltrials.gov/ct2/show/NCT04292899?cond=COVID-19&draw=4&rank=22
NCT04312997	The Use of PUL-042 Inhalation Solution to Reduce the Severity of COVID-19 in Adults Positive for SARS-CoV-2 Infection.	Improved clinical outcome.	Pulmotect, Inc.	20200324	2	https://clinicaltrials.gov/ct2/show/NCT04312997?cond=COVID-19&draw=4&rank=23
NCT04292730	Study to Evaluate the Safety and Antiviral Activity of Remdesivir (GS-5734™) in Participants With Moderate Coronavirus Disease (COVID-19) Compared to Standard of Care Treatment.	Not reported.	Gilead Sciences.	20200402	3	https://clinicaltrials.gov/ct2/show/NCT04292730?cond=COVID-19&draw=4&rank=24
NCT04273529	The Efficacy and Safety of Thalidomide in the Adjuvant Treatment of Moderate New Coronavirus (COVID-19) Pneumonia.	Improve lung function.	First Affiliated Hospital of Wenzhou Medical University.	20200221	2	https://clinicaltrials.gov/ct2/show/NCT04273529?cond=COVID-19&draw=4&rank=29
NCT04273581	The Efficacy and Safety of Thalidomide Combined With Low-dose Hormones in the Treatment of Severe COVID-19.	Improve lung function.	First Affiliated Hospital of Wenzhou Medical University.	20200221	2	https://clinicaltrials.gov/ct2/show/NCT04273581?cond=COVID-19&draw=4&rank=30
NCT04280588	Fingolimod in COVID-19.	Immunology modulation.	First Affiliated Hospital of Fujian Medical University.	20200221	2	https://clinicaltrials.gov/ct2/show/NCT04280588?cond=COVID-19&draw=5&rank=33
NCT04315896	Hydroxychloroquine Treatment for Severe COVID-19 Pulmonary Infection (HYDRA Trial) (HYDRA).	Reduced hospital mortality in patients with severe respiratory COVID-19 disease.	National Institute of Respiratory Diseases, Mexico.	20200220	3	https://clinicaltrials.gov/ct2/show/NCT04315896?cond=COVID-19&draw=5&rank=34
NCT04325061	Efficacy of Dexamethasone Treatment for Patients With ARDS Caused by COVID-19 (DEXA-COVID19).	Reduce the duration of mechanical ventilation and hospital mortality.	Dr. Negrin University Hospital.	20200401	4	https://clinicaltrials.gov/ct2/show/NCT04325061?cond=COVID-19&draw=5&rank=35
NCT04317040	CD24Fc as a Non-antiviral Immunomodulator in COVID-19 Treatment (SAC-COVID).	Not reported.	OncoImmune, Inc.	20200323	3	https://clinicaltrials.gov/ct2/show/NCT04317040?cond=COVID-19&draw=5&rank=37
NCT04286503	The Clinical Study of Carrimycin on Treatment Patients With COVID-19.	Not reported.	Beijing YouAn Hospital.	20200227	4	https://clinicaltrials.gov/ct2/show/NCT04286503?cond=COVID-19&draw=5&rank=40

Patent number	Patent title	Target/key results	Organization	Priority date	Phase	Links
NCT04318444	Hydroxychloroquine Post Exposure Prophylaxis for Coronavirus Disease (COVID-19).	Reduce the risk of developing symptoms of COVID-19 among people at high risk of infection.	Columbia University.	20200325	2 and 3	https://clinicaltrials.gov/ct2/show/NCT04318444?cond=COVID-19&draw=6&rank=43
NCT04318015	Hydroxychloroquine Chemoprophylaxis in Healthcare Personnel in Contact With COVID-19 Patients (PHYDRA Trial) (PHYDRA).	Reduce the risk of developing symptoms of COVID-19	National Institute of Respiratory Diseases, Mexico.	20200323	3	https://clinicaltrials.gov/ct2/show/NCT04318015?cond=COVID-19&draw=6&rank=44
NCT04295551	Multicenter Clinical Study on the Efficacy and Safety of Xiyangping Injection in the Treatment of New Coronavirus Infection Pneumonia (General and Severe).	Not reported.	Jiangxi Qingfeng Pharmaceutica l Co. Ltd.	20200304	Not Applicable	https://clinicaltrials.gov/ct2/show/NCT04295551?cond=COVID-19&draw=7&rank=60
NCT04303507	Chloroquine/ Hydroxychloroquine Prevention of Coronavirus Disease (COVID-19) in the Healthcare Setting (COPCOV).	Reduce the risk of developing symptoms of COVID-19	University of Oxford.	20200327	Not Applicable	https://clinicaltrials.gov/ct2/show/NCT04303507?cond=COVID-19&draw=8
NCT04273763	Evaluating the Efficacy and Safety of Bromhexine Hydrochloride Tablets Combined with Standard Treatment/ Standard Treatment in Patients with Suspected and Mild Novel Coronavirus Pneumonia (COVID-19).	Not reported.	Second Affiliated Hospital of Wenzhou Medical University.	20200323	Not Applicable	https://clinicaltrials.gov/ct2/show/NCT04273763?cond=COVID-19&draw=8
NCT04303299	Various Combination of Protease Inhibitors, Oseltamivir, Favipiravir, and Hydroxychloroquine for Treatment of COVID19: A Randomized Control Trial (THDMS-COVID19).	Reduce the risk of developing symptoms of COVID-19	Rajavithi Hospital.	20200325	3	https://clinicaltrials.gov/ct2/show/NCT04303299?cond=COVID-19&draw=8
NCT04312009	Losartan for Patients With COVID-19 Requiring Hospitalization.	Not reported.	University of Minnesota.	20200323	2	https://clinicaltrials.gov/ct2/show/NCT04312009?cond=COVID-19&draw=11&rank=93
NCT04252664	Mild/Moderate 2019-nCoV Remdesivir RCT	Not reported.	Capital Medical University.	20200224	3	https://clinicaltrials.gov/ct2/show/NCT04252664?cond=COVID-19&draw=10&rank=90
NCT04315948	Trial of Treatments for COVID-19 in Hospitalized Adults (DisCoVeRy).	Not reported.	Institut National de la Santé Et de la Recherche Médicale, France.	20200325	3	https://clinicaltrials.gov/ct2/show/NCT04315948?cond=COVID-19&draw=11&rank=94
NCT04311177	Losartan for Patients With COVID-19 Not Requiring Hospitalization.	Not reported.	University of Minnesota.	20200323	2	https://clinicaltrials.gov/ct2/show/NCT04311177?cond=COVID-19&draw=11&rank=95
NCT04255017	A Prospective/Retrospective, Randomized Controlled Clinical Study of Antiviral Therapy in the 2019-nCoV Pneumonia.	Not reported.	Tongji Hospital.	20200317	4	https://clinicaltrials.gov/ct2/show/NCT04255017?cond=COVID-19&draw=11&rank=99
NCT04254874	A Prospective/Retrospective, Randomized Controlled Clinical Study of Interferon Atomization in the 2019-nCoV Pneumonia	Not reported.	Tongji Hospital.	20200317	4	https://clinicaltrials.gov/ct2/show/NCT04254874?cond=COVID-19&draw=11&rank=100
NCT04323761	Expanded Access Treatment Protocol: Remdesivir (RDV; GS-	Not reported.	Gilead Sciences.	20200402	Not Applicable	https://clinicaltrials.gov/ct2/show/NCT04323761?c

Patent number	Patent title	Target/key results	Organization	Priority date	Phase	Links
	5734) for the Treatment of SARS-CoV2 (CoV) Infection.					ond=COVID-19&draw=12&rank=103
NCT04261270	A Randomized, Open, Controlled Clinical Study to Evaluate the Efficacy of ASC09F and Ritonavir for 2019-nCoV Pneumonia.	Not reported.	Tongji Hospital.	20200317	3	https://clinicaltrials.gov/ct2/show/NCT04261270?cond=COVID-19&draw=12&rank=104
NCT04311697	Intravenous Aviptadil for COVID-19 Associated Acute Respiratory Distress (COVID-AIV).	Not reported.	NeuroRx, Inc.	20200326	2	https://clinicaltrials.gov/ct2/show/NCT04311697?cond=COVID-19&draw=12&rank=105
NCT02735707	Randomized, Embedded, Multifactorial Adaptive Platform Trial for Community-Acquired Pneumonia (REMAP-CAP).	Not reported.	MJM Bonten.	20200330	4	https://clinicaltrials.gov/ct2/show/NCT02735707?cond=COVID-19&draw=12&rank=107
NCT04263402	The Efficacy of Different Hormone Doses in 2019-nCoV Severe Pneumonia.	Not reported.	Tongji Hospital.	20200317	4	https://clinicaltrials.gov/ct2/show/NCT04263402?cond=COVID-19&draw=12&rank=108
NCT04305457	Nitric Oxide Gas Inhalation Therapy for Mild/Moderate COVID-19 (NoCovid).	Not reported.	Massachusetts General Hospital.	20200324	2	https://clinicaltrials.gov/ct2/show/NCT04305457?cond=COVID-19&draw=13&rank=112
NCT04324463	Anti-Coronavirus Therapies to Prevent Progression of Coronavirus Disease 2019 (COVID-19) Trial (ACT COVID19).	Not reported.	Population Health Research Institute.	20200327	3	https://clinicaltrials.gov/ct2/show/NCT04324463?cond=COVID-19&draw=13&rank=113
NCT04320277	Baricitinib in Symptomatic Patients Infected by COVID-19: an Open-label, Pilot Study. (BARI-COVID).	Not reported.	Hospital of Prato.	20200324	3	https://clinicaltrials.gov/ct2/show/NCT04320277?cond=COVID-19&draw=13&rank=114
NCT04280705	Adaptive COVID-19 Treatment Trial (ACTT).	Not reported.	National Institute of Allergy and Infectious Diseases (NIAID).	20200327	3	https://clinicaltrials.gov/ct2/show/NCT04280705?cond=COVID-19&draw=13&rank=117
NCT04279197	Treatment of Pulmonary Fibrosis Due to 2019-nCoV Pneumonia With Fuzheng Huayu.	Not reported.	ShuGuang Hospital.	20200221	2	https://clinicaltrials.gov/ct2/show/NCT04279197?cond=COVID-19&draw=13&rank=118
NCT04321174	COVID-19 Ring-based Prevention Trial With Lopinavir/Ritonavir (CORIPREV-LR).	Not reported.	Darrell Tan, St. Michael's Hospital, Toronto.	20200325	3	https://clinicaltrials.gov/ct2/show/NCT04321174?cond=COVID-19&draw=13&rank=120
NCT04323592	Efficacy of Methylprednisolone for Patients With COVID-19 Severe Acute Respiratory Syndrome (MP-C19).	Not reported.	University of Trieste.	20200327	2 and 3	https://clinicaltrials.gov/ct2/show/NCT04323592?cond=COVID-19&draw=14&rank=123
NCT04322565	Colchicine Efficacy in COVID-19 Pneumonia.	Not reported.	Lucio Manenti, Azienda Ospedaliero-Universitaria di Parma	20200326	2	https://clinicaltrials.gov/ct2/show/NCT04322565?cond=COVID-19&draw=14&rank=124
NCT04312243	NO Prevention of COVID-19 for Healthcare Providers (NOpreventCOVID).	Not reported.	Massachusetts General Hospital.	20200318	2	https://clinicaltrials.gov/ct2/show/NCT04312243?cond=COVID-19&draw=14&rank=127
NCT04293887	Efficacy and Safety of IFN- $\alpha 2\beta$ in the Treatment of Novel Coronavirus Patients.	Not reported.	Tongji Hospital.	20200303	1	https://clinicaltrials.gov/ct2/show/NCT04293887?cond=COVID-19&draw=14&rank=128
NCT04321616	The Efficacy of Different Anti-viral Drugs in (Severe Acute Respiratory Syndrome-Corona Virus-2) SARS-CoV-2.	Not reported.	Oslo University Hospital.	20200325	2 and 3	https://clinicaltrials.gov/ct2/show/NCT04321616?cond=COVID-19&draw=14&rank=130
NCT04290871	Nitric Oxide Gas Inhalation for Severe Acute	Not reported.	Xijing Hospital.	20200324	2	https://clinicaltrials.gov/ct2/show/NCT04290871?cond=COVID-19&draw=14&rank=131

Patent number	Patent title	Target/key results	Organization	Priority date	Phase	Links
	Respiratory Syndrome in COVID-19. (NOSARSCOVID).					ond=COVID-19&draw=15&rank=137
NCT04320238	Experimental Trial of rhIFN α Nasal Drops to Prevent 2019-nCoV in Medical Staff.	Not reported.	Shanghai Jiao Tong University School of Medicine.	20200331	3	https://clinicaltrials.gov/ct2/show/NCT04320238?cond=COVID-19&draw=15&rank=139
NCT04322396	Proactive Prophylaxis With Azithromycin and Chloroquine in Hospitalized Patients With COVID-19 (ProPAC-COVID).	Decreased COVID-19 complications	Chronic Obstructive Pulmonary Disease Trial Network, Denmark.	20200326	4	https://clinicaltrials.gov/ct2/show/NCT04322396?cond=COVID-19&draw=16&rank=147
NCT04325893	Hydroxychloroquine Versus Placebo in Patients Presenting COVID-19 Infection and at Risk of Secondary Complication: a Prospective, Multicentre, Randomised, Double-blind Study (HYCOVID).	Not reported.	University Hospital, Angers	20200330	3	https://clinicaltrials.gov/ct2/show/NCT04325893?cond=COVID-19&draw=16&rank=150
NCT04321278	Safety and Efficacy of Hydroxychloroquine Associated With Azithromycin in SARS-CoV2 Virus (Coalition Covid-19 Brasil II).	Not reported.	Hospital Israelita Albert Einstein.	20200401	3	https://clinicaltrials.gov/ct2/show/NCT04321278?cond=COVID-19&draw=17&rank=151
NCT04260594	Clinical Study of Arbidol Hydrochloride Tablets in the Treatment of Pneumonia Caused by Novel Coronavirus.	Not reported.	Jieming QU, Ruijin Hospital.	20200207	4	https://clinicaltrials.gov/ct2/show/NCT04260594?cond=COVID-19&draw=17&rank=152
NCT04326426	COVIDL1: A Study to Investigate the Efficacy of Tradipitant in Treating Severe or Critical COVID-19 Infection.	Not reported.	Vanda Pharmaceuticals	20200330	3	https://clinicaltrials.gov/ct2/show/NCT04326426?cond=COVID-19&draw=17&rank=154
NCT04290858	Nitric Oxide Gas Inhalation Therapy for Mild/Moderate COVID19 Infection (NoCovid).	Not reported.	Xijing Hospital.	20200324	2	https://clinicaltrials.gov/ct2/show/NCT04290858?cond=COVID-19&draw=17&rank=157
NCT04257656	Severe 2019-nCoV Remdesivir RCT.	Not reported.	Capital Medical University.	20200224	3	https://clinicaltrials.gov/ct2/show/NCT04257656?cond=COVID-19&draw=17&rank=158
NCT04306393	Nitric Oxide Gas Inhalation in Severe Acute Respiratory Syndrome in COVID-19 (NOSARSCOVID).	Not reported.	Massachusetts General Hospital.	20200324	2	https://clinicaltrials.gov/ct2/show/NCT04306393?cond=COVID-19&draw=18&rank=163
NCT04322344	Escin in Patients With Covid-19 Infection (add-on-COV2).	Not reported.	University of Catanzaro.	20200327	2 and 3	https://clinicaltrials.gov/ct2/show/NCT04322344?cond=COVID-19&draw=18&rank=164
NCT04322773	Anti-il6 Treatment of Serious COVID-19 Disease With Threatening Respiratory Failure (TOCIVID).	Not reported.	Frederiksberg University Hospital.	20200330	2	https://clinicaltrials.gov/ct2/show/NCT04322773?cond=COVID-19&draw=18&rank=165
NCT04322786	The Use of Angiotensin Converting Enzyme Inhibitors and Incident Respiratory Infections, Are They Harmful or Protective?	Not reported.	University College, London.	20200326	Not Applicable	https://clinicaltrials.gov/ct2/show/NCT04322786?cond=COVID-19&draw=18&rank=167
NCT04322123	Safety and Efficacy of Hydroxychloroquine Associated With Azythromycin in SARS-Cov-2 Virus (Coalition-I).	Not reported.	Hospital do Coracao.	20200326	3	https://clinicaltrials.gov/ct2/show/NCT04322123?cond=COVID-19&draw=18&rank=168
NCT04261907	Evaluating and Comparing the Safety and Efficiency of ASC09/Ritonavir and Lopinavir/Ritonavir for Novel Coronavirus Infection.	Not reported.	First Affiliated Hospital of Zhejiang University.	20200210	Not Applicable	https://clinicaltrials.gov/ct2/show/NCT04261907?cond=COVID-19&draw=19&rank=174

Patent number	Patent title	Target/key results	Organization	Priority date	Phase	Links
NCT04302766	Expanded Access Remdesivir (RDV; GS-5734™).	Not reported.	U.S. Army Medical Research and Development Command.	20200320	Not Applicable	https://clinicaltrials.gov/ct2/show/NCT04302766?cond=COVID-19&draw=20&rank=181
NCT04323527	Chloroquine Diphosphate for the Treatment of Severe Acute Respiratory Syndrome Secondary to SARS-CoV2 (CloroCOVID19).	Not reported.	Fundação de Medicina Tropical Dr. Heitor Vieira Dourado	20200330	2	https://clinicaltrials.gov/ct2/show/NCT04323527?cond=COVID-19&draw=20&rank=182
NCT04275388	Xiyanping Injection for the Treatment of New Coronavirus Infected Pneumonia.	Not reported.	Jiangxi Qingfeng Pharmaceutica l Co. Ltd.	20200219	Not Applicable	https://clinicaltrials.gov/ct2/show/NCT04275388?cond=COVID-19&draw=20&rank=183
NCT03331445	Inhaled Gaseous Nitric Oxide (gNO) Antimicrobial Treatment of Difficult Bacterial and Viral Lung (COVID-19) Infections (NONTM).	Not reported.	University of British Columbia.	20200331	2	https://clinicaltrials.gov/ct2/show/NCT03331445?cond=COVID-19&draw=20&rank=186
NCT04322682	Colchicine Coronavirus SARS-CoV2 Trial (COLCORONA) (COVID-19).	Not reported.	Montreal Heart Institute.	20200327	3	https://clinicaltrials.gov/ct2/show/NCT04322682?cond=COVID-19&draw=20&rank=188
NCT04252274	Efficacy and Safety of Darunavir and Cobicistat for Treatment of Pneumonia Caused by 2019-nCoV (DACO-nCoV).	Not reported.	Shanghai Public Health Clinical Center.	20200304	3	https://clinicaltrials.gov/ct2/show/NCT04252274?cond=COVID-19&draw=21&rank=195
NCT04261517	Efficacy and Safety of Hydroxychloroquine for Treatment of Pneumonia Caused by 2019-nCoV (HC-nCoV).	Not reported.	Shanghai Public Health Clinical Center.	20200324	3	https://clinicaltrials.gov/ct2/show/NCT04261517?cond=COVID-19&draw=21&rank=196
NCT04244591	Glucocorticoid Therapy for Novel Coronavirus Critically Ill Patients With Severe Acute Respiratory Failure (Steroids-SARI).	Not reported.	Peking Union Medical College Hospital.	20200213	2 and 3	https://clinicaltrials.gov/ct2/show/NCT04244591?cond=COVID-19&draw=23&rank=211
NCT04316377	Norwegian Coronavirus Disease 2019 Study (NO COVID-19).	Not reported.	University Hospital, Akershus.	20200320	4	https://clinicaltrials.gov/ct2/show/NCT04316377?cond=COVID-19&draw=23&rank=212
NCT04276688	Lopinavir/ Ritonavir, Ribavirin and IFN-beta Combination for nCoV Treatment.	Not reported.	The University of Hong Kong.	20200228	2	https://clinicaltrials.gov/ct2/show/NCT04276688?cond=COVID-19&draw=5&rank=213
NCT04308668	Post-exposure Prophylaxis / Preemptive Therapy for SARS-Coronavirus-2 (COVID-19 PEP).	Not reported.	University of Minnesota.	20200327	3	https://clinicaltrials.gov/ct2/show/NCT04308668?cond=COVID-19&draw=5&rank=217
NCT04328467	Pre-exposure Prophylaxis for SARS-Coronavirus-2.	Not reported.	University of Minnesota.	20200406	3	https://clinicaltrials.gov/ct2/show/NCT04328467?cond=COVID-19&draw=4

3.2. Natural substances.

Several patents, in particular, Chinese evolving the anti-COVID-19 effects of medicinal plants from China, are filed today in the various clinical phases (Table 5). The action of these plant mixtures has not been specified. However, these plants are known for their antioxidant and anti-inflammatory properties, which could either decrease the promoter's action of ROS on the inflammatory process or inhibit the inflammation itself. Among the patents filed are nutritional supplements, traditional Chinese medicine, honey, and ascorbic acid.

Table 5. Clinical trial patents of natural targeted SARS-CoV2.

Patent number	Patent title	Organization	Priority date	Phase	Links
NCT04323228	Anti-inflammatory/Antioxidant Oral Nutrition Supplementation in COVID-19 (ONSCOV19).	King Saud University.	20200327	4	https://clinicaltrials.gov/ct2/show/NCT04323228?cond=COVID-19&draw=2&rank=3
NCT04323332	Traditional Chinese Medicine for Severe COVID-19.	Xiyuan Hospital of China Academy of Chinese Medical Sciences.	20200326	3	https://clinicaltrials.gov/ct2/show/NCT04323332?cond=COVID-19&draw=2&rank=4
NCT04306497	Clinical Trial on Regularity of Traditional Chinese Medicines Syndrome and Differentiation Treatment of COVID-19. (CTOROTSADTOC).	Jiangsu Famous Medical Technology Co., Ltd.	20200317	Not applicable	https://clinicaltrials.gov/ct2/show/NCT04306497?cond=COVID-19&draw=2&rank=7
NCT04308317	Tetrandrine Tablets Used in the Treatment of COVID-19 (TT-NPC).	Henan Provincial People's Hospital.	20200316	4	https://clinicaltrials.gov/ct2/show/NCT04308317?cond=COVID-19&draw=5&rank=31
NCT04323345	Efficacy of Natural Honey Treatment in Patients With Novel Coronavirus.	Misr University for Science and Technology.	20200326	3	https://clinicaltrials.gov/ct2/show/NCT04323345?cond=COVID-19&draw=6&rank=42
NCT04323514	Use of Ascorbic Acid in Patients With COVID 19.	University of Palermo	20200326	Not applicable	https://clinicaltrials.gov/ct2/show/NCT04323514?cond=COVID-19&draw=7&rank=51
NCT04278963	Yinhu Qingwen Decoction for the Treatment of Mild / Common CoVID-19.	China Academy of Chinese Medical Sciences	20200317	2 and 3	https://clinicaltrials.gov/ct2/show/NCT04278963?cond=COVID-19&draw=8&rank=64
NCT04310865	Yinhu Qingwen Granula for the Treatment of Severe CoVID-19.	China Academy of Chinese Medical Sciences.	20200317	2 and 3	https://clinicaltrials.gov/ct2/show/NCT04310865?cond=COVID-19&draw=8
NCT04285190	The Effect of T89 on Improving Oxygen Saturation and Clinical Symptoms in Patients With COVID-19.	Tasly Pharmaceuticals, Inc.	20200226	Not applicable	https://clinicaltrials.gov/ct2/show/NCT04285190?cond=COVID-19&draw=10&rank=82
NCT04264533	Vitamin C Infusion for the Treatment of Severe 2019-nCoV Infected Pneumonia.	Zhongnan Hospital.	20200310	2	https://clinicaltrials.gov/ct2/show/NCT04264533?cond=COVID-19&draw=19&rank=180
NCT04251871	Treatment and Prevention of Traditional Chinese Medicines on 2019-nCoV Infection.	Beijing 302 Hospital.	20200205	Not applicable	https://clinicaltrials.gov/ct2/show/NCT04251871?cond=COVID-19&draw=21&rank=198
NCT03680274	Lessening Organ Dysfunction With VITamin C (LOVIT).	Université de Sherbrooke.	20200324	3	https://clinicaltrials.gov/ct2/show/NCT03680274?cond=COVID-19&draw=5&rank=215

3.3. Specific antibody.

Among the therapeutic strategies that are under development against COVID-19, antibodies represent a promising choice. Indeed, several patents evolving the clinical effects of antibodies against COVID-19 disease are today in the various clinical phases (Table 6). Antibodies neutralizing IL-6, such as Tocilizumab, Sarilumab, and Emapalumab, are in clinical phases II/III (Table 6). The monoclonal antibody Bevacizumab directed against Vascular

endothelial growth factor is developed by the organization Qilu Hospital of Shandong University and is now in phases II/III. Mepolizumab is also a monoclonal antibody, blocks the CD147 receptor, is developed by Tang-Du Hospital in the initial clinical phases I/II (Table 6). The complement system has also been targeted by Eculizumab-like antibodies which are under development by Hudson Medical. In addition, other types of antibodies with an immunomodulatory and anti-inflammatory effect are under development (Table 6).

Table 6. Clinical trial patents of antibody-targeted SARS-CoV2.

Patent number	Patent title	Target/key results	Organization	Priority date	Phase	Links
NCT04317092	Tocilizumab in COVID-19 Pneumonia (TOCIVID-19) (TOCIVID-19).	Interleukin-6 (IL-6)	National Cancer Institute, Naples.	20200320	2	https://clinicaltrials.gov/ct2/show/NCT04317092?cond=COVID-19&draw=3&rank=11
NCT04315298	Evaluation of the Efficacy and Safety of Sarilumab in Hospitalized Patients With COVID-19.	Interleukin-6 (IL-6)	Regeneron Pharmaceuticals.	20200330	2 and 3	https://clinicaltrials.gov/ct2/show/NCT04315298?cond=COVID-19&draw=3&rank=12
NCT04305106	Bevacizumab in Severe or Critically Severe Patients With COVID-19 Pneumonia-RCT (BEST-RCT).	Vascular endothelial growth factor (VEGF).	Qilu Hospital of Shandong University.	20200326	Not applicable	https://clinicaltrials.gov/ct2/show/NCT04305106?cond=COVID-19&draw=4&rank=26
NCT04320615	A Study to Evaluate the Safety and Efficacy of Tocilizumab in Patients With Severe COVID-19 Pneumonia (COVACTA).	Interleukin-6 (IL-6)	Hoffmann-La Roche.	20200330	3	https://clinicaltrials.gov/ct2/show/NCT04320615?cond=COVID-19&draw=4&rank=27
NCT04310228	Favipiravir Combined with Tocilizumab in the Treatment of Corona Virus Disease 2019.	Interleukin-6 (IL-6)	Guiqiang Wang, Peking University First Hospital.	20200317	Not applicable	https://clinicaltrials.gov/ct2/show/NCT04310228?cond=COVID-19&draw=7&rank=58
NCT04324021	Efficacy and Safety of Emapalumab and Anakinra in Reducing Hyperinflam	Interleukin 1 receptor antagonist protein.	Swedish Orphan Biovitrum.	20200327	2 and 3	https://clinicaltrials.gov/ct2/show/NCT04324021?cond=COVID-19&draw=8

Patent number	Patent title	Target/key results	Organization	Priority date	Phase	Links
	mation and Respiratory Distress in Patients With COVID-19 Infection.					
NCT04268537	Immunoregulatory Therapy for 2019-nCoV.	Interleukin-6 (IL-6)	Southeast University, China.	20200213	2	https://clinicaltrials.gov/ct2/show/NCT04268537?cond=COVID-19&draw=10&rank=86
NCT04306705	Tocilizumab vs CRRT in Management of Cytokine Release Syndrome (CRS) in COVID-19 (TACOS).	Interleukin-6 (IL-6)	Tongji Hospital.	20200317	Not applicable	https://clinicaltrials.gov/ct2/show/NCT04306705?cond=COVID-19&draw=10&rank=87
NCT04261426	The Efficacy of Intravenous Immunoglobulin Therapy for Severe 2019-nCoV Infected Pneumonia.	Proving passive immunity and anti-inflammatory, immunomodulatory effect.	Peking Union Medical College Hospital.	20200207	2 and 3	https://clinicaltrials.gov/ct2/show/NCT04261426?cond=COVID-19&draw=11&rank=98
NCT04275414	Bevacizumab in Severe or Critical Patients With COVID-19 Pneumonia (BEST-CP).	VEGF	Qilu Hospital of Shandong University.	20200219	2 and 3	https://clinicaltrials.gov/ct2/show/NCT04275414?cond=COVID-19&draw=12&rank=101
NCT04264858	Treatment of Acute Severe 2019-nCoV Pneumonia With Immunoglobulin From Cured Patients.	Immunoglobulin	Wuhan Union Hospital, China.	20200317	Not applicable	https://clinicaltrials.gov/ct2/show/NCT04264858?cond=COVID-19&draw=14&rank=125
NCT04324073	Cohort Multiple Randomized Controlled Trials Open-label of Immune Modulatory Drugs and Other Treatments in COVID-19 Patients - Sarilumab Trial - CORIMUNO-19 - SARI (CORIMUNO-SARI).	sIL-6R α and mIL-6R α .	Assistance Publique - Hôpitaux de Paris.	20200401	2 and 3	https://clinicaltrials.gov/ct2/show/NCT04324073?cond=COVID-19&draw=16&rank=149

Patent number	Patent title	Target/key results	Organization	Priority date	Phase	Links
NCT04288713	Ecilizumab (Soliris) in Covid-19 Infected Patients (SOLID-C19).	Complement system	Hudson Medical.	20200330	Not applicable	https://clinicaltrials.gov/ct2/show/NCT04288713?cond=COVID-19&draw=17&rank=160
NCT04315480	Tocilizumab for SARS-CoV2 Severe Pneumonitis	Interleukin-6 (IL-6)	Università Politecnica delle Marche.	20200319	2	https://clinicaltrials.gov/ct2/show/NCT04315480?cond=COVID-19&draw=20&rank=190
NCT04275245	Clinical Study of Anti-CD147 Humanized Meplazumab for Injection to Treat With 2019-nCoV Pneumonia.	CD147.	Tang-Du Hospital.	20200219	1 and 2	https://clinicaltrials.gov/ct2/show/NCT04275245?cond=COVID-19&draw=21&rank=200
NCT04322773	Anti-il6 Treatment of Serious COVID-19 Disease With Threatening Respiratory Failure (TOCIVID).	Interleukin-6 (IL-6)	Frederiksborg University Hospital.	20200403	2	https://clinicaltrials.gov/ct2/show/NCT04322773?cond=COVID-19&draw=4&rank=224

3.4. Cell therapy.

Different patents related to the use of cell therapy as a therapeutic strategy to treat COVID-19 are presented in Table 7. As summarized, the most of these approaches use mesenchymal stem cells (MSC), and the most these patents are in only in the phase I. MSC can inhibit the overactivation of the immune system and promoting endogenous repair, and reduce non-productive inflammation and affect tissue regeneration. Other cells are developed in phase I, such as NK, which activate the adaptive immune system.

Table 7. Clinical trial patents of cell therapy targeted SARS-CoV2.

Patent number	Patent title	Target/key results	Organization	Priority date	Phase	Links
NCT04315987	NestCell® Mesenchymal Stem Cell to Treat Patients With Severe COVID-19 Pneumonia (HOPE)	Inhibition of the overactivation of the immune system and promoting endogenous repair	Azidus Brasil.	20200331	1	https://clinicaltrials.gov/ct2/show/NCT04315987?cond=COVID-19&draw=4&rank=25
NCT04313322	Treatment of COVID-19 Patients Using Wharton's Jelly-Mesenchymal Stem Cells.	Inhibition of the overactivation of the immune system and promoting endogenous repair	Stem Cells Arabia.	20200318	1	https://clinicaltrials.gov/ct2/show/NCT04313322?cond=COVID-19&draw=4&rank=28

Patent number	Patent title	Target/key results	Organization	Priority date	Phase	Links
NCT04288102	Treatment With Mesenchymal Stem Cells for Severe Corona Virus Disease 2019(COVID-19).	Reduce non-productive inflammation and affect tissue regeneration.	Beijing 302 Hospital.	20200323	1 and 2	https://clinicaltrials.gov/ct2/show/NCT04288102?cond=COVID-19&draw=5&rank=38
NCT04302519	Novel Coronavirus Induced Severe Pneumonia Treated by Dental Pulp Mesenchymal Stem Cells.	Inhibition of the overactivation of the immune system and promoting endogenous repair	CAR-T (Shanghai) Biotechnology Co., Ltd.	20200310	1	https://clinicaltrials.gov/ct2/show/NCT04302519?cond=COVID-19&draw=7&rank=59
NCT04321096	The Impact of Camostat Mesilate on COVID-19 Infection (CamoCO-19).	Not reported.	University of Aarhus.	20200325	1 and 2	https://clinicaltrials.gov/ct2/show/NCT04321096?cond=COVID-19&draw=10&rank=85
NCT04273646	Study of Human Umbilical Cord Mesenchymal Stem Cells in the Treatment of Novel Coronavirus Severe Pneumonia.	Inhibition of the overactivation of the immune system and promoting endogenous repair	Wuhan Union Hospital, China.	20200221	Not applicable	https://clinicaltrials.gov/ct2/show/NCT04273646?cond=COVID-19&draw=11&rank=96
NCT04252118	Mesenchymal Stem Cell Treatment for Pneumonia Patients Infected With 2019 Novel Coronavirus.	Inhibition of the overactivation of the immune system and promoting endogenous repair	Beijing 302 Hospital.	20200226	1	https://clinicaltrials.gov/ct2/show/NCT04252118?cond=COVID-19&draw=11&rank=97
NCT04269525	Umbilical Cord(UC)-Derived Mesenchymal Stem Cells(MSCs) Treatment for the 2019-novel Coronavirus(nCoV) Pneumonia.	Inhibition of the overactivation of the immune system and promoting endogenous repair	Zhongnan Hospital of Wuhan University.	20200217	2	https://clinicaltrials.gov/ct2/show/NCT04269525?cond=COVID-19&draw=19&rank=175
NCT04276987	A Pilot Clinical Study on Inhalation of Mesenchymal Stem Cells Exosomes Treating Severe Novel Coronavirus Pneumonia.	Inhibition of the overactivation of the immune system and promoting endogenous repair	Ruijin Hospital.	20200225	1	https://clinicaltrials.gov/ct2/show/NCT04276987?cond=COVID-19&draw=5&rank=220

Patent number	Patent title	Target/key results	Organization	Priority date	Phase	Links
NCT0429152	Stem Cell Educator Therapy Treat the Viral Inflammation Caused by Severe Acute Respiratory Syndrome Coronavirus 2.	Inhibition of the overactivation of the immune system and promoting endogenous repair	Tianhe Stem Cell Biotechnologies Inc.	20200330	2	https://clinicaltrials.gov/ct2/show/NCT0429152?cond=COVID-19&draw=4&rank=264
NCT04280224	NK Cells Treatment for Novel Coronavirus Pneumonia.	Activation of adaptative immune system	Xinxiang medical university.	20200221	1	https://clinicaltrials.gov/ct2/show/NCT04280224?cond=COVID-19&draw=4&rank=272

3.5. Plasma therapy.

Another way to fight COVID-19 is to use the plasma of people who are cured of this disease and administer it to COVID-19 patients (Table 8). Certain clinical patents are filed on plasma therapy, two of which are in clinical phase III. This is a patent that evaluated the effect of plasma on immunocompromised individuals (NCT03808922) and another patent that aims to decrease the severe complications of COVID-19.

Table 8. Clinical trial patents of plasma therapy targeted SARS-CoV2.

Patent number	Patent title	Organization	Priority date	Phase	Links
NCT04321421	Hyperimmune Plasma for Critical Patients With COVID-19 (COV19-PLASMA).	Foundation IRCCS San Matteo Hospital.	20200325	Not applicable	https://clinicaltrials.gov/ct2/show/NCT04321421?cond=COVID-19&draw=2&rank=6
NCT04324996	A Phase I/II Study of Universal Off-the-shelf NKG2D-ACE2 CAR-NK Cells for Therapy of COVID-19.	Chongqing Public Health Medical Center.	20200327	1 and 2	https://clinicaltrials.gov/ct2/show/NCT04324996?cond=COVID-19&draw=2&rank=9
NCT04273321	Efficacy and Safety of Corticosteroids in COVID-19.	Beijing Chao Yang Hospital.	20200401	Not applicable	https://clinicaltrials.gov/ct2/show/NCT04273321?cond=COVID-19&draw=6&rank=41
NCT04323800	Efficacy and Safety Human Coronavirus Immune Plasma (HCIP) vs. Control (SARS-CoV-2 Non-immune Plasma) Among Adults Exposed to COVID-19 (CSSC-001).	Sidney Kimmel Comprehensive Cancer Center at Johns Hopkins.	20200402	2	https://clinicaltrials.gov/ct2/show/NCT04323800?cond=COVID-19&draw=10&rank=84
NCT04325672	Convalescent Plasma to Limit Coronavirus Associated Complications.	Mayo Clinic.	20200327	3	https://clinicaltrials.gov/ct2/show/NCT04325672?cond=COVID-19&draw=19&rank=177

Patent number	Patent title	Organization	Priority date	Phase	Links
NCT03808922	Phase III DAS181 Lower Tract PIV Infection in Immunocompromised Subjects (Substudy: DAS181 for COVID-19): RCT Study.	Ansun Biopharma, Inc.	20200402	3	https://clinicaltrials.gov/ct2/show/NCT03808922?cond=COVID-19&draw=5&rank=219

3.6. Vaccine trials.

Some clinical vaccine trials are being evaluated with different phases (Table 9). These trials are based primarily on decreasing the complications of COVID-19 and directing the immune system against the antigens of SARS-CoV-2. So far, only two vaccine trials have reached the third clinical phase. The first trial, carried out by the Mayo Clinic organization, developed convalescent plasmas in order to limit the complications associated with the coronavirus (NCT04325672), while the second trial in clinical phase 3, evaluated the injection of *Parainfluenza* virus in Immunocompromised Subjects (NCT03808922). Another trial patent in phase 2 has evaluated the effect of efficacy and safety of human coronavirus immune plasma (NCT04323800).

Table 9. Clinical trial patents of vaccine strategies against SARS-CoV2.

Patent number	Patent title	Target/key results	Organization	Priority date	Phase	Links
NCT04299724	Safety and Immunity of Covid-19 aAPC Vaccine.	Not reported.	Shenzhen Geno-Immune Medical Institute.	20200309	1	https://clinicaltrials.gov/ct2/show/NCT04299724?cond=COVID-19&draw=6&rank=47
NCT04276896	Immunity and Safety of Covid-19 Synthetic Minigene Vaccine.	Not reported.	Shenzhen Geno-Immune Medical Institute.	20200319	1 and 2	https://clinicaltrials.gov/ct2/show/NCT04276896?cond=COVID-19&draw=6&rank=50
NCT04313127	A Phase I Clinical Trial in 18-60 Adults (APICHT).	Recombinant Novel Coronavirus Vaccine (Adenovirus Type 5 Vector).	CanSino Biologics Inc.	20200331	1	https://clinicaltrials.gov/ct2/show/NCT04313127?cond=COVID-19&draw=7&rank=55
NCT04324606	A Study of a Candidate COVID-19 Vaccine (COV001).	Not reported.	University of Oxford.	20200327	1 and 2	https://clinicaltrials.gov/ct2/show/NCT04324606?cond=COVID-19&draw=10&rank=83
NCT04283461	Safety and Immunogenicity Study of 2019-nCoV Vaccine (mRNA-1273) for Prophylaxis SARS CoV-2 Infection.	Spike protein.	National Institute of Allergy and Infectious Diseases.	20200330	1	https://clinicaltrials.gov/ct2/show/NCT04283461?cond=COVID-19&draw=20&rank=185
NCT04283461	Safety and Immunogenicity Study of 2019-nCoV Vaccine (mRNA-1273) for	Spike protein.	National Institute of Allergy and Infectious Diseases.	20200330	1	https://clinicaltrials.gov/ct2/show/NCT04283461?cond=COVID-19&draw=20&rank=185

Patent number	Patent title	Target/key results	Organization	Priority date	Phase	Links
	Prophylaxis SARS CoV-2 Infection.					

4. Conclusions

The COVID-19 epidemic posed a real danger with extremely powerful damage. In the absence of effective treatments such as a vaccine, the spread of the virus is continuously emerging. However, recent works that have evaluated the antiviral activity of natural and synthetic molecules against SARS-CoV-2 have shown promising results and could introduce effective drugs. In addition, the use of other old antivirals has revealed that these molecules are also effective against SARS-CoV2, which could make their use an effective means against COVID-19, as in the case of chloroquine and hydroxy-chloroquine. There are also a number of recently filed patents on various proposed therapies, such as monoclonal antibody therapy, cell therapy, plasma therapy, and vaccine trials. These patents are in the different clinical phases and will certainly lead to clinical validations in the future weeks or months.

Funding

This research received no external funding.

Acknowledgments

This research has no acknowledgment.

Conflicts of Interest

The authors declare no conflict of interest.

References

- Gupta, V.; Know the unknown fact of novel COVID -19 corona virus. *Letters in Applied NanoBioScience* **2020**, *9*, 1083 – 1088, <https://doi.org/10.33263/LIANBS92.10831088>.
- Nadjib, B.M. Effective Antiviral Activity of Essential Oils and Their Characteristic Terpenes against Coronaviruses: An Update. *Journal of Pharmacology & Clinical Toxicology* **2020**, *9*.
- Fischer, A.; Sellner, M.; Neranjan, S.; Lill, M.A. Inhibitors for Novel Coronavirus Protease Identified by Virtual Screening of 687 Million Compounds. *Chemrxiv* **2020**, *21*, <https://doi.org/10.26434/chemrxiv.11923239>.
- Phan, L.T.; Nguyen, T.V.; Luong, Q.C.; Nguyen, T.V.; Nguyen, H.T.; Le, H.Q.; Nguyen, T.T.; Cao, T.M.; Pham, Q.D. Importation and Human-to-Human Transmission of a Novel Coronavirus in Vietnam. *New England Journal of Medicine* **2020**, *382*, 872–874, <https://doi.org/10.1056/NEJMc2001272>.
- Shereen, M.A.; Khan, S.; Kazmi, A.; Bashir, N.; Siddique, R. COVID-19 Infection: Origin, Transmission, and Characteristics of Human Coronaviruses. *Journal of Advanced Research* **2020**, *24*, 91–98, <https://doi.org/10.1016/j.jare.2020.03.005>.
- Hong, H.; Wang, Y.; Chung, H.T.; Chen, C.J. Clinical Characteristics of Novel Coronavirus Disease 2019 (COVID-19) in Newborns, Infants and Children. *Pediatrics & Neonatology* **2020**, *0*, <https://doi.org/10.1016/j.pedneo.2020.03.001>.
- Rothan, H.A.; Byrareddy, S.N. The Epidemiology and Pathogenesis of Coronavirus Disease (COVID-19) Outbreak. *Journal of Autoimmunity* **2020**, *109*, <https://doi.org/10.1016/j.jaut.2020.102433>.
- Yang, Y.; Islam, M. S.; Wang, J.; Li, Y.; Chen, X. Traditional Chinese Medicine in the Treatment of Patients Infected with 2019-New Coronavirus (SARS-CoV-2): A Review and Perspective. *Int. J. Biol. Sci.* **2020**, *16*, 1708–1717, <https://doi.org/10.7150/ijbs.45538>.
- Corman, V.M.; Landt, O.; Kaiser, M.; Molenkamp, R.; Meijer, A.; Chu, D.K.; Bleicker, T.; Brünink, S.; Schneider, J.; Schmidt, M.L.; Mulders, D.G.; Haagmans, B.L.; van der Veer, B.; van den Brink, S.; Wijsman, L.; Goderski, G.; Romette, J.L.; Ellis, J.; Zambon, M.; Peiris, M.; Goossens, H.; Reusken, C.; Koopmans,

- M. P.; Drosten, C. Detection of 2019 Novel Coronavirus (2019-NCoV) by Real-Time RT-PCR. *Euro Surveill* **2020**, *25*, <https://doi.org/10.2807/1560-7917.ES.2020.25.3.2000045>.
10. Zhang, L.; Liu, Y. Potential Interventions for Novel Coronavirus in China: A Systematic Review. *J Med Virol* **2020**, *92*, 479–490, <https://doi.org/10.1002/jmv.25707>.
11. Mohammadi, N.; Shaghaghi, N. Inhibitory Effect of Eight Secondary Metabolites from Conventional Medicinal Plants on COVID-19 Virus Protease by Molecular Docking Analysis. *Preprint* **2020**, <https://doi.org/10.26434/chemrxiv.11987475.v1>.
12. Liu, C.; Zhu, X.; Lu, Y.; Jia, X.; Yang, T. Potential Treatment of Chinese and Western Medicine Targeting Nsp14 of 2019-NCoV. *Chinaxiv* **2020**.
13. Tsai, Y.C.; Lee, C.L.; Yen, H.R.; Chang, Y.S.; Lin, Y.P.; Huang, S.H.; Lin, C.W. Antiviral Action of Tryptanthrin Isolated from *Strobilanthes cusia* Leaf against Human Coronavirus NL63. *Biomolecules* **2020**, *10*, <https://doi.org/10.3390/biom10030366>.
14. Lin, C.W.; Tsai, F.J.; Tsai, C.H.; Lai, C.C.; Wan, L.; Ho, T.Y.; Hsieh, C.C.; Chao, P.D.L. Anti-SARS Coronavirus 3C-like Protease Effects of *Isatis indigotica* Root and Plant-Derived Phenolic Compounds. *Antiviral Research* **2005**, *68*, 36–42, <https://doi.org/10.1016/j.antiviral.2005.07.002>.
15. Liang, W.; He, L.; Ning, P.; Lin, J.; Li, H.; Lin, Z.; Kang, K.; Zhang, Y. (+)-Catechin Inhibition of Transmissible Gastroenteritis Coronavirus in Swine Testicular Cells Is Involved Its Antioxidation. *Research in Veterinary Science* **2015**, *103*, 28–33, <https://doi.org/10.1016/j.rvsc.2015.09.009>.
16. Yu, M.S.; Lee, J.; Lee, J.M.; Kim, Y.; Chin, Y.W.; Jee, J.G.; Keum, Y.S.; Jeong, Y.J. Identification of Myricetin and Scutellarein as Novel Chemical Inhibitors of the SARS Coronavirus Helicase, Nsp13. *Bioorganic & Medicinal Chemistry Letters* **2012**, *22*, 4049–4054, <https://doi.org/10.1016/j.bmcl.2012.04.081>.
17. Cho, J.K.; Curtis-Long, M.J.; Lee, K.H.; Kim, D.W.; Ryu, H.W.; Yuk, H.J.; Park, K.H. Geranylated Flavonoids Displaying SARS-CoV Papain-like Protease Inhibition from the Fruits of *Paulownia tomentosa*. *Bioorganic & Medicinal Chemistry* **2013**, *21*, 3051–3057, <https://doi.org/10.1016/j.bmc.2013.03.027>.
18. Utomo, R.Y.; Ikawati, M.; Meiyanto, E. Revealing the Potency of Citrus and Galangal Constituents to Halt SARS-CoV-2 Infection. *Preprint; Medicine & Pharmacology* **2020**, <https://doi.org/10.20944/preprints202003.0214.v1>.
19. Cheng, L.; Zheng, W.; Li, M.; Huang, J.; Ma, Z. Citrus Fruits Are Rich in Flavonoids for Immunoregulation and Potential Targeting ACE2. *Preprints* **2020**, *13*.
20. Jo, S.; Kim, S.; Shin, D.H.; Kim, M.S. Inhibition of SARS-CoV 3CL Protease by Flavonoids. *Journal of Enzyme Inhibition and Medicinal Chemistry* **2020**, *35*, 145–151, <https://doi.org/10.1080/14756366.2019.1690480>.
21. Nguyen, T.T.H.; Woo, H.J.; Kang, H.K.; Nguyen, V.D.; Kim, Y.M.; Kim, D.W.; Ahn, S.A.; Xia, Y.; Kim, D. Flavonoid-Mediated Inhibition of SARS Coronavirus 3C-like Protease Expressed in *Pichia pastoris*. *Biotechnol Lett* **2012**, *34*, 831–838, <https://doi.org/10.1007/s10529-011-0845-8>.
22. Ryu, Y.B.; Jeong, H.J.; Kim, J.H.; Kim, Y.M.; Park, J.Y.; Kim, D.; Nguyen, T.T.H.; Park, S.J.; Chang, J.S.; Park, K.H. Biflavonoids from *Torreya nucifera* Displaying SARS-CoV 3CLpro Inhibition. *Bioorganic & Medicinal Chemistry* **2010**, *18*, 7940–7947, <https://doi.org/10.1016/j.bmc.2010.09.035>.
23. Wen, C.C.; Kuo, Y.H.; Jan, J.T.; Liang, P.H.; Wang, S.Y.; Liu, H.G.; Lee, C.K.; Chang, S.T.; Kuo, C.J.; Lee, S.S.; Hou, C.C.; Hsiao, P.W.; Chien, S.C.; Shyr, L.F.; Yang, N.S. Specific Plant Terpenoids and Lignoids Possess Potent Antiviral Activities against Severe Acute Respiratory Syndrome Coronavirus. *J. Med. Chem.* **2007**, *50*, 4087–4095, <https://doi.org/10.1021/jm070295s>.
24. Park, J.Y.; Kim, J.H.; Kwon, J.M.; Kwon, H.J.; Jeong, H.J.; Kim, Y.M.; Kim, D.; Lee, W.S.; Ryu, Y.B. Dieckol, a SARS-CoV 3CLpro Inhibitor, Isolated from the Edible Brown Algae *Ecklonia cava*. *Bioorganic & Medicinal Chemistry* **2013**, *21*, 3730–3737, <https://doi.org/10.1016/j.bmc.2013.04.026>.
25. Kwon, H.J.; Ryu, Y.B.; Kim, Y.M.; Song, N.; Kim, C.Y.; Rho, M.C.; Jeong, J.H.; Cho, K.O.; Lee, W.S.; Park, S.J. In Vitro Antiviral Activity of Phlorotannins Isolated from *Ecklonia cava* against Porcine Epidemic Diarrhea Coronavirus Infection and Hemagglutination. *Bioorganic & Medicinal Chemistry* **2013**, *21*, 4706–4713, <https://doi.org/10.1016/j.bmc.2013.04.085>.
26. Khalifa, I.; Zhu, W.; Nafie, M.S.; Dutta, K.; Li, C. Anti-COVID-19 Effects of Ten Structurally Different Hydrolysable Tannins through Binding with the Catalytic-Closed Sites of COVID-19 Main Protease: An In-Silico Approach. *Preprint other* **2020**, <https://doi.org/10.20944/preprints202003.0277.v1>.
27. Ho, T.; Wu, S.; Chen, J.; Li, C.; Hsiang, C. Emodin Blocks the SARS Coronavirus Spike Protein and Angiotensin-Converting Enzyme 2 Interaction. *Antiviral Research* **2007**, *74*, 92–101, <https://doi.org/10.1016/j.antiviral.2006.04.014>.
28. Schwarz, S.; Wang, K.; Yu, W.; Sun, B.; Schwarz, W. Emodin Inhibits Current through SARS-Associated Coronavirus 3a Protein. *Antiviral Research* **2011**, *90*, 64–69, <https://doi.org/10.1016/j.antiviral.2011.02.008>.
29. Park, J.Y.; Ko, J.A.; Kim, D.W.; Kim, Y.M.; Kwon, H.J.; Jeong, H.J.; Kim, C.Y.; Park, K.H.; Lee, W.S.; Ryu, Y.B. Chalcones Isolated from *Angelica keiskei* Inhibit Cysteine Proteases of SARS-CoV. *Journal of Enzyme Inhibition and Medicinal Chemistry* **2014**, *31*, 23–30, <https://doi.org/10.3109/14756366.2014.1003215>.

30. Cheng, J.; Tang, Y.; Zhang, P. Exploring the Active Compounds of Traditional Mongolian Medicine Agsirga in Intervention of Novel Coronavirus (2019- NCoV) Based on HPLC-Q-Exactive-MS/MS and Molecular Docking Method. *Chemrxiv* **2020**, 31.
31. Hoefer, G.; Baltina, L.; Michaelis, M.; Kondratenko, R.; Baltina, L.; Tolstikov, G. A.; Doerr, H. W.; Cinatl, J. Antiviral Activity of Glycyrrhizic Acid Derivatives against SARS–Coronavirus. *J. Med. Chem.* **2005**, 48, 1256–1259, <https://doi.org/10.1021/jm0493008>.
32. Park, J.Y.; Kim, J.H.; Kim, Y.M.; Jeong, H.J.; Kim, D.W.; Park, K.H.; Kwon, H.J.; Park, S.J.; Lee, W.S.; Ryu, Y.B. Tanshinones as Selective and Slow-Binding Inhibitors for SARS-CoV Cysteine Proteases. *Bioorganic & Medicinal Chemistry* **2012**, 20, 5928–5935, <https://doi.org/10.1016/j.bmc.2012.07.038>.
33. Park, J.Y.; Yuk, H.J.; Ryu, H.W.; Lim, S.H.; Kim, K.S.; Park, K.H.; Ryu, Y.B.; Lee, W.S. Evaluation of Polyphenols from *Broussonetia Papyrifera* as Coronavirus Protease Inhibitors. *Journal of Enzyme Inhibition and Medicinal Chemistry* **2017**, 32, 504–512, <https://doi.org/10.1080/14756366.2016.1265519>.
34. Hsieh, L.E.; Lin, C.N.; Su, B.L.; Jan, T.R.; Chen, C.M.; Wang, C.H.; Lin, D.S.; Lin, C.T.; Chueh, L.L. Synergistic Antiviral Effect of Galanthus Nivalis Agglutinin and Nelfinavir against Feline Coronavirus. *Antiviral Research* **2010**, 88, 25–30, <https://doi.org/10.1016/j.antiviral.2010.06.010>.
35. Jo, S.; Kim, S.; Shin, D.H.; Kim, M.S. Inhibition of SARS-CoV 3CL Protease by Flavonoids. *Journal of Enzyme Inhibition and Medicinal Chemistry* **2020**, 35, 145–151, <https://doi.org/10.1080/14756366.2019.1690480>.
36. Galasiti Kankanamalage, A.C.; Kim, Y.; Damalanka, V.C.; Rathnayake, A.D.; Fehr, A.R.; Mehzebeen, N.; Battaille, K.P.; Lovell, S.; Lushington, G.H.; Perlman, S.; Chang, K.O.; Groutas, W.C. Structure-Guided Design of Potent and Permeable Inhibitors of MERS Coronavirus 3CL Protease That Utilize a Piperidine Moiety as a Novel Design Element. *European Journal of Medicinal Chemistry* **2018**, 150, 334–346, <https://doi.org/10.1016/j.ejmech.2018.03.004>.
37. Ho, T.; Wu, S.; Chen, J.; Wei, Y.; Cheng, S.; Chang, Y.; Liu, H.; Hsiang, C. Design and Biological Activities of Novel Inhibitory Peptides for SARS-CoV Spike Protein and Angiotensin-Converting Enzyme 2 Interaction. *Antiviral Research* **2006**, 69, 70–76, <https://doi.org/10.1016/j.antiviral.2005.10.005>.
38. Hanh Nguyen, T.T.; Ryu, H.J.; Lee, S.H.; Hwang, S.; Breton, V.; Rhee, J.H.; Kim, D. Virtual Screening Identification of Novel Severe Acute Respiratory Syndrome 3C-like Protease Inhibitors and in Vitro Confirmation. *Bioorganic & Medicinal Chemistry Letters* **2011**, 21, 3088–3091, <https://doi.org/10.1016/j.bmcl.2011.03.034>.
39. Mirza, M.U.; Froeyen, M. Structural Elucidation of SARS-CoV-2 Vital Proteins: Computational Methods Reveal Potential Drug Candidates Against Main Protease, Nsp12 RNA-Dependent RNA Polymerase and Nsp13 Helicase. *Preprint life sciences* **2020**, <https://doi.org/10.20944/preprints202003.0085.v1>.
40. Karypidou, K.; Ribone, S.R.; Quevedo, M.A.; Persoons, L.; Pannecouque, C.; Helsen, C.; Claessens, F.; Dehaen, W. Synthesis, Biological Evaluation and Molecular Modeling of a Novel Series of Fused 1,2,3-Triazoles as Potential Anti-Coronavirus Agents. *Bioorganic & Medicinal Chemistry Letters* **2018**, 28, 3472–3476, <https://doi.org/10.1016/j.bmcl.2018.09.019>.
41. Thanigaimalai, P.; Konno, S.; Yamamoto, T.; Koiwai, Y.; Taguchi, A.; Takayama, K.; Yakushiji, F.; Akaji, K.; Kiso, Y.; Kawasaki, Y.; Chen, S.E.; Naser-Tavakolian, A.; Schön, A.; Freire, E.; Hayashi, Y. Design, Synthesis, and Biological Evaluation of Novel Dipeptide-Type SARS-CoV 3CL Protease Inhibitors: Structure–Activity Relationship Study. *European Journal of Medicinal Chemistry* **2013**, 65, 436–447, <https://doi.org/10.1016/j.ejmech.2013.05.005>.
42. Turlington, M.; Chun, A.; Tomar, S.; Egger, A.; Grum-Tokars, V.; Jacobs, J.; Daniels, J. S.; Dawson, E.; Saldanha, A.; Chase, P.; Baez-Santos, Y.M.; Lindsley, C.W.; Hodder, P.; Mesecar, A.D.; Stauffer, S.R. Discovery of N-(Benzo[1,2,3]Triazol-1-Yl)-N-(Benzyl)Acetamido)Phenyl) Carboxamides as Severe Acute Respiratory Syndrome Coronavirus (SARS-CoV) 3CLpro Inhibitors: Identification of ML300 and Noncovalent Nanomolar Inhibitors with an Induced-Fit Binding. *Bioorganic & Medicinal Chemistry Letters* **2013**, 23, 6172–6177, <https://doi.org/10.1016/j.bmcl.2013.08.112>.
43. Kim, M.K.; Yu, M.S.; Park, H.R.; Kim, K.B.; Lee, C.; Cho, S.Y.; Kang, J.; Yoon, H.; Kim, D.E.; Choo, H.; Jeong, Y.J.; Chong, Y. 2,6-Bis-Arylmethoxy-5-Hydroxychromones with Antiviral Activity against Both Hepatitis C Virus (HCV) and SARS-Associated Coronavirus (SCV). *European Journal of Medicinal Chemistry* **2011**, 46, 5698–5704, <https://doi.org/10.1016/j.ejmech.2011.09.005>.
44. Yang, C.W.; Lee, Y.Z.; Kang, I.J.; Barnard, D.L.; Jan, J.T.; Lin, D.; Huang, C.W.; Yeh, T.K.; Chao, Y.S.; Lee, S.J. Identification of Phenanthroindolizines and Phenanthroquinolizidines as Novel Potent Anti-Coronaviral Agents for Porcine Enteropathogenic Coronavirus Transmissible Gastroenteritis Virus and Human Severe Acute Respiratory Syndrome Coronavirus. *Antiviral Research* **2010**, 88, 160–168, <https://doi.org/10.1016/j.antiviral.2010.08.009>.
45. Zhang, H.; Saravanan, K.M.; Yang, Y.; Hossain, M.T.; Li, J.; Ren, X.; Wei, Y. Deep Learning Based Drug Screening for Novel Coronavirus 2019-NCov. *Preprints* **2020**, <https://doi.org/10.20944/preprints202002.0061.v1>.
46. Cao, J.; Forrest, J.C.; Zhang, X. A Screen of the NIH Clinical Collection Small Molecule Library Identifies Potential Anti-Coronavirus Drugs. *Antiviral Research* **2015**, 114, 1–10, <https://doi.org/10.1016/j.antiviral.2014.11.010>.

47. Cheng, K.W.; Cheng, S.C.; Chen, W.Y.; Lin, M.H.; Chuang, S.J.; Cheng, I.H.; Sun, C.Y.; Chou, C.Y. Thiopurine Analogs and Mycophenolic Acid Synergistically Inhibit the Papain-like Protease of Middle East Respiratory Syndrome Coronavirus. *Antiviral Research* **2015**, *115*, 9–16, <https://doi.org/10.1016/j.antiviral.2014.12.011>.
48. Kim, M.K.; Yu, M.S.; Park, H.R.; Kim, K.B.; Lee, C.; Cho, S.Y.; Kang, J.; Yoon, H.; Kim, D.E.; Choo, H.; Jeong, Y.J.; Chong, Y. 2,6-Bis-Arylmethoxy-5-Hydroxychromones with Antiviral Activity against Both Hepatitis C Virus (HCV) and SARS-Associated Coronavirus (SCV). *European Journal of Medicinal Chemistry* **2011**, *46*, 5698–5704, <https://doi.org/10.1016/j.ejmech.2011.09.005>.
49. Elfiky, A.A. Anti-HCV, Nucleotide Inhibitors, Repurposing against COVID-19. *Life Sciences* **2020**, *248*, <https://doi.org/10.1016/j.lfs.2020.117477>.
50. Smith, M.; Smith, J.C. Repurposing Therapeutics for COVID-19: Supercomputer-Based Docking to the SARS-CoV-2 Viral Spike Protein and Viral Spike Protein-Human ACE2 Interface. *Chemrxiv* **2020**, <https://doi.org/10.26434/chemrxiv.11871402.v3>.
51. Ruan, Z.; Liu, C.; Guo, Y.; He, Z.; Huang, X.; Jia, X.; Yang, T. Potential Inhibitors Targeting RNA-Dependent RNA Polymerase Activity (NSP12) of SARS-CoV-2. *Preprints* **2020**, <https://doi.org/10.20944/preprints202003.0024.v1>.
52. Simmons, G.; Gosalia, D.N.; Rennekamp, A.J.; Reeves, J.D.; Diamond, S.L.; Bates, P. Inhibitors of Cathepsin L Prevent Severe Acute Respiratory Syndrome Coronavirus Entry. *PNAS* **2005**, *102*, 11876–11881, <https://doi.org/10.1073/pnas.0505577102>.
53. Sheahan, T.P.; Sims, A.C.; Leist, S.R.; Schäfer, A.; Won, J.; Brown, A.J.; Montgomery, S.A.; Hogg, A.; Babusis, D.; Clarke, M.O.; Spahn, J.E.; Bauer, L.; Sellers, S.; Porter, D.; Feng, J.Y.; Cihlar, T.; Jordan, R.; Denison, M.R.; Baric, R.S. Comparative Therapeutic Efficacy of Remdesivir and Combination Lopinavir, Ritonavir, and Interferon Beta against MERS-CoV. *Nature Communications* **2020**, *11*, 1–14, <https://doi.org/10.1038/s41467-019-13940-6>.
54. Wang, M.; Cao, R.; Zhang, L.; Yang, X.; Liu, J.; Xu, M.; Shi, Z.; Hu, Z.; Zhong, W.; Xiao, G. Remdesivir and Chloroquine Effectively Inhibit the Recently Emerged Novel Coronavirus (2019-NCoV) in Vitro. *Cell Research* **2020**, *30*, 269–271, <https://doi.org/10.1038/s41422-020-0282-0>.
55. Yao, X.; Ye, F.; Zhang, M.; Cui, C.; Huang, B.; Niu, P.; Liu, X.; Zhao, L.; Dong, E.; Song, C.; Zhan, S.; Lu, R.; Li, H.; Tan, W.; Liu, D. In Vitro Antiviral Activity and Projection of Optimized Dosing Design of Hydroxychloroquine for the Treatment of Severe Acute Respiratory Syndrome Coronavirus 2 (SARS-CoV-2). *Clin Infect Dis* **2020**, <https://doi.org/10.1093/cid/ciaa237>.
56. de Wilde, A.H.; Falzarano, D.; Zevenhoven-Dobbe, J.C.; Beugeling, C.; Fett, C.; Martellaro, C.; Postuma, C.C.; Feldmann, H.; Perlman, S.; Snijder, E.J. Alisporivir Inhibits MERS- and SARS-Coronavirus Replication in Cell Culture, but Not SARS-Coronavirus Infection in a Mouse Model. *Virus Research* **2017**, *228*, 7–13, <https://doi.org/10.1016/j.virusres.2016.11.011>.
57. Cheng, K.W.; Cheng, S.C.; Chen, W.Y.; Lin, M.H.; Chuang, S.J.; Cheng, I.H.; Sun, C.Y.; Chou, C.Y. Thiopurine Analogs and Mycophenolic Acid Synergistically Inhibit the Papain-like Protease of Middle East Respiratory Syndrome Coronavirus. *Antiviral Research* **2015**, *115*, 9–16, <https://doi.org/10.1016/j.antiviral.2014.12.011>.